Department of Physics and Astronomy, University of Canterbury,
Private Bag 4800, Christchurch, New Zealand

Suitability of Tumour Tracking For The Verification of Respiratory Gated Radiation Therapy

by

Marco A. Serpa Lopez

A thesis submitted in partial fulfilment of the requirements for the award of Master of Science from the University of Canterbury

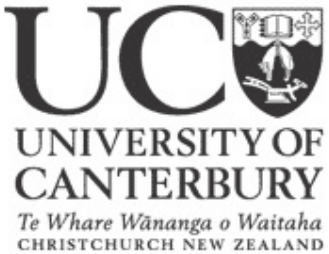

Senior Supervisor: Dr. Jürgen Meyer
Co-Supervisor: Dr. Florian Cremers

September 14th, 2011

Abstract

External beam radiotherapy (RT) is the primary treatment modality for patients with inoperable lung tumours. Respiration-induced motion and related intra-/interfractional variations present a series of limitations to the success of existing conventional treatment modalities for lung cancer. Subsequently, to minimise the effects of respiration different management techniques have been proposed and are available. Respiratory gated radiotherapy (RGRT) holds promise to improve dose conformity, reduce the normal tissue control probability while increasing the tumour control probability. Its effectiveness depends on precise tumour localisation and targeting during dose delivery. In this thesis, the suitability of RGRT for the compensation of breathing induced motion was investigated by means of phantom studies and film dosimetry. Both regular and irregular trajectories were simulated during gated dose delivery and their effects on dose distributions analysed. Respiration-induced motion led to dose blurring and hence to less conformal dose distributions, which resulted overall in underdose of the treatment planning volume and an overdose of healthy surrounding tissue. Compared to non-gated dose delivery, RGRT improved dose conformity by enabling steeper dose gradients, resulting in an increased sparing of healthy tissue, at the expenses of increased delivery times. In the presence of irregular motion paths the dosimetric advantages of RGRT were observed to decrease. In the absence of a clinical tool for treatment verification such irregularities may pass unnoticeable and may lead to poor treatment outcomes.

Investigations of the suitability of a software tool for tracking lung tumours in portal images during RGRT demonstrated that it is possible to determine and track tumour motion during gated treatment. Both the residual tumour motion inside the gating window as well as the probability density function were used as measures to quantify tumour position and variability. Tracking information was sufficient to quantify residual motion and variability. Baseline drifts as well as sudden fluctuations in tumour positions were detected and quantified, which led to considerable variations in residual motion which in turn may result in marginal miss. Although this was a retrospective analysis of motion data, the tool showed a great potential for verification of the tumour position during RGRT and may possibly be useful for adaptation of the gating window.

Contents

List of Figures

List of Tables

Chapter 1

Introduction

1.1 Background

Lung cancer has long been recognised as one of the major causes of cancer-related deaths worldwide [1], ranking first and second in terms of incidences for males and females in 2008 [2]. Based on the World Health Organisation (WHO) histologic lung cancer classification, the four major types of lung cancer are squamous cell carcinoma, adenocarcinoma, non-small cell lung cancer (NSCLC), and small-cell undifferentiated carcinoma [1], with NSCLC accounting for most of the lung cancer cases reported. For patients suffering from NSCLC, tumour stage is the most important prognosis factor, which determines treatment modality. Although, surgery is the primary treatment choice for patients suffering from stage I-II tumours as well as some selective cases of stage III tumours, only the minority of them (about 20%) are suitable to undergo surgery due to co-morbid conditions, such as compromised lung function, bleeding tendency [3]. External-beam radiotherapy (RT), either alone for patients who present with stage I/II or combined with concurrent chemotherapy, in case of locally advanced (stage III) disease, is the treatment of choice for patients who are inoperable due to medical co-morbidities [3]. However, despite the increased efforts to control or eradicate the disease, the treatment of pulmonary tumours is among one of the most technically challenging procedures in radiation oncology [4]. This has been reflected in the limited improvements in survival rates observed in the last years, with one Radiation Therapy Oncology Group (RTOG) report indicating the 5-year survival rate between 13% - 16% [5].

Since the beginnings of the application of x-rays in radiation therapy, several attempts have been made to concentrate the dose distributions within specified treatment volumes [6]. Initially, rectangular cross-fired fields of uniform fluences were used to treat tumours [7], which delivered unwanted doses to surrounding structures. Then over the following years, the need to concentrate the treatment radiation fields within the target volumes was better understood, which led to the development and combined implementation of a series of mechanical devices and treatment planning techniques to fulfill this objective [4, 8]. Subsequently, conformal radiotherapy (CFRT) was developed and then three dimensional conformal radiotherapy (3D-CRT). An important step in 3D-CRT was the use of metal blocks, made from low melting points alloy, to generate irregularly shaped irradiations field [9]. Although this improved dose conformity, it turned out to be time-consuming and expensive as the blocks had to be customized based on patient-/beam-specific characteristics.

Alternatively, a great progress in conformal radiotherapy was achieved with the development of multileaf collimators (MLCs), which offered dose conformity similar or equivalent to conformal blocks. With MLCs more convenient irregular field shapes could be created and soon became a standard feature implemented into most clinical linear accelerators.

3D-CRT is an extension of CFRT, which has allowed the inclusion of 3D anatomic information into the process of treatment planning [9]. This enabled the design of dose distributions that can be shaped to conform to target volumes by the use of forward planning process, multimodality imaging and sophisticated delivery techniques [3, 9]. The overall goal was to conform the dose distributions as close as possible to target volume in terms of adequate dose to the tumour and minimum possible dose to the normal tissue. This objective involves both physical and biological rationales, such as maximising tumour control probability (TCP) and minimising normal tissue complications probability (NTCP), to achieve the desired clinical result.

In the last decades, a more advanced form of (CFRT), known as intensity-modulated radiation therapy (IMRT) [8], has emerged as the result of the improved physical basis of radiation therapy [6]. IMRT combines geometrical and fluence shaping to the clinical requirements, allowing photon fields fluence modulation pixel-by-pixel [8]. This way, a high dose distribution can be tailored to concave target volumes with greater sparing of healthy tissue. Intensity-modulated beams are generated via inverse planning techniques [6], which are the opposite to existing trial-and-error forward planning, in which the planner start out by specifying the prescribed dose and algorithms seeks to arrive at the "optimum plan", consisting of the most acceptable compromised beam segments closest to optimum. The beginnings of IMRT can be attributed to works by Brahme in early 1980s [8]. In 1982, Brahme put into effect his newly introduced planning technique, which reversed the order of existent trial-and-error forward method used at that times [8]. Brahme demonstrated how to create a circular uniform dose D, with outer radius R_{out} enclosing a smaller concentric circle of radius r_{in} with zero dose by a rotation technique [8]. Figure 1.1 shows how by blocking the inner central region (OARs) and then rotating the beam, a non-uniform dose distribution is formed in surrouding outer circle with almost zero fluence from origin out to r_{in} [6].

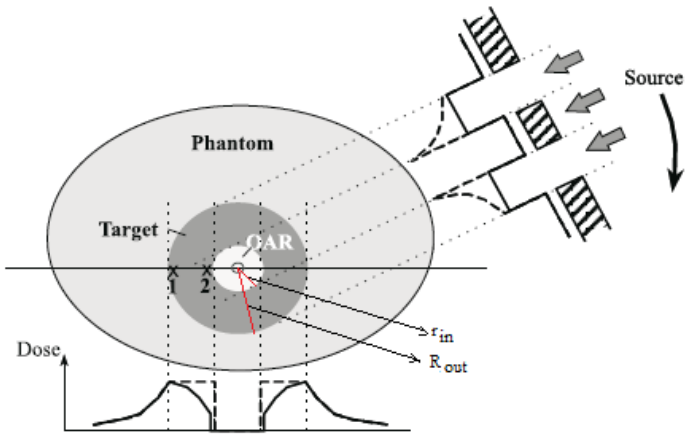

Figure 1.1: *Brahme's 1982 rotation technique with central blocking used to generate an inhomogeneous dose distribution in the target, with zero fluence around a critical structure.(Modified figure taken from Image-guide IMRT [4])*

The success of lung cancer RT relies on accurate imaging (tumour definition/localisation), treatment planning and delivery (tumour targeting) [10, 11]. However, because of the fractionated-nature of RT and the associated treatment workflow [9], organ movement due to different physiological processes results in a series of inherent geometrical uncertainties, which may lead to poor outcomes of RT. Respiration has been recognised as a major limiting factor to the success of RT for lung tumours, inducing uncertainties during imaging, planning, and delivery. Normally, all such uncertainties in combination with intrafractional tumour motion are compensated with large margins [12, 13, 14]. This, inevitably results in exposure of surrounding healthy lung tissue and other organs-at-risk (OAR) to often unacceptable levels of dose [11, 15, 16]. On the other hand, if healthy tissue toxicity is to be kept below permissible levels, insufficient dose would be delivered to the tumour [17, 18]. Furthermore, there is evidence from dose-escalation studies, which have reported improved local control and survival rates when higher doses compared to those of conventional fractionated (60 - 66Gy in 1.8 or 2Gy/fractions) are used [19, 20], although these gains may be compromised by the effects of respiration. This indicates the inability of existing modalities and treatment protocols to control the disease [3, 17, 21] and the need for improvement of local control.

Radiation therapy remains the main treatment modality for inoperable non-small cell lung cancer despite some progress with the use of other treatment modalities such as surgery and chemotherapy. Clinical studies have reported improved local controls and survival in patients with early-stage non-small cell lung cancer (NSCLC) treated with 3D-CRT, compared to conventional 2D RT [22]. On the other hand, the use of IMRT to treat tumours in the lung has largely been delayed due to concerns with the low dose tolerance of lung tissue, as well as organ motion due to physiological processes, namely respiration, and other changes in anatomy during course of treatment [4]. Although IMRT may be effective in minimising NTCP while maximising TCP, its sharper fall-off of dose and conformity requires high level of precision in tumour targeting during dose delivery [3, 9]. Therefore, it has been suggested that if IMRT is to be more effective in treating NSCLC, the integration of other motion management technologies with IMRT, such as respiratory gating and tumour tracking, should be explored [3, 4].

1.2 Motivation and Thesis Outline

The unpredictable nature of respiration and related uncertainties have presented a series of challenges to existing modalities for the treatment of mobile tumour in the lung. Subsequently, further improvements are still required to exploit their full potential. This has prompted the development of motion management technologies, such as more representative imaging systems and treatment techniques. Among existing techniques, respiratory gated radiotherapy (RGRT) has gained increased popularity recently. RGRT has the potential to reduce motion-induced irradiation of healthy lung tissue, which may in turn allow for the reduction in treatment fields and ultimately dose escalation [23, 24, 25]. On the other hand, many clinical institutions have developed gated treatment techniques that rely on the monitoring of external surrogates to gate the delivery of treatment beams. Such technique is advantageous provided that the correlation between the external surrogate and the tumour

does not change in an unpredictable way throughout the treatment [26]. However, intra-/interfractional variations in internal tumour mobility as well as breathing patterns have been reported [27, 28], which may be the source of uncertainty. This in turn has caused much ongoing debate about how well the monitoring of the external surrogate can predict the internal tumour location. Therefore, it has been suggested that RGRT requires a verification system to ensure that the treatment scenario mimics the scenario observed during treatment planning [29, 30]. It is hypothesized that tumour tracking can play an important role to maximise the potential benefits of RGRT. This provided the impetus for this research.

In this work, the capabilities of a commercially available gating system were first tested to investigate its suitability for the compensation of respiration induced motion. The main objective was to simulate the effects of possible irregularities in tumour motion, which are observed in real treatment procedures, on the system's performance. In addition to this, for the first time the suitability and potential of a clinical tool, denoted PortalTrack, for treatment verification and markerless tracking of lung tumours in respiratory gated RT was investigated.

This thesis consists of 6 chapters. The first chapter introduces the role that radiotherapy plays to treat mobile tumours in the lung. **Chapter 2** gives a general background of the challenges presented by respiration and introduces some of the motion management techniques for its compensation. In **Chapter 3**, a respiratory gated study was conducted in order to give a preliminary insight into gated beam delivery. Both regular and irregular tumour trajectories were simulated and their effects on dose distributions assessed by means of film dosimetry. In **Chapter 4**, the suitability and potential of a clinical tool, denoted PortalTrack, for tumour position verification during gated RT was investigated. In **Chapter 5**, the suitability of the approach presented in Chapter 4 is evaluated with a clinical case study. Lastly, **Chapter 6** concludes this thesis by summarising the main results and pointing out future developments.

Chapter 2

Respiration Management

Radiotherapy (RT) of tumours located in the thoracic and abdominal region is associated with a series of complex geometrical uncertainties, such as setup errors, respiratory motion, intra-/interfractional variation and anatomic changes due to treatment response, which can act during treatment preparation and execution [10, 14, 18]. In the case of patients suffering from tumours in the lungs, respiratory motion has been regarded as a major source of uncertainties which degrades the accuracy of RT at all stages of the treatment workflow [18, 31]: imaging, treatment planning and delivery. Consequently, leading to poor locoregional control and treatment outcome, which is correlated with poor survival rates [21].

To date, much research and development has been directed towards accounting for respiratory motion. With the advent of recent technological advances several treatment techniques have been proposed and are available with the attempt to take into account the limitations presented by respiration motion. This, has led to an improved identification, quantification and integration of uncertainties into treatment workflow of external-beam RT for lung carcinoma. In principle, a full characterization of all such deviations as well as their respective integration into the planning process should facilitate the generation of optimal treatment margins. In section 2.1 and 2.2 an analysis of tumour motion is given. This is followed in section 2.3 by introducing some techniques for its management, and then in section 2.4 by outlining some issues associated with their use.

2.1 Tumour Motion

Numerous studies have been directed towards assessing, characterising and quantifying the magnitude of respiration induced tumour motion in lung tissue [13, 27, 32], as well as, its dosimetric impact [33, 34, 35]. Understanding the behaviour of tumour motion may potentially lead to the design of more representative and robust models of tumour movement [27, 36], and ultimately its prediction [37], which will allow for its better integration into the treatment workflow and adaptation, and thus, improving the accuracy and effectiveness of RT for mobile tumours in the lung.

Besides cardiac, muscular and peristaltic activity, which have been also reported to contribute to organ motion [18, 27], respiratory activity has been regarded as the major source of motion for tumours in pulmonary region with motion amplitudes over 2 cm reported in

the literature [13, 27]. Studies such as those conducted by Seppenwoolde *et al.* [27] and Shirato *et al.* [32], where the investigators used fiducial markers implanted in or near the tumour, which were imaged in 3D via stereoscopic diagnostic x-ray fluoroscopy, have indicated that tumour motion in the superior-inferior (SI) direction is more pronounced compared to motion in the anterior-posterior (AP) and left-to-right (LR) directions, as shown in figure 2.1. This was observed, specially for tumours located in lower lobes and not attached to rigid structures, compared to tumours located in other sites. Moreover, the exhalation phase appeared to be more stable and last longer than the inhalation phase. Hysteresis in the tumour trajectories, which is the different motion paths the tumour follows during inhalation and exhalation, was also observed [27], suggesting that it may be due to the asymmetry in the coupling two driving mechanisms, the diaphragm and intercostal muscles in the ribcage, involved during respiration; or due to the lung's dynamic properties so that due to the elasticity of lung tissue, which can be further impaired by pulmonary diseases (emphysema, fibrosis), the tumour motion lags behind (delayed) relative to the motion of chest wall or diaphragm [27].

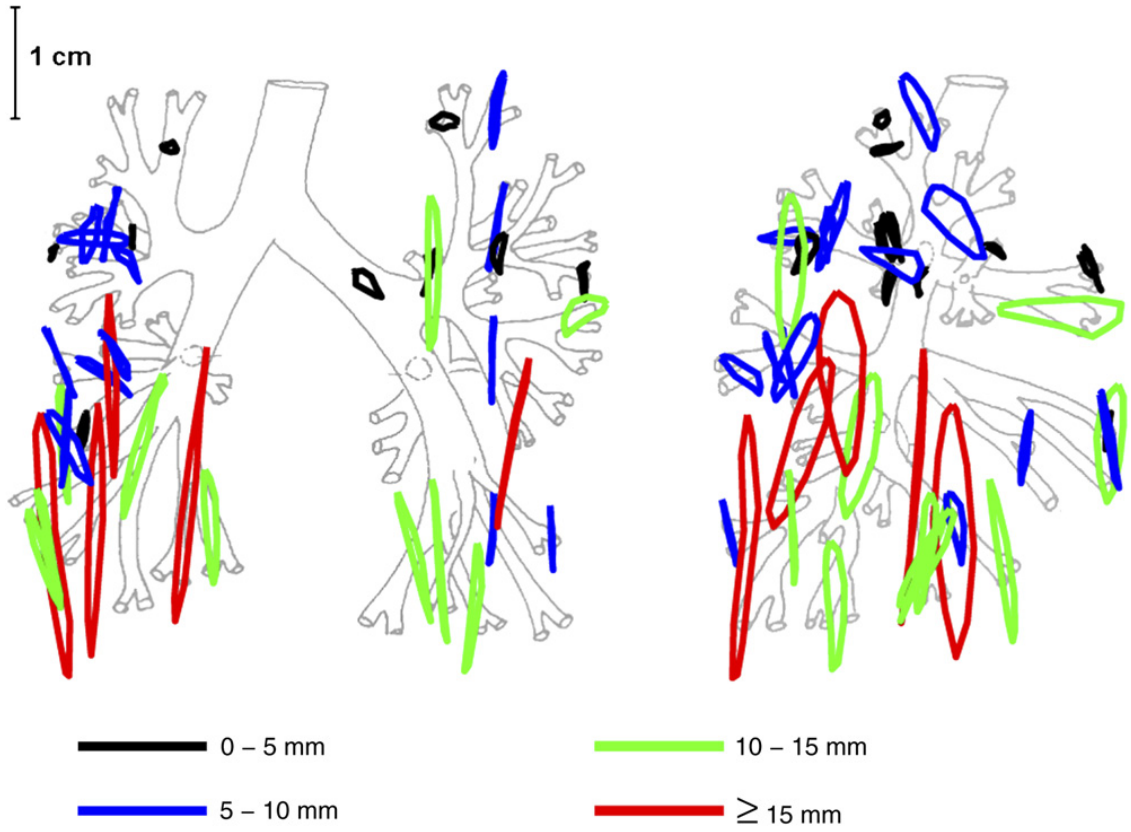

Figure 2.1: *Position and shape of trajectories of 23 tumours on the coronal (left) and sagittal (right) plane measured with implanted marker and real-time fluoroscopy. This illustration shows that tumour motion is more pronounced in the superior-inferior direction for tumour located in lower lobes compared to tumours in upper-lobes. (Figure taken from Sonke et al. [38])*

In addition to this, significant intra-/interfractional variations in tumours' paths as well as

in breathing level and intensity, are also described in the literature [26, 27, 28, 32, 34, 38, 39]. These studies have reported tumour motion variations in amplitude, period, mean (baseline drifts) and in inhale/exhale (exhale/inhale fluctuations) position. Furthermore, the correlation between the occurrence/magnitude of tumour motion and tumour size, location and pulmonary function has been observed to be controversial among studies. These observations have led to the conclusions that there are no general patterns of respiratory behaviour that can be assumed prior to treatment, suggesting that tumour motion should be characterised and assessed individually for each patient [18]. Therefore, because of the above-mentioned variations in the tumour trajectories, with clinically observed variations, i.e., baseline drifts, tumour motion can not be easily modelled by a simple function [34], such as in the case of a popular model described in the work of Shirato *et al.* [27]:

$$S(t) = S_o - Acos^{2n}(\pi t/T - \phi) \tag{2.1}$$

where S_o is the tumour position at exhalation, A the peak-to-peak motion amplitude, T the period of breathing cycle and ϕ the starting phase. n is an integer, taking normally values between 1-2, which makes the function model the fact that the tumour spends more time at the exhale compared to the inhale position.

2.2 Respiration-induced Uncertainties

2.2.1 Systematic and Random Uncertainties

Geometric uncertainties induced by respiratory motion can be modeled as the combination of systematic and random components, which can take place intra-/interfractionally [34, 38, 40]. The systematic component can be defined as errors that are introduced during the preparation phase of treatment, i. e. imaging artifacts leading to erroneous target definition/and delineation due to the use of a non-time resolved CT, which will affect all fractions throughout the treatment in the same way. The random component can be thought of as uncertainties introduced or acting during execution phase of treatment, i.e., daily patient setup and intrafractional motion, with day-to-day variations in magnitude and direction [10, 14].

External-beam RT of lung cancer is a form of localised treatment [17] that demand as a prerequisite high geometrical accuracy for its success. However, owing to the treatment workflow [9] and fractionated nature associated with the treatment of mobile tumours, respiration and its variations can present a series of limitations at each stage of treatment process [18]: (*i*) imaging, (*ii*) treatment planning and (*iii*) delivery.

Imaging and Treatment Planning

Accurate imaging is a prerequisite for accurate treatment planning and delivery [21]. However, respiration-induced motion during initial image acquisition can give rise to a series of

imaging artifacts, which may in turn translate into treatment planning uncertainties, leading to a poor definition of microscopic spread of the tumour, degrading target/normal tissue delineation accuracy [18, 41]. Delineation uncertainties are purely systematic (affect all fraction in same way) [10], and have adverse affects on the selection of safety margin and dose calculation during treatment planning.

Different imaging artifacts observed during conventional (non-time resolved) computed tomography, i.e. partial volume effect (image distortion) and image blurring, have been reported in the literature [10]. Moreover, although it is undeniable that the introduction of 4D computed tomography (4DCT) into clinical routine has improved image quality, providing time-resolved data sets with reliable spatial-temporal information of patient anatomy, there are some residual errors which still remain. For example, the patient may breath at a different level during delivery than of during imaging [34], or the tumour will be targeted at another arbitrary position that had during imaging [10]. Furthermore, variability in tumour motion, such as changes in mean tumour position (baseline drift), have added an extra degree of complexity to time-resolved imaging modalities that account for the effects of respiration. Baseline drifts are not visible under 4DCT as reported in the work by Sonke *et al.* [38].

Set-up

Tumour motion influence both systematic and random setup errors [10, 13, 14]. Van Herk *et al.* [10] reported that motion of skin relative to internal organs was a major limiting factor preventing reproducibility of patient setup. With the systematic component mainly due to the patient setup with regards to skin markers during imaging, whereas the random component due to day-to-day variations in the reproducibility of the patient setup during delivery. Recent Image-guided setup protocols, such as those using cone-beam CT (kV and MV) imaging, have the potential to reduce systematic and random errors [11, 40]. Studies by Wolthaus *et al.* [40] and Guckenberger *et al.* [11] have indicated that by targeting the soft-tissue tumour itself (using kV CBCT) and bringing its mean position to isocentre prior to delivery, the systematic component can be largely eliminated, leaving the random component unattended (intrafractional tumour motion), which can be considered as random error, requiring smaller margins for its compensation.

Delivery

Dose delivery in the presence of intrafractional motion leads to dose blurring over the direction of motion, which is the dominant effect on dose distributions [33], resulting in underdosage in the tumour and overdose of surrounding healthy tissue and other organs at risk (OARs). Interfractional motion, such as in the case of systematic changes in mean tumour position (baseline drifts) [18, 34, 42], on the other hand causes a shift of dose distributions relative to its planned position [18]. In addition to this, respiration may also lead to spatial deformation of dose distributions, such as, interplay effects [33] during IMRT. Moreover, asymmetric deviations in the shape of dose distributions are also possible, which are not negligible for motions amplitudes 10 mm, requiring nonuniform margins for compensation, as discussed in the work by van Herk *et al* [43].

Overall, the dosimetric implications are such that random errors results in blurring of dose distributions while systematic uncertainties result in a shift of dose distributions relative to its planned position [10, 14, 34, 40], as shown in Figure 2.2 (b). More importantly, the magnitude of the shift may in some cases lead to marginal miss of target in the way that the tumour moves away from the high dose region, which is a major limiting factor for motion management techniques designed to facilitate the reduction of treatment margins, such as gated radiotherapy, which will be discussed in section 2.3.3. Furthermore, it has been noted in the literature that effects of systematic errors on dose distribution are greater than those of random errors, which may require 3 to 4 time larger margins than random errors [10].

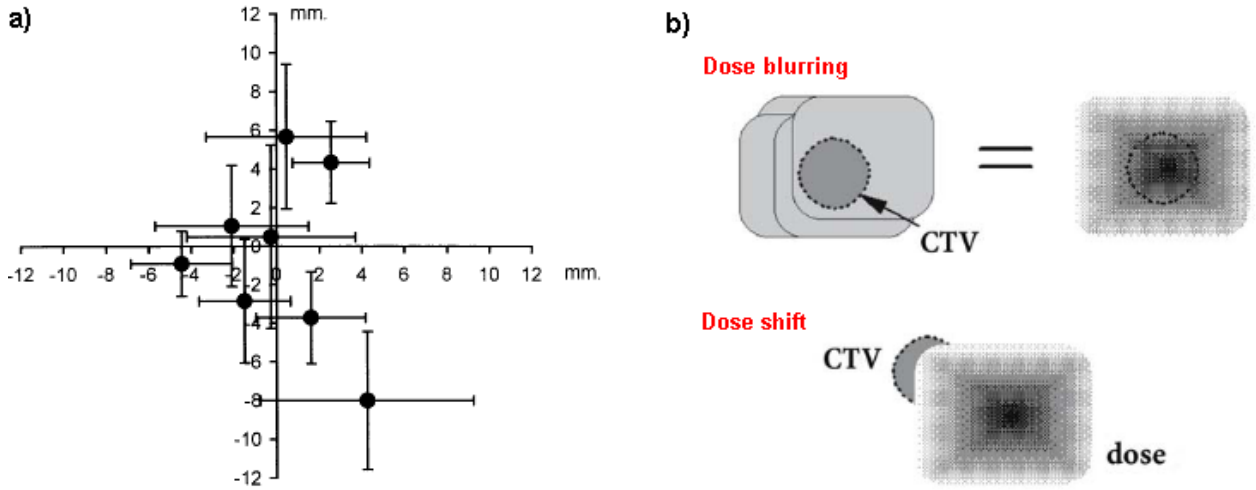

Figure 2.2: *(a) Systematic uncertainties in mean positions (black dots) and random errors represented by the deviation about mean (error bars). (b) Random errors lead blurring while systematic errors lead to a shift of the dose distribution* (Figures taking from Ekberg *et al.* [13] and van Herk *et al.* [14])

2.3 Management of Respiration-induced Motion

2.3.1 Rationale for Control of Respiration

External-beam RT of lung cancer is a form of localised treatment [17] that demand as a prerequisite high geometrical accuracy for it success at all stages of treatment workflow: imaging, treatment planning and dose delivery. However, as described above in section 2.2, different uncertainties are inherent in the treatment process, which degrades the accuracy and effectiveness of RT. Typically, all these uncertainties are compensated with large margins [12, 13, 14]. This, in turn increases the exposure of surrounding healthy lung tissue and other OAR to high levels of toxicity [11, 15, 16] increasing the normal tissue complication probability (NTCP).

Furthermore, the increase in data which support the dose-response relationship has provided the grounds for the consideration of the use of doses higher than those used conventionally for treatment of tumours in the lung with RT. Different escalation dose studies

have reported improved local control and survival rates when applying doses higher than conservative doses of (60 -66 Gy) [3]. Dose escalation requires high precision in targeting of tumours. However, this dosimetric gain can be obscured by limits imposed by normal tissue complications [4]. Moreover, dose escalation can be potentially even more detrimental compared to conventional doses in case of geographic miss of the tumour caused by error induced by respiration during dose delivery.

The challenges presented by respiration have prompted the development of more representative imaging modalities, as well as delivery techniques to mitigate the effects caused by respiration and hence improve local control of tumours in the lung. The following section is limited to introduce the motion management approaches that were used for this thesis.

2.3.2 Treatment Planning Solutions

Arguably, technological advances have enabled the development of sophisticated treatment systems and techniques, such as the Mitsubishi real time radiation therapy (RTRT) system developed by Shirato *et al.* [44], which have shown superior accuracy and management of pulmonary tumours, compared to other treatment modalities lacking of direct monitoring of the tumour during dose delivery. However, such high-precision systems are not yet an off-the-shelf available technology for most clinical institutions due to increased expenses associated with their clinical implementation [45]. Subsequently, treatment planning solutions, regarded as motion-encompassing methods [18, 41], for motion compensation have been developed, which are of relevance for clinics lacking of dedicated respiration management devices. On the other hand, some studies have proposed that it may be sufficient to account for intrafractional tumour motion during treatment by applying motion-encompassing methods [18, 41]. However, these techniques rely on the robustness of imaging, with reliable spatial-temporal information regarding the patient's internal anatomy over breathing cycle, such as in the case of 4DCT, for treatment planning.

The International Commission on Radiation Units (ICRU) Report No 62 [12] guidelines for determining the volumes have been applied to the treatment of mobile tumours in the lung, as shown in figure 2.3. The gross tumour volume (GTV) is the gross demonstrable extent of malignant growth, which consists of the primary tumour and possible other metastases where the tumour cell density is the greatest. The clinical target volume (CTV) is the tissue that contains the GTV or area believed to harbour the micrometastasis. The PTV is the geometrical concept, defined to select the appropriate beam arrangements and sizes to ensure that the CTV receives the prescribed dose, which is defined by adding extra margins to the CTV to compensate for set-up uncertainties (i.e. patient positioning and alignment of treatment beams during treatment planning and delivery), as well as internal geometric variations (i.e., motion induced by physiologic processes). This gives rise to the internal target volume (ITV), considered as an intermediate to construct the PTV from CTV. This is an extention of the CTV that has been added to explicitly compensate for the movement and variations in the shape of the tissue contained in or adjacent to the CTV, such as motion due to respiration, heart beat, and movement of the bowels [12].

Figure 2.3: *Definition of treatment volumes according to the ICRU Report 62.*

Moreover, the definition of the ITV by means of 4DCT has further enabled the generation of more representatives ITV for treating tumours in the lung. 4DCT data sets can be analysed to determine the tumour motion range for treatment planning and the relation of tumour motion to other organs. This in turn has allowed the characterization and design of patient-specific treatment volumes and dose conformity compared to population-based isotropic margins.

2.3.3 Treatment Delivery

Respiratory-gated RT

Respiratory gated radiotherapy (RGRT) is a relatively new technique used to reduce and/or mitigate the effects of respiration-induced motion [3]. In RGRT, the delivery of radiation is synchronized to a specific portion of the respiratory cycle [3, 18, 41]. The delivery of gated beams can be synchronised to either a particular position in the respiratory cycle of the actual tumour/or substitute (amplitude-based gating), or phase of the respiratory cycle (phase-based gating) [3]. The onset and duration of the gating window relies on the respiratory signal, which can be acquired either externally by a sensor, i.e., pressure belt, optical reflector, or by fluoroscopy of internal fiducial markers. The respiratory signal is assumed to be representative of the tumour motion, from which information regarding tumour internal trajectory and phase over the respiratory cycle can be inferred. Normally, a duty cycle, which is the ratio of beam-on to total treatment time, between 30% to 50% is used [18, 29, 41]. The gate is set to the portion or phase of the breathing cycle where motion is observed to the least and/or more stable and reproducible position, i.e. end-of-exhalation phase.

Depending on the type of surrogate used to acquire the respiratory signal, gating systems can be classified into external-/internal-based gating [29]. Internal based gating is an invasive treatment approach that uses internal surrogates (fiducial markers) implanted in or near the tumour site, which are tracked by either on-board or external fluoroscopic kilovoltage (kV) x-rays systems, to derive the tumour position and guide the delivery of gated treatment beams [18]. One example of such system is the Mitsubishi/Hokkaido real-time tumour tracking system (RTRT) developed by Shirato *et al* [44]. On the other hand, gating based on external surrogates is a non-invasive technique that relies on external respiratory monitors to indirectly derive an estimate of the internal tumour position [18, 29, 46, 47]. Based on the acquired respiratory signal the delivery of treatment fields can be either phase/or amplitude gated. Different research groups have investigated several external surrogates for deriving tumour position [46], and developed techniques based on the type of surrogate employed. Two widely commercialized systems [48] are : *(i)* the real-time position management (RPM) respiratory gating system (Varian Medical Systems, Palo Alto, CA); *(ii)* the ANZAI respiratory gating system (Anzai Medical, Japan). Both systems rely on the external monitoring of the abdominal wall motion, mainly limited to the 1D anterior-posterior direction, to provide a correlation of the tumour position. Figure 2.4, shows some of the major components of the Anzai gating system which was used for work. The operation of this system will be described in section 3.1.2.

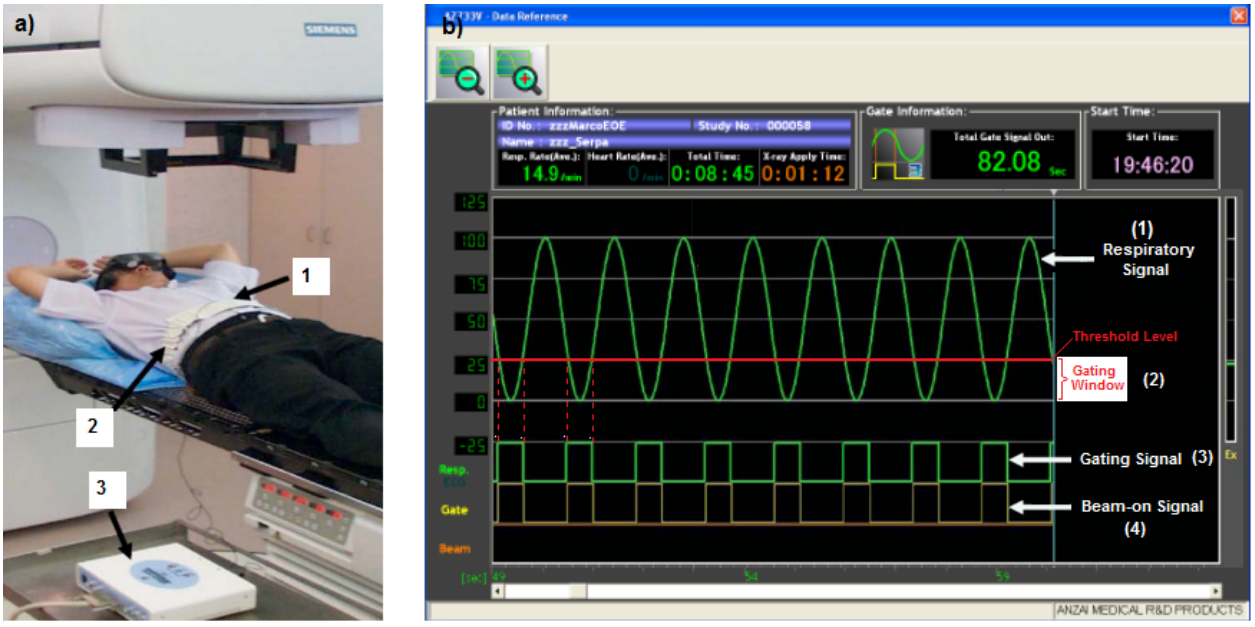

Figure 2.4: *(a) The Anzai gating system with a pressure sensor a(1), belt a(2) fastened around patient to record the respiratory signal, and sensor port a(3). In (b), the display window showing the respiratory signal b(1), gating window b(2), gating signal b(3) and beam-on signal b(4).*

Tumour Tracking

Real-time tumour tracking is one of the most advanced motion compensation methods for the management of respiration induced tumour motion [9]. In an ideal RT procedure, dose delivery would be dynamically shifted to accommodate or follow intra-fractional changes in tumour position. This will eliminate the need for additional margins, otherwise required to compensate for intrafractional tumour motion, maximizing dose delivery efficiency by maintaining a 100% beam-on duty cycle [18, 49]. To accomplish this, a tracking system should be able to [16, 49]: (*i*) image the tumour/ surrogate [50], (*ii*) determine or track tumour position directly [16] or indirectly [51], (*iii*) predict tumour position to allow for system's mechanical and computational delays [37], and (*iv*) adjust treatment parameters. All this has to be conducted in real-time.

Existing methods for the determination of target position can be grouped into three categories [39, 52]: external surrogate based [24, 51]; internal surrogate based (implant markers) [44, 53]; and markerless [16]. The information regarding tumour position is then coupled through a control loop to repositioning system that will adjust or shift the position of the beam relative to the moving target [49]. This can be accomplished, either by adjusting the MLCs, such as in the case of Dynamic MLC delivery; or by shifting the treatment table with a robotic couch [42]. An example of such dedicated systems, which is relevant to this thesis (chapter 4 and 5), is the Wuerzburg Adaptive Tumour Tracking System (Figure 2.5).

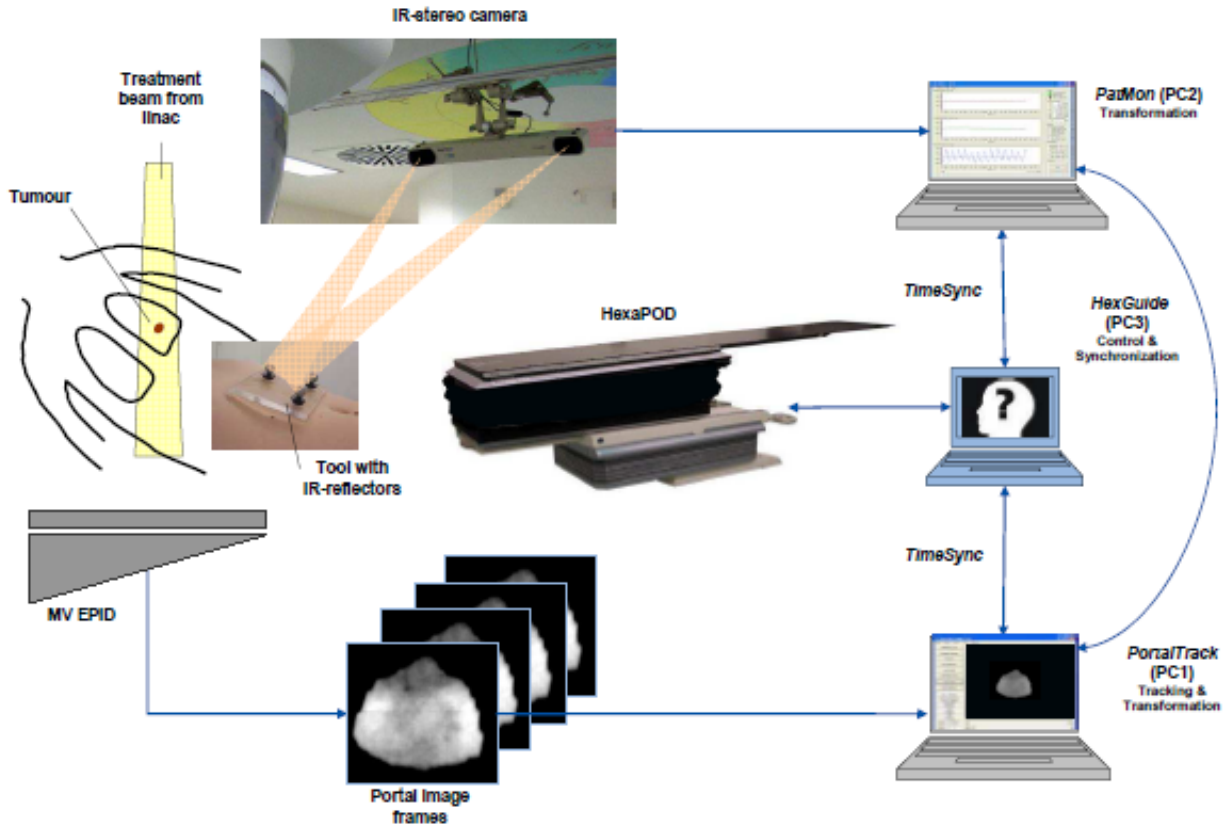

Figure 2.5: *Schematic representation of the Wuerzburg Adaptive Tumour Tracking System.*

The objective of this system is to compensate tumour motion in real-time by repositioning the patient, using a HexaPOD robotic couch with six degrees of freedom, relative to the stationary treatment beam. Repositioning of the couch is guided by 2 independent means. Megavoltage imaging, in which the tumour is automatically tracked in images acquired with the electronic portal imaging device (EPID) without the aid of markers using a dedicated tracking software, denoted PortalTrack, whose suitability for the verification of RGRT will be investigated in chapter 4 and 5. At the same time the external signal is obtained by tracking optical markers placed on the patient abdomen by an infrared camera (external signal). Both the internal and external signals are sent to a control system, which is used to predict the future tumour position. Using the prediction, appropriate repositioning commands are sent to the HexaPOD [42].

2.4 Issues with Motion Management Techniques

It is difficult and technically challenging to determine the tumour position directly, one has to rely on monitoring surrogates (external/internal) for tumour motion, i.e., abdominal wall, diaphragm, which are assumed to closely correlate with the actual tumour motion [18]. If a surrogate of tumour motion is used for the purpose of beam gating or tumour tracking without being able to directly monitor the tumour, and because of the above-mentioned variations in tumour motion that may take place intra-/inter-fractionally, this may result in uncertainties in the mechanical coupling between surrogate and tumour.

With regards to RGRT, although internal-based gating modalities allow the direct and more accurate internal localization of the tumour in 3D with improved image contrast and high sampling rate, compared to megavoltage imaging, day-to-day migration of markers is also possible [32]. As a result of this, more than one marker is required to measure their displacement relative to each other and hence rule out the possibility of marker migrations. This in turn increases the risks of infections, i.e. pneumothorax [49]. Another concern is the additional patient exposure to radiation dose during fluoroscopic tracking of markers, which is to have a greater impact on longer treatment session, such as in the case of hypofractionated RT, resulting in clinically unacceptable accumulative levels of imaging dose to patient [29, 49]. Because of the invasiveness, complexity and expenses associated with this procedure, many clinicians are reluctant to adopt this technique in clinical routine [15].

In the case of motion management modalities that rely on the monitoring of external surrogates, i.e., external-based gating, for deriving tumour position, the degree of internal(tumour)/external(surrogate) correlation represents the major source of geometric uncertainty. It is not clear how accurately the external surrogate represents the extent of internal tumour motion [3]. For example, the linear 1D motion of the abdominal wall may not accurately reflect the internal 3D tumour motion.

Effects of Correlation Variations

In the case of external-based gating, it has been identified that in clinical cases most patients exhibit unsynchronised amplitude variations, baseline drifts and time shifts between internal tumour motion and external surrogate signal [45, 46, 47, 54]. Figure 2.6 gives examples of

discrepancies in the correlation between the internal tumour and external surrogate, which may arise during external-based gating, reported in the work of Wu *et al.* [47].

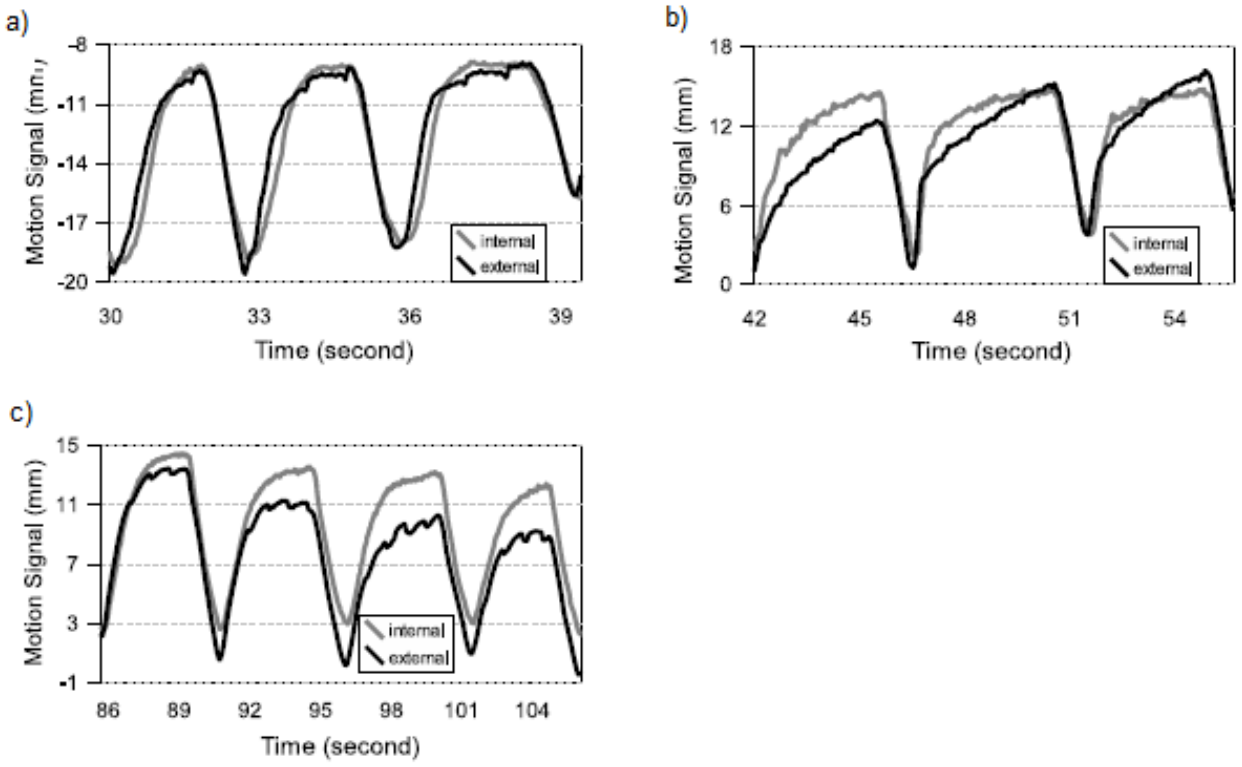

Figure 2.6: *Examples of discrepancies in the correlation between the internal/external signals with phase shifts (a), baseline drifts (b) and amplitude variations (c). (Figure taken from Wu et al. [47])*

Furthermore, it has been documented that the presence of intra/interfractional variations in tumour mobility and patient's breathing pattern and reproducibility further degrades the degree of internal/external correlation, decreasing the accuracy and effectiveness of RGRT. Such types of variations add uncertainty and delay to treatment, which can lead to false positives and false negative [29, 47]. During a false positive event the radiation beam is on while the tumour is out of the gating window (marginal miss) while during a false negative the beam is off while the tumour is inside the gating window. The clinical implications are such that during false positive more dose is given to healthy tissue and other critical structures whereas false negatives prolongs treatment, which in turn may lead to underdosage of the tumour. Variations in the external breathing levels and patterns a patient may be identified by only monitoring the breathing signal during treatment, and once a irregularity is identified the treatment can be interrupted. However, accounting for variations in the internal tumour trajectories during treatment, a clinical tool is required in which breathing-induced tumour motion can be imaged and quantified to the extent that variations such as baseline drifts and shifts can be identified [45].

2.5 Summary

This chapter introduced some of the major issues presented by respiration and related uncertainties, which limit the success of radiation therapy of tumours in the lung. Motion management techniques play an important role in the compensation of respiration-induced motion. One of these newly emerging techniques, which is being commercially implemented worldwide, is RGRT. RGRT holds promise to reduce the incidence of healthy tissue toxicity and improve the TCP. However, there is some controversy with existing gating techniques that has been reported in the literature and, which needs to be addressed. In the next chapter, the suitability of RGRT to mitigate the effects of respiration-induced motion will be investigated.

Chapter 3

Respiratory-Gated Study

This investigation is part of the University Medical Center Hamburg-Eppendorf (UKE)'s preliminary research on RGRT for its potential implementation into clinical routine. RGRT is a relatively new treatment technique for the management of mobile tumours in the thorax and abdomen [18, 24]. It has the potential to mitigate the effects of respiration induced motion, reducing the incidence of healthy tissue toxicity by facilitating the reduction of treatment fields, which may ultimately allow for dose escalation [23, 25]. Although external based gating systems are commercially available, there are some issues as to how well monitoring an external surface correlates to the internal tumour motion, which has discouraged many users [46, 47, 54]. Therefore, it is essential to conduct an assessment of the performance of such systems in order to identify their capabilities and limitations before they are introduced into the clinical routine. This may then lead to the design of treatment protocols, such as to establish criteria to select patients, i.e. patients with regular breathing, who are to benefit the most from this technique and those that might not, i.e. patients with irregular breathing.

For this study an external-based gating system (Anzai AZ-733V, Anzai Medical Solutions, Japan) was available and its suitability to reduce the effects of intrafractional breathing motion on dose distributions investigated. In addition to this, its performance under the influences of discrepancies in the correlation between the internal target motion and the external signal, which has been acknowledged as a major source of uncertainty for such treatment modalities and become the source of much debate [30, 45, 46], was also explored. This was accomplished by means of phantom studies and film dosimetry.

3.1 Method and Materials

3.1.1 Motion Phantom

An in-house developed motor-driven motion phantom, consisting of a movable wagon carrying a stack (9 cm x 7 cm x 7 cm) of water equivalent RW3 (PTV, Freiburg, Germany) plates each 1 cm thick, was used for the simulation of a series of periodic trajectories (see Figure 3.2(c)). This phantom has the ability to simulate coupled motions in two dimensions (2D) along the anterior-posterior (AP) and superior-inferior (SI) directions, with adjustable user-defined amplitude (A) and period (T) of oscillations. The motion patterns are generated by the rotation of eccentric discs, designed based on observed 4DCT data of patients with lung

tumours [55]. In addition to this, a contrast material (with a diameter 2 cm and thickness of 2 cm), serving as tumour substitute, was built-into the stack of plates (see Figure 3.1 and 3.2). The centroid of tumour surrogate was designed to be located at position x = 3.5 cm; y = 4.5 cm; and z = 4 cm relative to the stack of plates (between plates 4 and 5). The ICRU reference point was set to this point. Overall, all the motion patterns generated by the dynamic phantom are transmitted to the tumour substitute, which is moved in 2D in both the SI and AP directions and in synchrony with the motion phantom. It is worth indicating that this tumour substitute was originally designed for the purpose of running tumour tracking simulations, which will be discussed in the next chapter, due to its high contrast. Only for consistency in the overall aim of this work the same contrast material (tumour substitute) was used for this gated study.

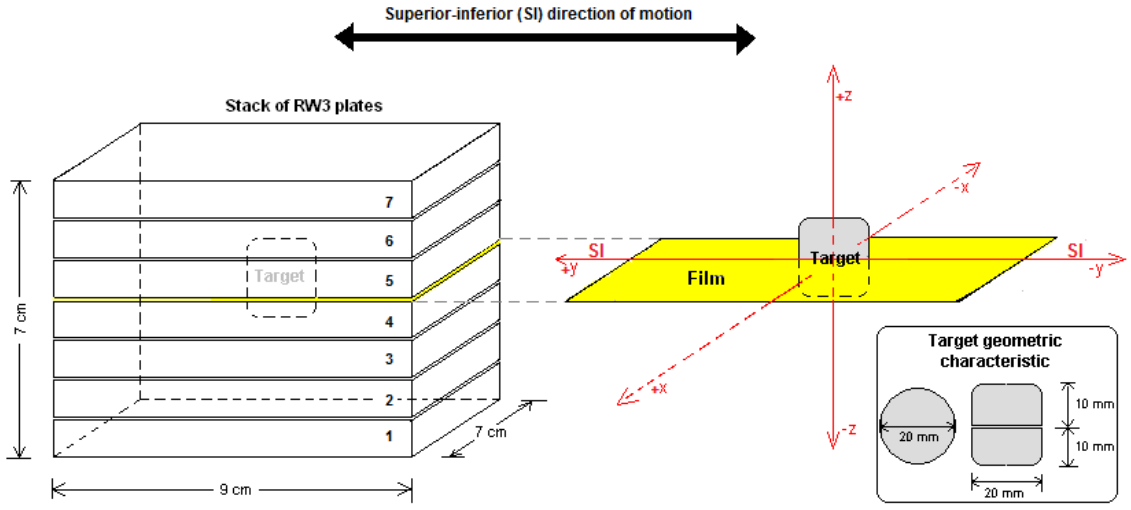

Figure 3.1: *Stack of water equivalent RW3 plates with tumour substitute embedded within it. Film was placed on a reference plane, with the ICRU reference point set to centroid of the tumour substitute, which was in the plane of the film.*

Target Paths

Different sinusoidal motion paths of tumour substitute were defined by a given peak-to-peak motion amplitude (A) and period (T) of oscillation. This study was only concerned with motion in the SI direction since it has been indicated to be the predominant direction of motion observed in clinical cases [13, 18, 27, 32], as well as, with relatively large motion amplitudes (A $\geq$ 10 mm) of the tumour substitute (target). The justification for the simulation of large motion amplitudes for this experiments are based on the literature [11, 34], which has suggested that gated RT is of more relevance for the treatment of tumours exhibiting large motion amplitudes. In a study by Engelsman *et al.* [34] the investigators noted that the relationship between the margins required for the compensation of intrafractional motion was not linearly proportional to the peak-to-peak motion amplitude (A), but quadratic. It was observed that small margins ($\leq$ 2 mm) were sufficient for the compensation of breathing amplitudes $\leq$ 10 mm. However, for motion amplitudes $\geq$ 10 mm these margins would

increased rapidly (quadratically). In a more recent study, Guckenberger *et al.* [11] also reported a quadratic relationship between tumour motion amplitude and the margins required for the compensation of cumulative dose loss to treatment planning volumes as result of respiratory induced tumour motion.

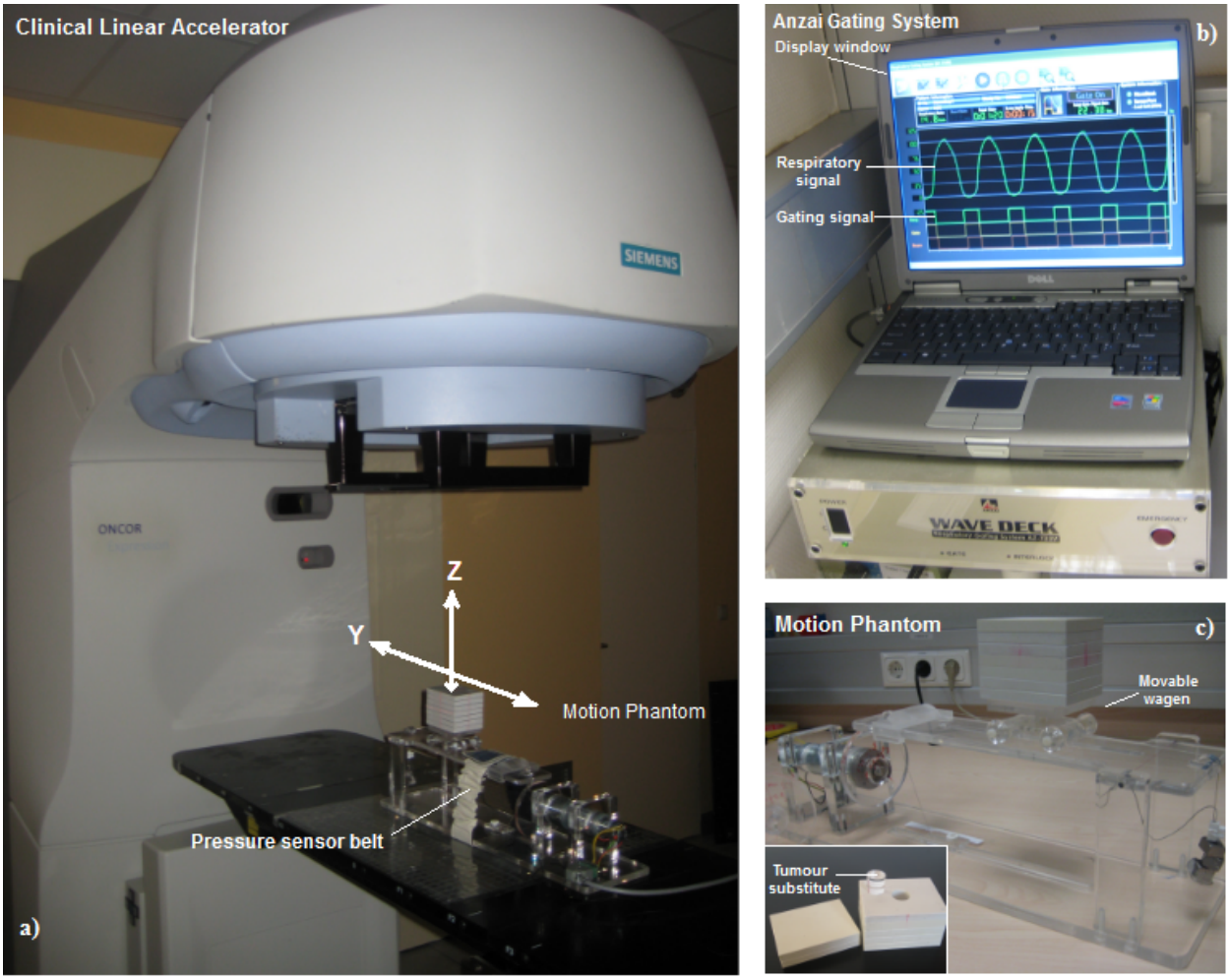

Figure 3.2: *(a) The orientation of room coordinates with the motion phantom set at delivery position with pressure sensor belt fasted around the main platform to acquire the 1D respiratory signal used to gate the linac, (b) the Anzai display window monitoring the respiratory signal which was used to direct the onset of gating signal sent to the linac, and (c) the major components of motion phantom with the tumour substitute to be irradiated*

3.1.2 Gated Delivery

The Anzai gating system, which is commercially available, was used to monitor respiratory motion and gate the delivery of treatment fields on a linear accelerator. This system uses a pressure sensor belt to monitor the external respiratory patterns (pressures changes) in real-time. The pressure sensor belt was placed around the main platform where the movable wagon rests (see Figure 3.2(a)). This platform was only exposed to changes in position along

the AP direction, which at the same time was responsible for the AP motion component of the tumour substitute. This way, the pressure sensor was only limited to detect changes in motion along the AP direction resulting in a 1D signal (breathing signal). In a real clinical procedure, the belt is normally placed around the patient's abdomen and let to monitor changes in the abdominal wall of the patient, resulting in an 1D signal, which is used to trigger the accelerator during gated treatment or for slice sorting during image reconstruction in 4DCT.

This signal is transfered to the sensor port and then to a processing deck where it is digitized and then input into the control computer for display and definition of gating parameters. In the display console, the respiratory signal is displayed between a 0% to 100% range, spanning from the end-of-exhale (EOE) to end-of-inhale (EOI) phases of respiration. To gate the linac, a gating window was defined on the external signal by setting a predefined amplitude threshold level on the respiratory signal, defining a range of the respiratory signal. Any time the signal falls below the threshold of the gating window the linac is ON (beam-on time); otherwise OFF. Gating windows of different sizes can be defined by setting different amplitude levels (between the 0% to 100% range) on external signal, as shown in Figure 3.3. Applying a 100% gating level means that the gate remains on over the whole breathing cycle, whereas for instance a 75% gating level means that the gate remains open for the 75% range of breathing signal.

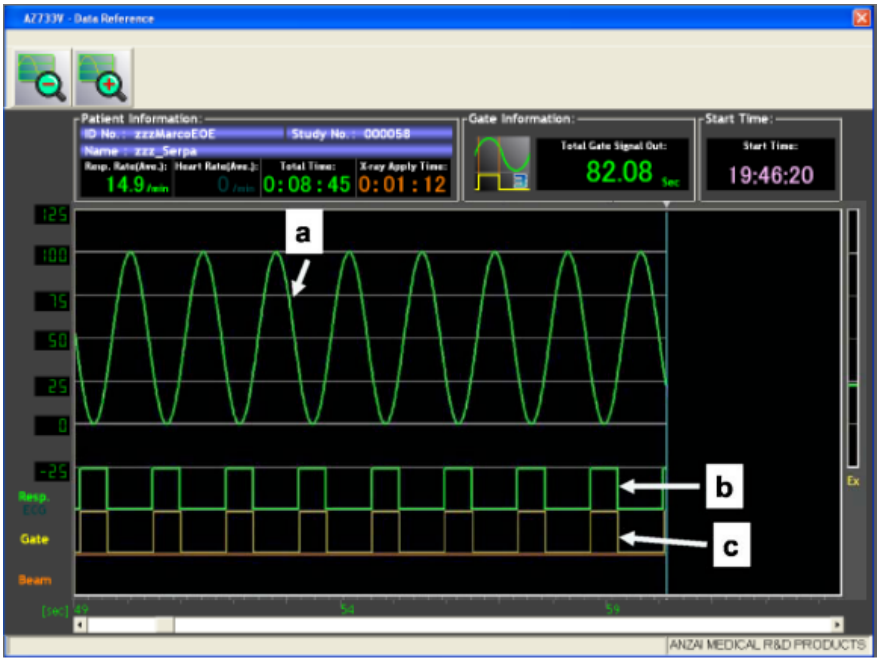

Figure 3.3: *Anzai display console showing the respiratory signal (a), the gating signal (b), and the beam-on signal sent to linac. The respiratory signal is normalized to 100%, with zero representing the EOE and 100 the EOI phases of respiration. For this example, a 25% amplitude threshold level was set to the signal with the gating window encompassing the EOE phase of respiration.*

For the phantom, the breathing signal (0% to 100% range), was equated to the total motion range (peak-to-peak displacement along SI direction) of target, which represented the longitudinal distance encompassed between the EOE and EOI positions of the target during dose delivery. Therefore there was a one-to-one (1:1) correlation between the changes in position of target and the breathing signal.

3.1.3 Treatment Planning

A 4DCT scan was acquired of the motion phantom with a helical 24-slice scanner (Somatom Sensation Open, Siemens Medical Solutions, Erlangen, Germany) together with a pressure belt sensor for generation of breathing signal. After the amplitude-based reconstruction of projections, eight phases were reconstructed. The recorded breathing signal was extracted from the system's data bank for analysis. The probability density function (PDF) of the signal, whose shape carries characteristic information of the motion signal indicating where the target spends more time, was used as criteria to select the corresponding phase from the 4DCT dataset for purpose of treatment planning.

The CT study corresponding to the EOE phase was chosen for treatment planning. A 6MV single-beam conformal plan was generated using the planning system XIO CMS, with the gantry set to 0° with beam direction perpendicular to the movement direction of the target in SI axis. The ICRU reference point was set to the centre of mass of the tumour substitute at a depth of 3 cm relative to stack of plates (see Figure 3.1). The MLCs were conformed to the geometry of delineated PTV with a field edge-to-PTV distance of 0.8 mm. The idea was to conform the 95% isodose level around PTV in the coronal central plane through the target centroid, delivering a prescribed dose of 2Gy to the ICRU reference point. Figure 3.4 shows the 4DCT data with the target contoured at both ends of the motion range between EOE(green) and EOI (red) phases of respiration. Note that both the target and the movable wagon move relative to the beam direction. The resulting dose dristributions obtained from treatment planning process are shown in Figure 3.5.

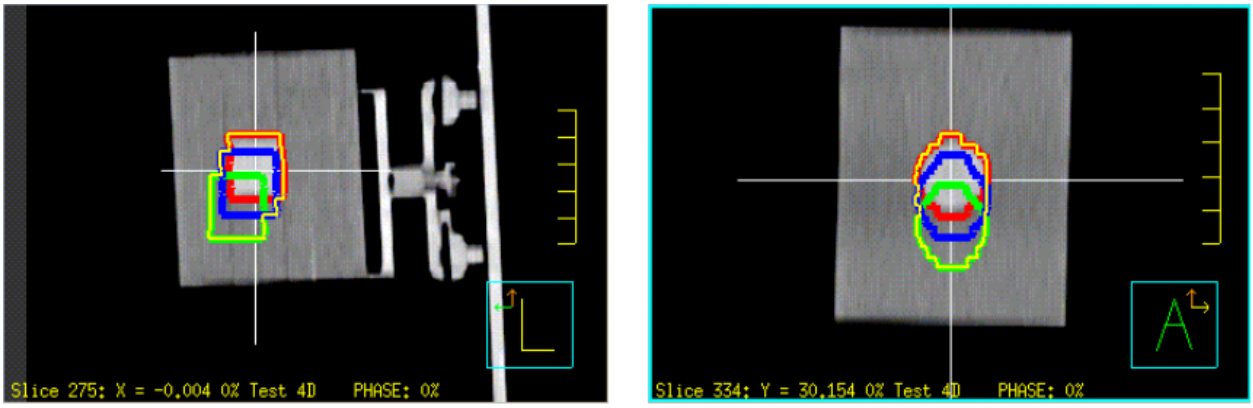

Figure 3.4: *4DCT of 2D phantom with tumour surrogate contoured at EOE phase (green), EOI phase (red), and middle phase (blue), and the internal target volume (ITV) encompassing the peak-to-peak excursion of the target (yellow).*

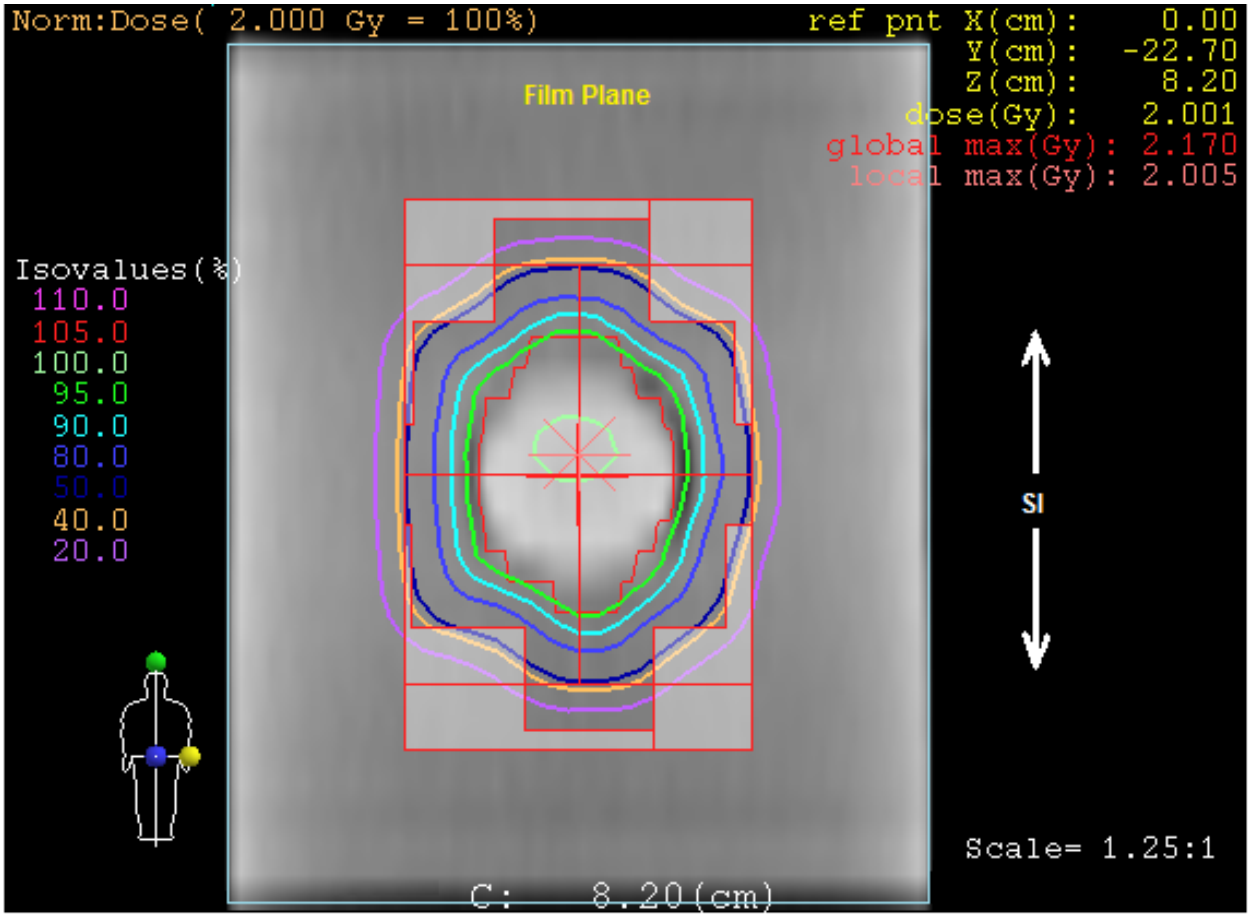

Figure 3.5: *The planned dose distributions in the plane of the film with the tumour substitute set at the EOE phase.*

3.1.4 Data Analysis

Film Dosimetry

Film measurements were performed in the coronal central plane, which contained (approximately) the tumour substitute's centroid, using GafChromic EBT2 films, as indicated in Figure 3.1. To convert the irradiated films to dose distributions a dose response curve was first obtained from one film for a pattern of nine 2 cm x 2 cm fields arranged in a 3 x 3 patter with a 1 cm gap between each field. Each field was irradiated with a different number of monitor units (MUs), corresponding to a dose range between 0.16 to 3.16 Gy (see Table 3.1). After irradiation the film was stored for 24 hours, during which the self-developing process took place. After this period, the film was digitized using a commercially available flatbed scanner Model ScanMarker 8700 (Microtek, Hsinchu, Taiwan). The scan was stored as 48 bit RGB images in the tagged image file format (TIFF). From this TIFF data file, the red channel was extracted and corresponding scan values, resulting from the 0.16 to 3.16 dose range, were obtained using in-house MATLAB (Mathworks, Inc., Natick, MA, USA) routines. A first order polynomial of first degree order was fit to the points, resulting in a dose response curve, as shown in Figure 3.6. The fitting of a first order polynomial and resulting dose response curve is a standard procedure, which is conducted at the Department.

Table 3.1: *Irradiated dose values to obtain the dose response curve*

Field	Dose (Gy)
1	0.16 ± 0.01
2	0.53 ± 0.01
3	0.91 ± 0.01
4	1.29 ± 0.01
5	1.67 ± 0.02
6	2.04 ± 0.03
7	2.44 ± 0.04
8	2.79 ± 0.04
9	3.16 ± 0.05

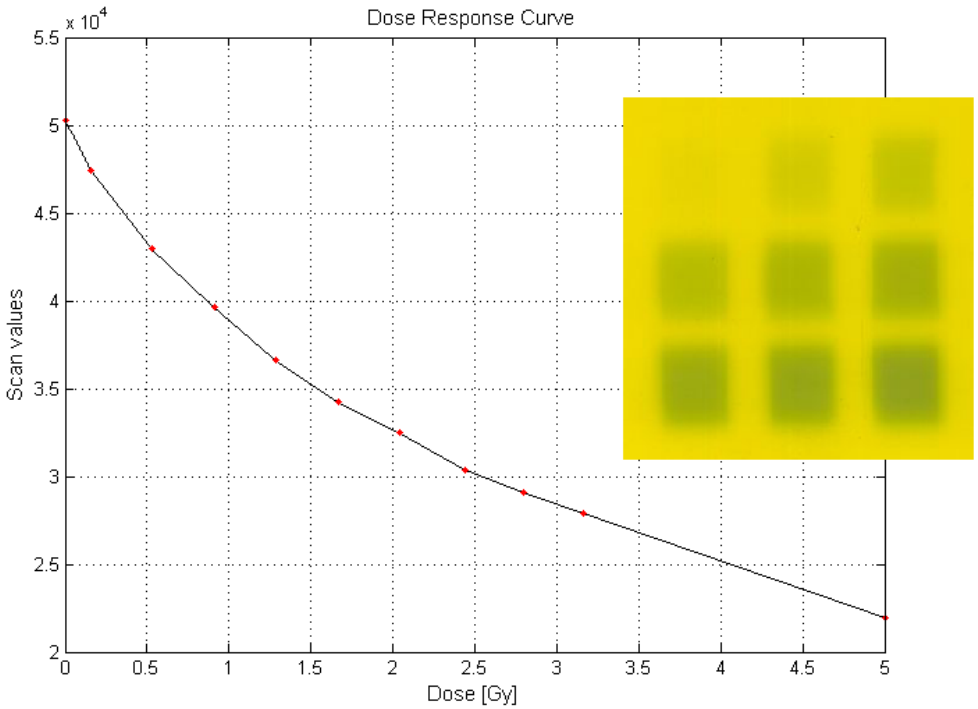

Figure 3.6: *Schematic representation of irradiated film with a pattern of nine 2 cm x 2 cm fields arranged in a 3 x 3 pattern, and resulting dose response curve*

All film measurements performed using the motion phantom were irradiated one at a time, digitized in the same way as described above, and converted by means of the dose response curve into a dose matrices (dose distribution), and retrospectively analysed. Figure 3.7 gives two examples of dose distribution extracted from irradiated films using the information from dose response curve and Matlab-based routines.

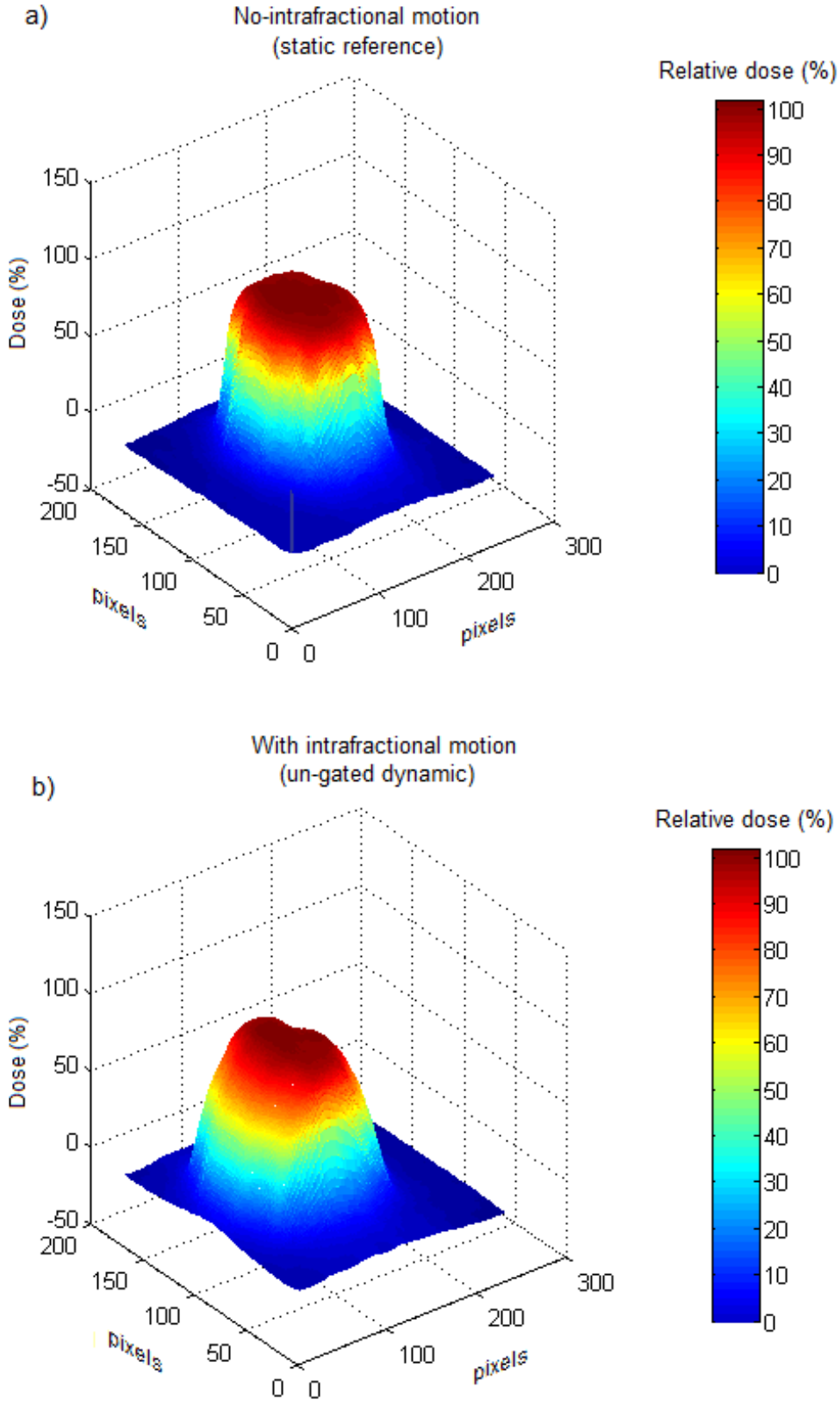

Figure 3.7: *Two examples of resulting dose distributions obtained from irradiated films in the absence (a), and in the presence (b) of intrafraction breathing motion simulated by the motion phantom.*

Dose Comparison Criteria

To evaluate the effects of intrafractional breathing motion the resulting dose distributions, obtained under the effects of different motion components simulated by the motion phantom, were compared against a reference dose distribution. This reference dose distribution was obtained from a delivery session having the tumour substitute stationary and set at its planned position, which modelled an idealised treatment procedure without the influences of breathing induced-motion on dose to the PTV. Note that initial comparisons between the planned and the measured reference dose showed a dose deviation of approximately + 2.5% between the two. Although this dose comparison was repeated 6 times (for 6 different irradiated films with target stationary at reference position), this dose deviation remained constant for all the 6 films. This was attributed to systematic uncertainties which may have been introduced throughout the experiment, i.e., scanner inistability and scanning artifacts, the small geometry of target and its set up, etc.

Differential Dose Area Histograms

To better appreciate the differences between dose distributions resulting from gated and un-gated dose delivery differential dose area histograms (DAH) were designed. The construction of dose area histograms were based on the approach presented in the work of Engelsman *et al.* [35]. Differential dose area histograms were constructed for both the PTV and area outside of it. To accomplish this, the area enclosed by the 95% isodose level ($IDL_{95\%}$) in the reference static dose distribution was chosen to represent the PTV, receiving a dose $\geq 95\%$ of the prescribed normalised dose, and with 100% target coverage. This area served as reference region, which was superimposed over the dose distribution to be evaluated. Then the dose values within the reference region were compared with those enclosed by its projected area over the dose distribution being evaluated. Figure 3.8 shows a schematic representation of the procedure used to construct dose area histograms for the evaluation of resulting dose distributions, relative to the reference dose distribution.

All the dose values within the reference PTV region were extracted and put into dose bins of 1% dose intervals generating a DAH, representative of the static reference dose distribution, with an area equivalent to the total number of dose values enclosed within selected reference region, which was normalised to 100%. Then, both the reference (static case) and the dose distribution to be evaluated were superimposed, and all dose values enclosed by the projected PTV area over the dose matrix being evaluated were extracted (see Figure 3.8). These extracted dose values were equally put into dose bins to generate a DAH representative of the dose distribution being evaluated. DAHs were contructed for all dose distributions and used to evaluate the influence of intrafractional motion and its variation (baseline drifts) during un-gated and gated beam delivery.

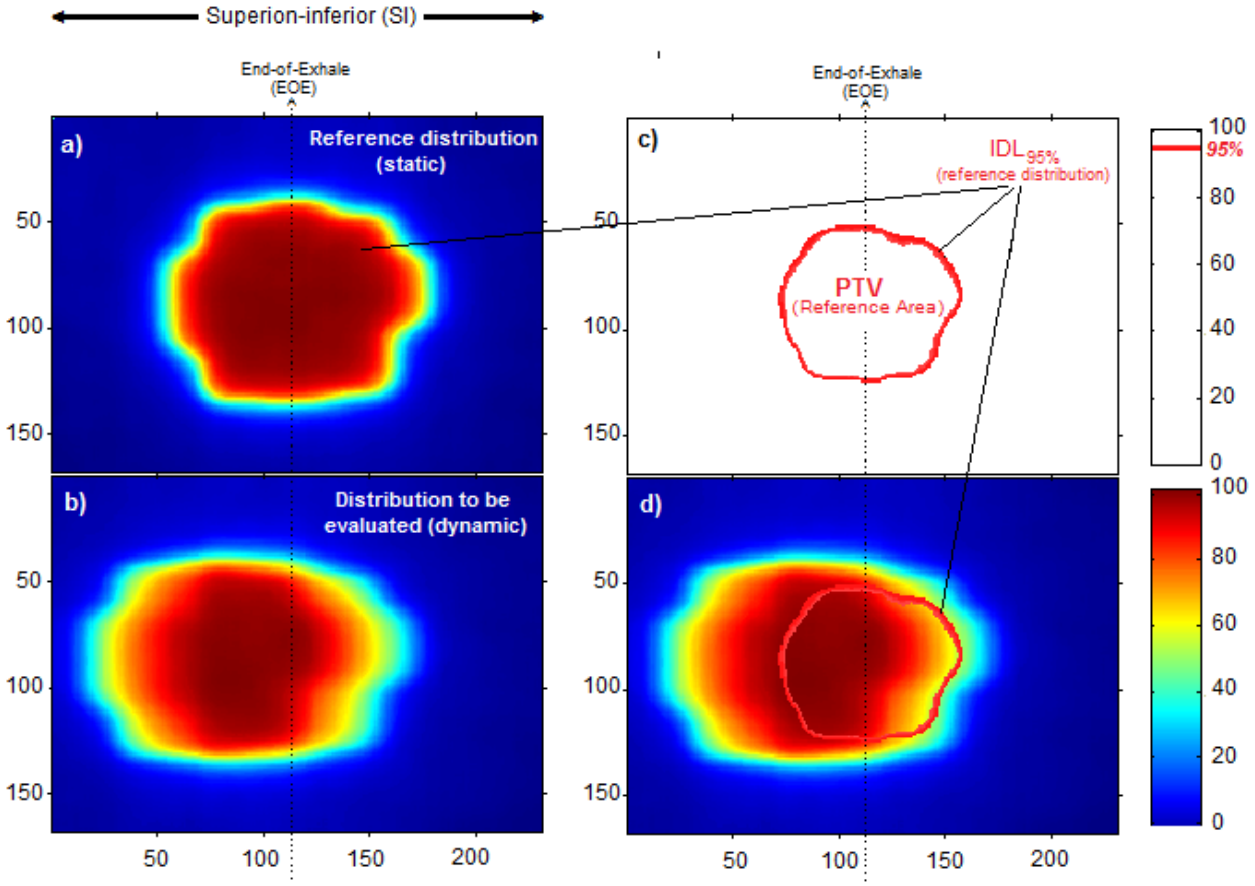

Figure 3.8: *An example of the procedure for the evaluation of dose distributions using DAHs. First both the reference (a) and the dose distribution to be evaluated (b) were aligned around the EOE, then the area enclosed by the $IDL_{95\%}$ in the reference distribution (c) was selected as reference PTV area. This is superimposed over the distribution being evaluated in (d). Only the dose values within the reference region of its projected area are used for the construction of DAHs.*

3.2 Intrafractional Motion and Gated Delivery

The dominant effect resulting from intrafractional motion is the blurring of dose distributions [33, 34]. Blurring leads to an enlarged beam penumbra and hence to less conformal dose distributions, which may have more detrimental effects on highly conformal treatments techniques such as intensity-modulated radiotherapy where steep dose gradient are tailored around OARs. The magnitude of blurring depends on the characteristics of motion, as well as the steepness of dose gradient and density of the medium [33, 34, 35]. The objective of this section was to investigate the effects of intrafraction motion on dose distributions and the suitability of gated beam delivery to minimise motion-induced blurring effects.

3.2.1 Gating Level Variations

This part of the study investigated the effects of applying different gating levels during dose delivery. For comparison both un-gated and gated dose delivery sessions were performed. The tumour substitute's centroid was positioned at the isocentre and set to oscillate with a peak-to-peak motion amplitude of $\approx$ 18 mm in the SI direction, perpendicular to beam direction with gantry at 0°, a breathing rate of 15 breaths per minute (f = 15 breath/min), corresponding to a 4-second long breathing cycle, which is within the range of clinically observed values (2.7 to 6.6 sec) [27].

Six delivery sessions (1-6) were conducted. For session 1, dose delivery was performed in the absence of intrafraction motion (target stationary centred at EOE phase), resulting in a static dose distribution. This static dose distribution served as reference against which the other dose distributions were compared to. For the remaining sessions the tumour substitute was allowed to move during dose delivery. Session 2 (dynamic delivery) corresponded to dose delivery without applying any control for motion (un-gated), which can be interpreted as allowing the delivery of dose over the whole breathing cycle (100% duty cycle). For the remaining sessions (3-6) an amplitude-based gating approach was performed applying gating duty cycles of 12%, 38%, 50% and 75%. Figure 3.9 shows the relative dose distributions resulting from delivery sessions (1-6). By comparing both the static (reference) and un-controlled (un-gated) dynamic distribution, it can be observed that intrafractional motion results in a degradation of dose conformity manifested by an enlarged penumbra at the edges of the field in the direction of motion. Conversely, with gating, the blurred dose distribution (dynamic distribution) resulting from un-gated delivery of dose is reduced progressively as smaller gating levels are applied. For instance, applying a 12% gating duty cycle resulted in a dose distribution that closely resembled that of the static distribution.

The dose profiles through the PTV along the SI direction, containing the target centroid (white dashed line drawn on static dose distribution in Figure 3.9), are shown in Figure 3.10. The PTV represents the area enclosed by the prescribed $IDL_{95\%}$, with the target centred at the EOE phase of respiration and static. The target moves along the SI direction from EOE to EOI phases of respiration a certain distace (ΔSI) and perpendicular to the beam direction. Since the gating window was defined to encompass the EOE phase of respiration, any time the target moved towards the EOI the area of the film to the left of the PTV was exposed to more dose, whereas the area to the right of the PTV to less dose. This explains the shapes of dose profiles, which have been smeared towards the EOE phase (to the left of the PTV). The profile correponding to the un-gated dynamic dose delivery shows that the gate (beam-on time) remained on over the whole breathing cycle length, which resulted in maximum dose smearing towards the left of the PTV. Less dose blurring can be observed for gated deliveries in which the gate was opened for only 75%, 50%, 38% and 12% of breathing cycle length.

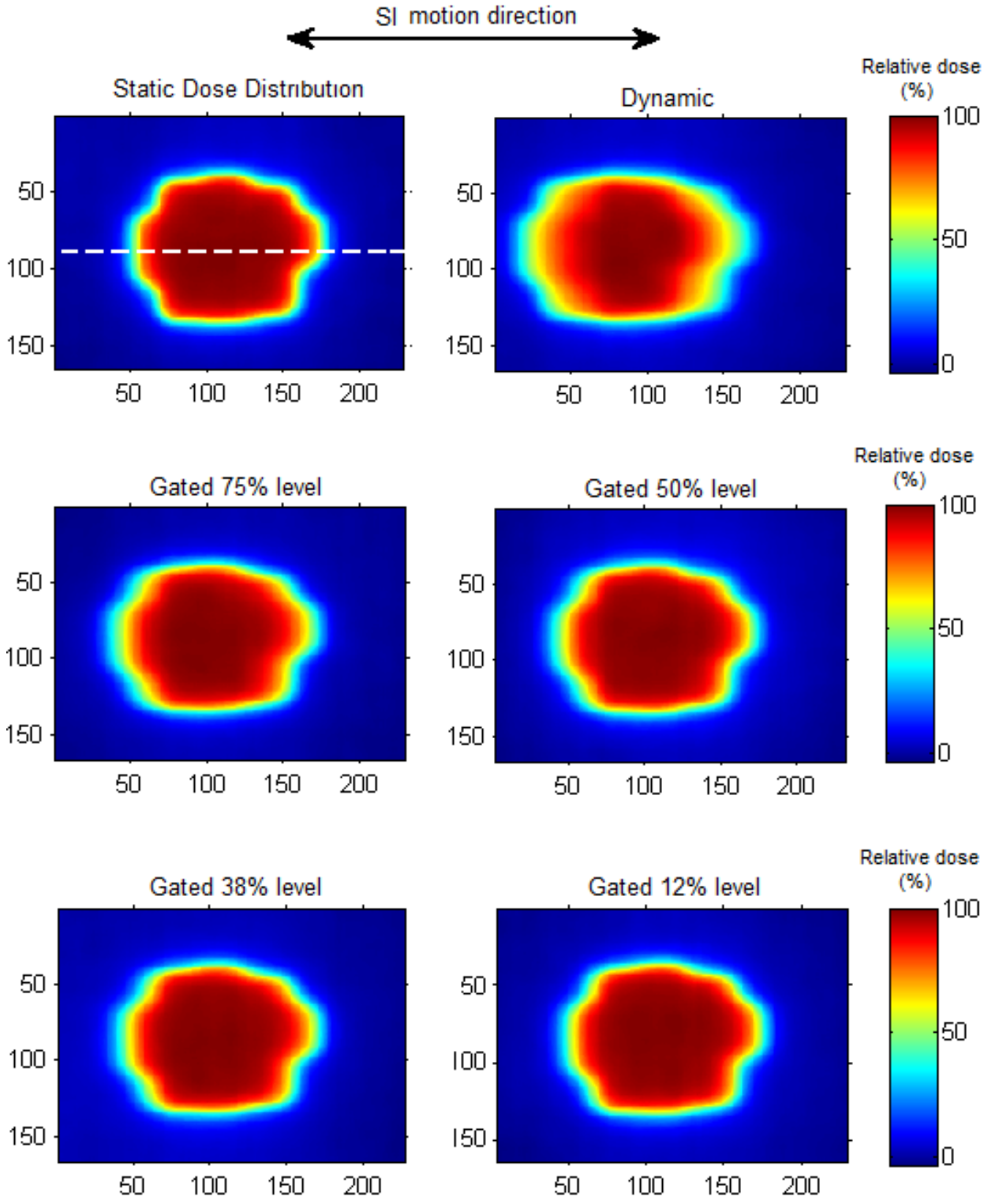

Figure 3.9: *Comparison of dose distributions (in pixels) corresponding to delivery sessions (1-6). Reducing the gating level decreases dose blurring effects (dynamic distribution) resulting in improved dose conformity. The white dashed line indicates the position at which the penumbra widening was measured for each dose distribution.*

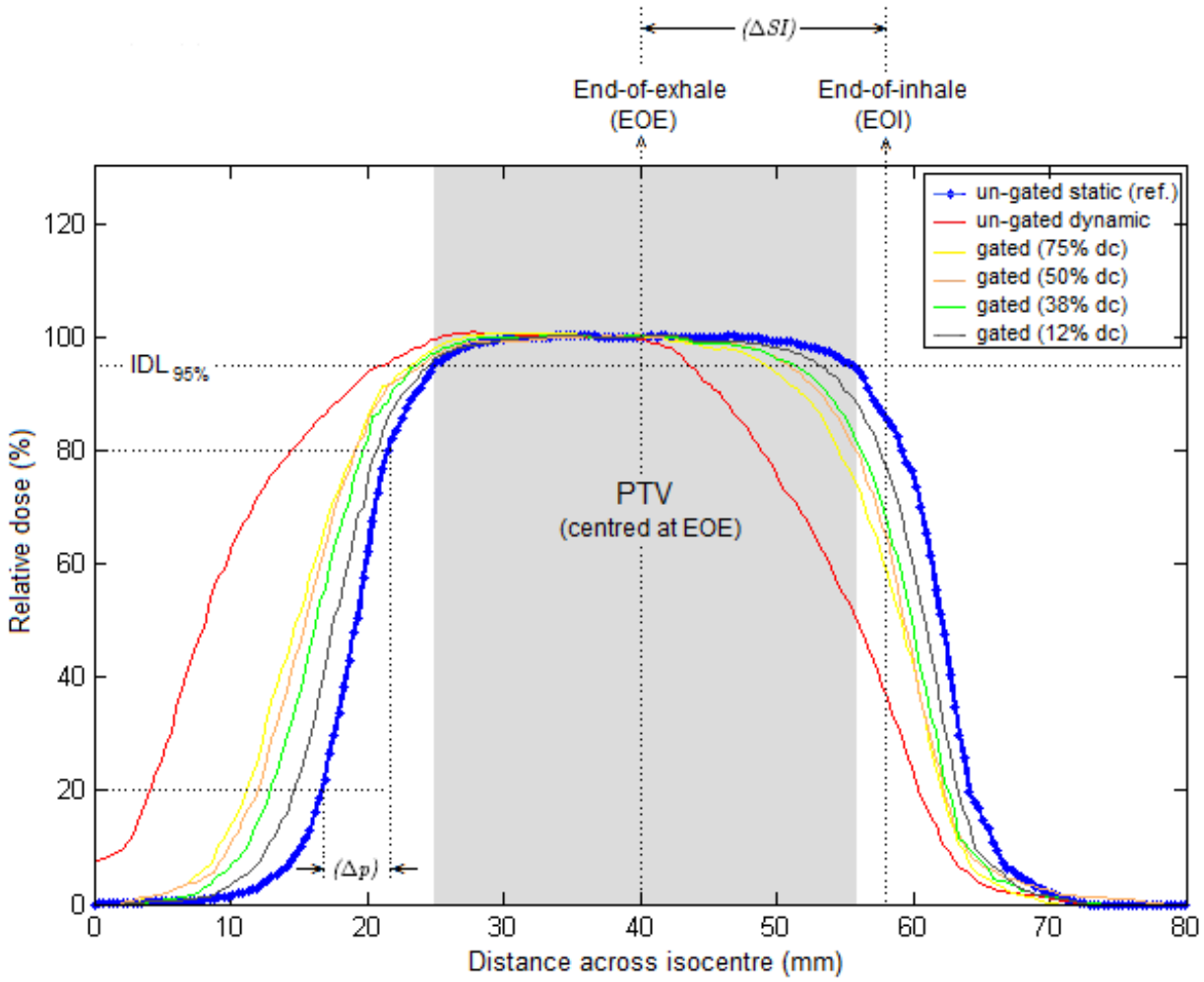

Figure 3.10: *Dose profiles along the superior-inferior (SI) through target centroid for delivery sessions (1-6). The change in position of tumour substitute during dose delivery (ΔSI) represents the peak-to-peak motion amplitude. The penumbra widening (Δp) was measured between the 80% and 20% isodose level.*

Table 3.2 shows a summary of measured parameters for penumbra widening (Δp) and their relative change with respect to the reference distribution (static case), as well as delivery time and resulting treatment efficiency. Intrafractional motion without any control (dynamic case) leads to an increase in penumbra by up to 121%, relative to static delivery. On the other hand, for applied gating levels of 75%, 50%, 38% and 12%, the blurred penumbra was reduced to 158%, 144%, 131% and 120%. This was at the expense of an increase in treatment efficiency which was reduced to 73%, 71%, 69% and 51%, respectively. Such prolonged treatment times represents a major disadvantage of gated delivery, compared to other motion management techniques such as tumour tracking. It has been suggested that such prolonged treatment times are not only relevant in terms of patient treatment output, but that it may also add uncertanties to the treatment, i.e. patient setup, as result of patient discomfort.

Table 3.2: *Measurements of penumbra widening (Δp) and treatment efficiency for delivery sessions(1-6)*

Session #	Delivery mode	Duty cycle (%)	Penumbra (Δp)		Delivery	
			mean (mm)	perct.Δ (%)	time (sec)	efficiency (%)
1	un-gated (static)	-	5.1	100	64.5	100
2	un-gated (dynamic)	-	11.2	221	-	-
3	gated	75	8.0	158	81.7	73
4		50	7.4	144	83.1	71
5		38	6.7	131	84.4	69
6		12	6.1	120	95.9	51

Overall, the presence of intrafractional breathing motion results in an underdose of the PTV and overdose of the area outside of it, representing surrounding healthy tissue. Figure 3.11 compares the effects of intrafractional motion on the dose to the PTV (central plane of the PTV) corresponding to delivery sessions without control (dynamic cases) and with control for respiration with duty cycles of 75%, 50%, 38% and 12%, relative to the static ideal case (no-intrafractional motion). From these plots, it can be observed that dose delivery without any control result in the PTV receiving less than 95% of the prescribed dose (decrease in TCP), with a decrease in the minimum prescribed dose from 94% (static case) to 49% (dynamic case). Conversely, gating improved PTV coverage, increasing the minimum dose to the PTV from 49 (un-controlled dynamic case) to 73, 79, 81, and 86% for gating level of 75%, 50%, 38% and 12%, respectively.

Furthermore, with presence of intrafractional motion the percentage of the PTV area receiving a dose less than 95% of the prescribed (area enclosed by the $IDL_{95\%}$) decreases from 3.6% (static case) to 41.8% (dynamic case), whereas with gating the underdosed area inside the PTV is decreased from 41.8 (dynamic case) to 28.2%, 20.3%, 15.8% and 10.8 % for gating levels of 75%, 50%, 38% and 12%, respectively (see Table 3.3). These improvements in the coverage of the PTV observed with gated beam delivery are correlated with improvements in dose conformity, and hence a decrease in overdose area outside PTV, which represents surrounding healthy tissue.

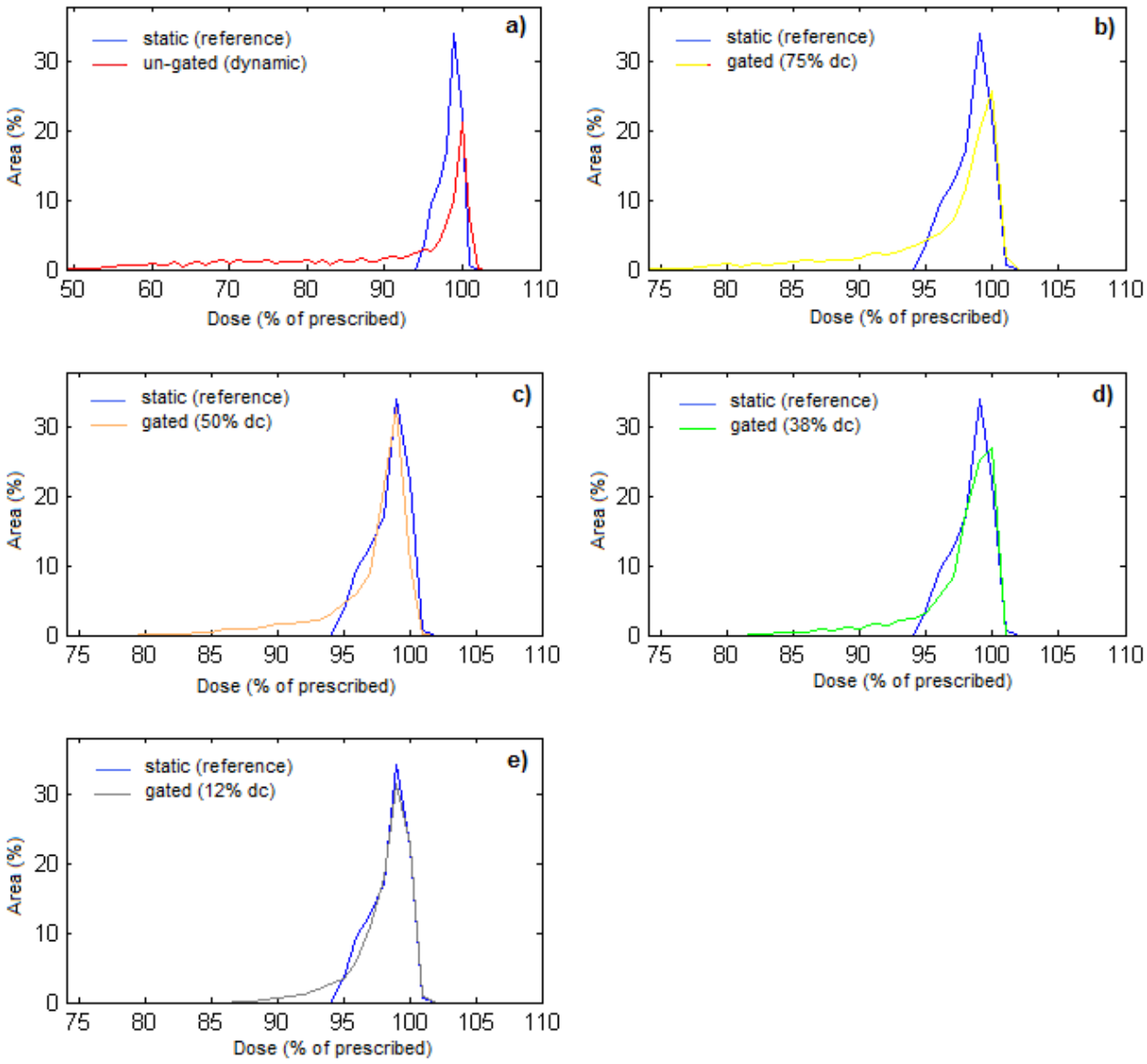

Figure 3.11: *Comparison of dose area histograms (DAHs) of the central plane (plane of the film) of the PTV (area enclosed by the $IDL_{95\%}$) for dose delivery sessions, without (un-gated) and with control for respiration using gating. The PTV dose area histogram corresponding to static dose distribution served as reference, which is compared to dose DAHs resulting from un-gated (a) and gated dose delivery with duty cycles of 75% (b), 50% (c), 38% (d), and 12% (e), respectively.*

Alternatively, if target coverage is to be kept constant when using gating to compensate for the blurring effects induced by intrafractional motion, the margins designed during treatment planning should be modified. Applying the approach suggested by Engelsman *et al.* [34], in which the investigators used the displacement of the prescribed isodose as a measure to quantify the margins required to compensate for intrafractional motion, measurements of the displacement of the 95% isodose level ($IDL_{95\%}$) indicate that the treatment portals can be reduced with gating. Table 3.3 gives a summary of the measurements of the displacement of $IDL_{95\%}$ corresponding to the left-hand and right-hand side of dose profiles from figure 3.10, relative to the static case. This one dimensional analysis indicates that having the

target positioned at EOE, the field sizes would have to be enlarged by 6.3 mm, 4.6 mm, 4.2 mm, 2.4 mm towards the EOI direction, whereas towards the EOE direction decrease by 1.8 mm, 1.1 mm, 1.3 mm, 0.7 mm for duty cycles (gating levels) of 75%, 50%, 38% and 12%, respectively. For example, an increase in field sizes of ≈ 3 mm ($\Delta\,|right - lefthand|$) would be sufficient to ensure that the target remains within the high dose region during gated beam delivery with a 38% gating duty cycle at the expense of 31% (from Table 3.2) decrease in treatment efficiency. This reduction in field sizes with gating may in turn result in an increase in the sparing of surrounding healthy tissue and other OARs.

Table 3.3: *Minimum relative dose to PTV and its percentage area receiving less than 95% of prescribed dose. Measurements of the displacement of the $IDL_{95\%}$ represent the decrease (-ve) and increase (+ve) in field sizes towards the left-/ and right-hand side direction.*

Session #	Delivery mode	Duty cycle (%)	PTV		$IDL_{95\%}$ displacement	
			Min. dose (%)	Area prcnt. with dose < 95%	to Left (mm)	to Right (mm)
1	(un-gated) static	-	94	3.6	-	-
2	dynamic	-	49	41.8	-	-
3	(gated)	75	73	28.2	- 1.8	+ 6.3
4		50	79	20.3	- 1.1	+ 4.6
5		38	81	15.3	- 1.3	+ 4.2
6		12	86	10.8	- 0.7	+ 2.4

3.3 Discrepancies in the Internal/External Correlation

The aim of this section was to investigate the effects of the discrepancies in the correlation between target motion and the ANZAI respiratory signal on gated beam delivery. Variations, which may arise during delivery, i.e. baseline drifts, can lead to uncertainties resulting in poor tumour control [40].

Baseline-drifts of 4 different magnitudes (3, 6, 9 and 12 mm) were simulated by making respective discrete changes to the couch position over fractionated delivery. For a dose of 2Gy, resulting in 212 monitor units (MU), the delivery was interrupted three times, splitting a single fraction into 4 equally divided subfractions of 53 MUs each. Each time the dose delivery was interrupted, the treatment couch was displaced a certain distance away from central beam axis until the whole number of MUs was delivered. The total displacement of the couch by the end of fraction delivery represents the magnitude of simulated drift (d), as shown in Figure 3.12. Overall, this resulted in the target centroid deviating caudally away from its central beam axis and its planned position, while the breathing signal used for the onset of gated beams remaining regular. A schematic representation of the procedure can

be observed in Figure 3.12. All measurements performed on the motion phantom had the target set to oscillate at a frequency of 15 cycles/min and a peak-to-peak motion amplitude $\approx$ 18 mm.

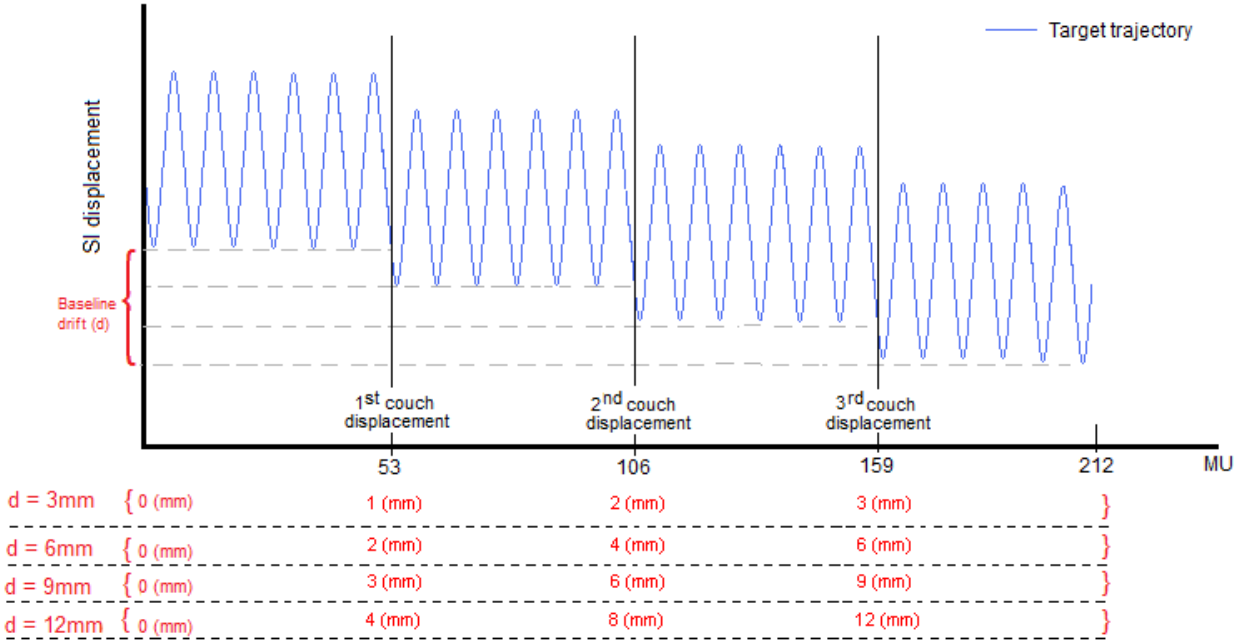

Figure 3.12: *Simulation of baseline drifts along the SI motion direction of tumour substitute.*

3.3.1 Effects of Baseline Drifts

To assess the dosimetric impact of baseline drifts on gated beam delivery, all measurements were performed with a common reference gating duty cycle of 38%. The first delivery session was performed in the absence of baseline drift, which served as reference. For the remaining sessions a different magnitude of baseline drift was simulated. Figure 3.13 shows the dose profiles measured in the plane of film resulting from delivery sessions performed in the absence (blue profile), as well as under the effects of 3 (grey profile), 6 (green profile), 9 (yellow profile) and 12 mm (red profile) baseline drifts. From this figure, it can be observed that baseline drifts diminished the dosimetric gains of gated beam delivery, resulting from a 38% gating duty cycle. In addition to leading to less conformal dose distributions, such drifts resulted in a general shift of dose distributions relative to the intended position ($PTV_{gated\_38\%dc}$), which was the region enclosed by $IDL_{95\%}$ under a 38% duty cycle, in the direction and with a magnitude proportional to that of the simulated drift (see Figure 3.13).

With respect to the reference dose profile, baseline drifts led to an increase in penumbra by 10%, 23%, 49% and 70% for simulated drifts of 3, 6, 9 and 12 mm, respectively. Furthermore, measurements of the displacement of high dose region, showed asymmetric changes in the position of the $IDL_{95\%}$ for the left-hand side (between 1.3 to 7.7 mm) and right-hand side (between 1.6 to 3.7 mm) dose profiles, as also pointed out in studies by van Herk *et al.*

and Engelsman *et al.* [10, 34]. Moreover, it is interesting to note that the combined (left-/right-hand side) displacement of $IDL_{95\%}$ resulted in corresponding shifts of 2.9 mm, 5.9 mm, 8.9 mm and 11.4 mm, which were within 0.3 - 4.8% in magnitude with those simulated. From a clinical point of view, such measurements of the $IDL_{95\%}$ displacement can be used to determine the margins required to compensate for the effects of such drifts.

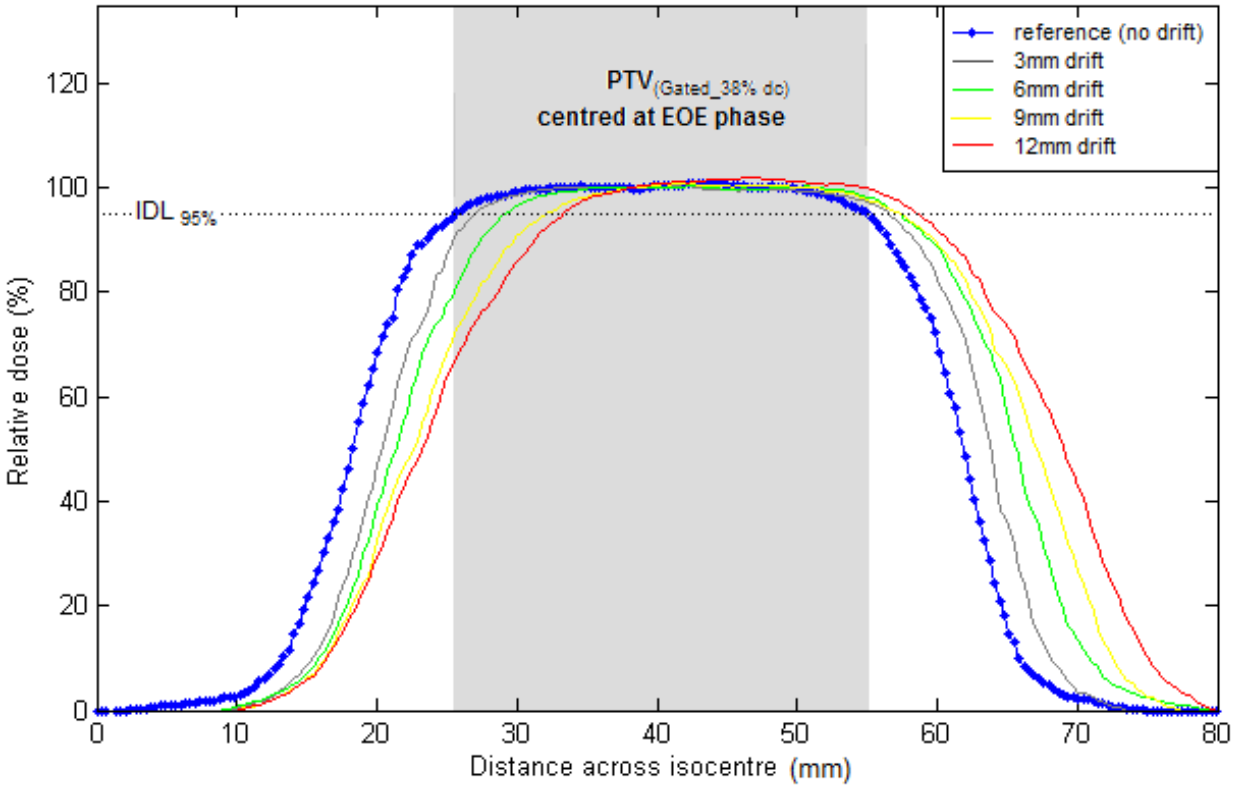

Figure 3.13: *Resulting dose profiles measured in the plane of the film, with respect to* $PTV_{(Gated\_38\%dc)}$*, marked by region enclosed by 95% IDL*

On the other hand, to assess the the influence of such drifts on relative dose delivered to region of interest ($PTV_{(Gated\_38\%dc)}$), the dose area histograms (DAHs) of the central plane, corresponding to each delivery session, are also shown (Figure 3.14). Baseline drifts resulted in the $PTV_{(Gated\_38\%dc)}$ receiving a dose less than 95% of prescribed dose, while at the same time increasing the percentage of the $PTV_{(Gated\_38\%dc)}$ area receiving a dose of less than 95%. For instance, a 3 mm baseline drift resulted in a decrease in minimum dose to $PTV_{(Gated\_38\%dc)}$ from 94% (gated reference in absence of drift) to 89%, as well as in an increase in area receiving a dose less than the minimum prescribed of 95% from 2.8 % to 11.1%, respectively. Conversely, for the case of simulated drifts of 6, 9 and 12 mm the minimum relative dose delivered to $PTV_{(gated\_38\%dc)}$, with respect to reference DAH (gated without baseline drift) decreased to 80%, 71% and 66%. Additionally, the $PTV_{(Gated\_38\%dc)}$

area receiving a dose less than 95% increased to 16.2%, 30.1% and 32.1%, respectively. Table 3.4 gives a summary of calculated parameters.

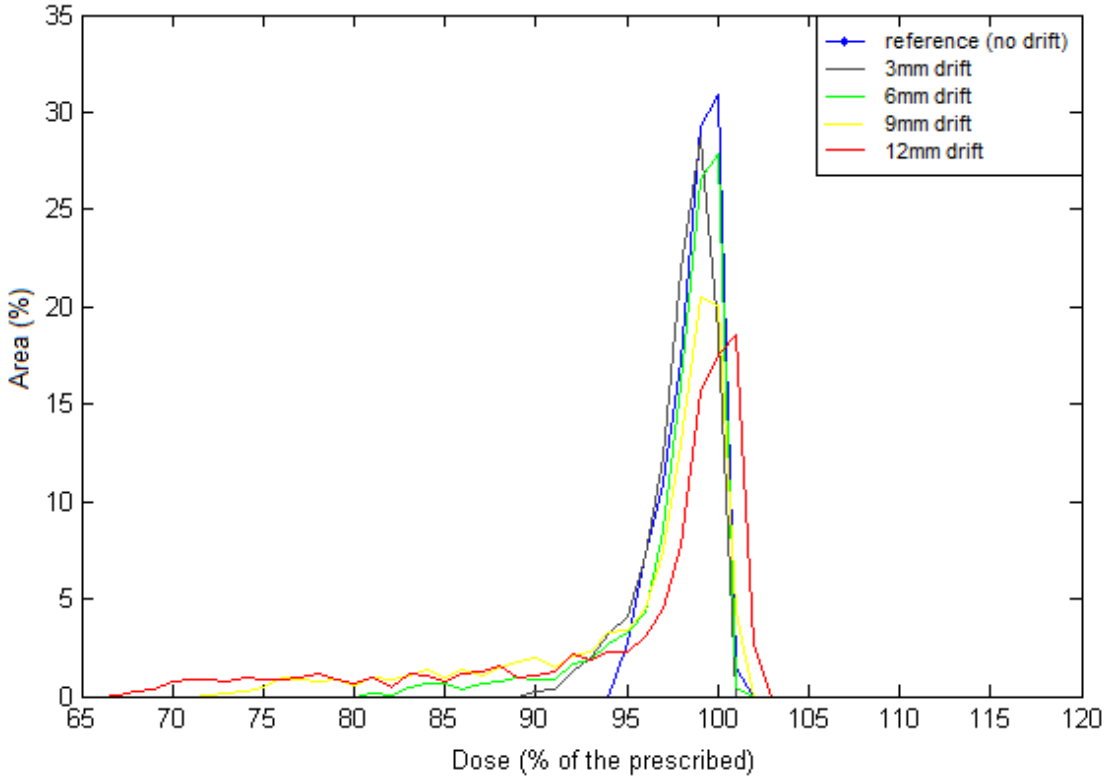

Figure 3.14: *Dose area histograms of the central plane of the region of interest (PTV) showing the effects of baseline drifts on the dose to* $PTV_{(Gated\_38\%dc)}$ *during gated delivery with 38% duty cycle.*

Table 3.4: *Effects of baseline drifts of different magnitudes on the dose delivered to the PTV during gated delivery using a 38% gating duty cycle*

Delivery mode	Magnitude of baseline drift (mm)	Penumbra		PTV	
		mean (mm)	perct.Δ (%)	min. rel. Dose (%)	perct.(%) Area with < 95% rel. Dose
gated (reference)	-	6.2	117	94	2.8
gated 38% dc	3	6.6	127	89	11.1
	6	7.4	140	80	16.2
	9	8.8	166	71	30.1
	12	9.8	187	66	32.1

3.3.2 Variations in Gating Levels

Different gating duty cycles (12%, 38%, 75%) were tested under the effects of a 6 mm baseline drift, which was equally applied over each delivery session, in order to investigate whether such effects could be compensated by only adjusting the gating window. It has been suggested in some studies [17, 29], by making respective adjustment to gating window so to accommodate for increases/decreases in residual motion by widening/narrowing the gating window.

Table 3.5 gives a summary of the calculated parameters corresponding to both un-gated (static and dynamic) and gated delivery sessions with applied gating duty cycles of 12%, 38% and 75% under the effects of a 6 mm baseline drift. The dynamic distribution represented the worst case scenario, resulting purely from the effects of intrafractional motion and baseline drifts, without applying any control for motion compensation (ungated). With respect to the reference distribution, a 6 mm baseline drift degraded dose conformity and compromised $PTV_{(ref)}$ coverage, increasing the penumbra region by 113% and reducing the minimum dose delivered to $PTV_{(ref)}$ to 66% (see Figure 3.15), while at the same time increasing the $PTV_{(ref)}$ area with dose less than prescribed to 34.9%. Conversely, with gating the blurring effects were minimised, reducing the blurred penumbra (un-gated dynamic) by 27.9%, 34.2% and 40% when applying gating duty cycles of 75%, 38% and 12%, respectively. A similar trend towards improving dose coverage was observed by decreasing the gating duty cycle. Overall, the underdosed area was reduced between 46.7 to 72.2% with respect ungated dynamic delivery (down from 34.9% to 18.6% and from 34.9% to 9.7%) for duty cycles of 75% and 12%. For instance, for a reference 38% duty cycle, the underdosed area was reduced by almost 62% (down from 34.9% to 13.3%) and minimum dose to $PTV_{(ref)}$ increased to 87% (see Table 3.5).

Table 3.5: *Effects of varying gating levels on the dose delivered to the $PTV_{(ref)}$ under the effects of 6 mm baseline drift*

Baseline drift (mm)	Delivery mode	Window level (%)	Penumbra		$PTV_{(ref)}$	
			mean (mm)	perct.Δ (%)	min. rel. Dose (%)	perct. Area with $< 95\%$ rel. Dose
-	(un-gated) static	-	5.3	100	94	3.4
6 mm	dynamic	-	11.2	213	66	34.9
6 mm	(gated)	75	8.1	153	86	18.6
6 mm		38	7.4	140	87	13.3
6 mm		12	6.7	128	88	9.7

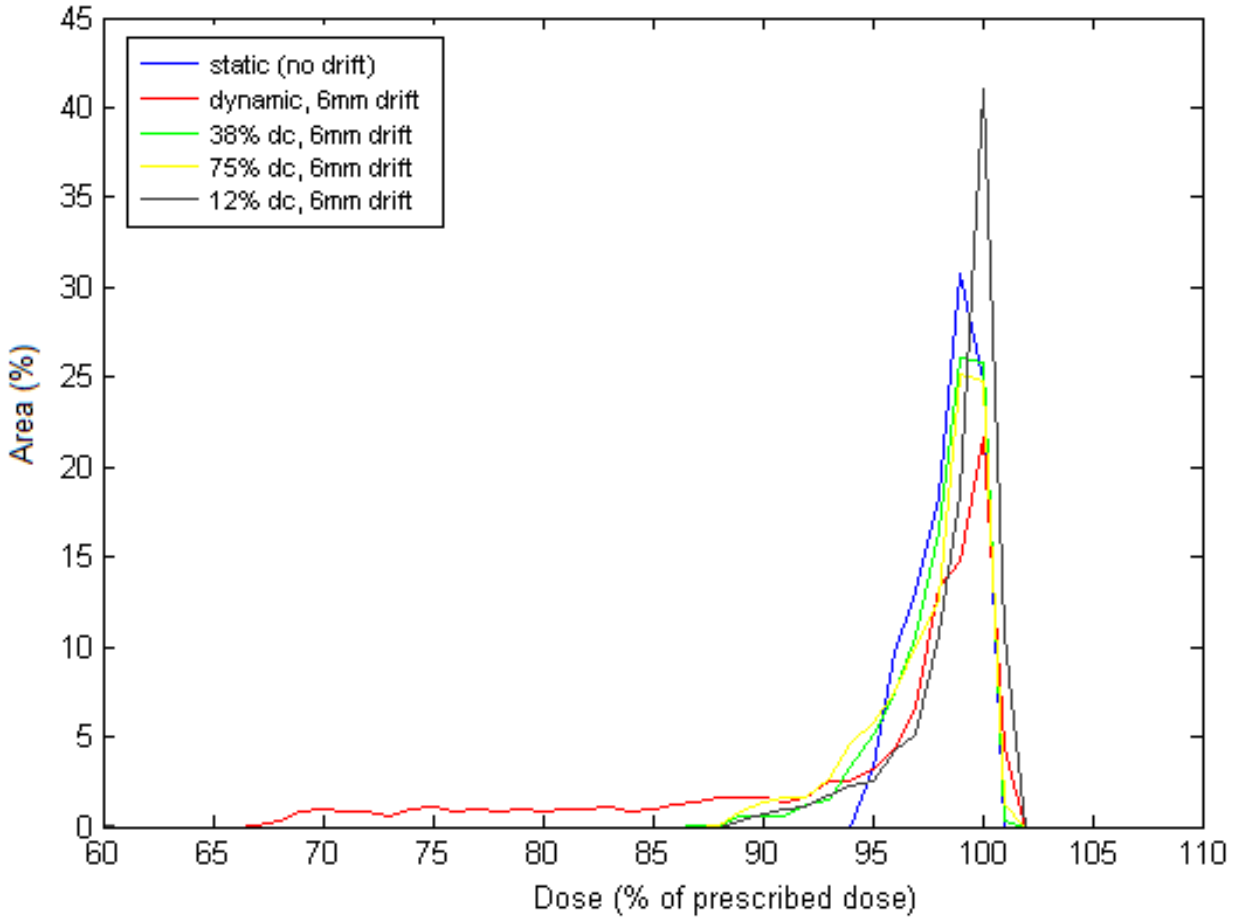

Figure 3.15: *Comparison of dose area histograms for delivery sessions with duty cycles of 75%, 38% and 12% in the presence of a 6 mm baseline drift.*

Figure 3.16 shows the dose profiles corresponding to sessions delivered under the combined effects of intrafractional motion and baseline drifts. By inspecting the dose profiles, it can be observed that applying a 12% duty cycle reduced the effects of baseline drift significantly, improving dose conformity and PTV coverage. Although, this may be accomplished at the expenses of a prolonged treatment time associated with the small gating duty cycle applied, as previously demonstrated in section 3.2.1. Furthermore, when considering the amount of dose delivered outside the $\text{PTV}_{(ref)}$ region, which may be correlated with the amount of dose deposited in the surrounding healthy tissue or organs at risk, the dosimetric benefits were also significant. From Figure 3.16, it can be observed that the amount of dose smeared outside $\text{PTV}_{(ref)}$, towards the end-exhalation direction (left-hand side relative to static profile), could be almost compensated by reducing the gating window from 75% to 38 and 12% dc. However, because of the effects of baseline drift, reducing the duty cycle resulted in slightly more dose being delivered to the region outside $\text{PTV}_{(ref)}$ towards the inhalation direction (right-hand side relative to static profile). Moreover, it appears that with smaller duty cycles (38% and 12%) slightly more dose was concentrated outside $\text{PTV}_{(ref)}$ region, compared to dose delivery with a 75% duty cycle (see Figure 3.16).

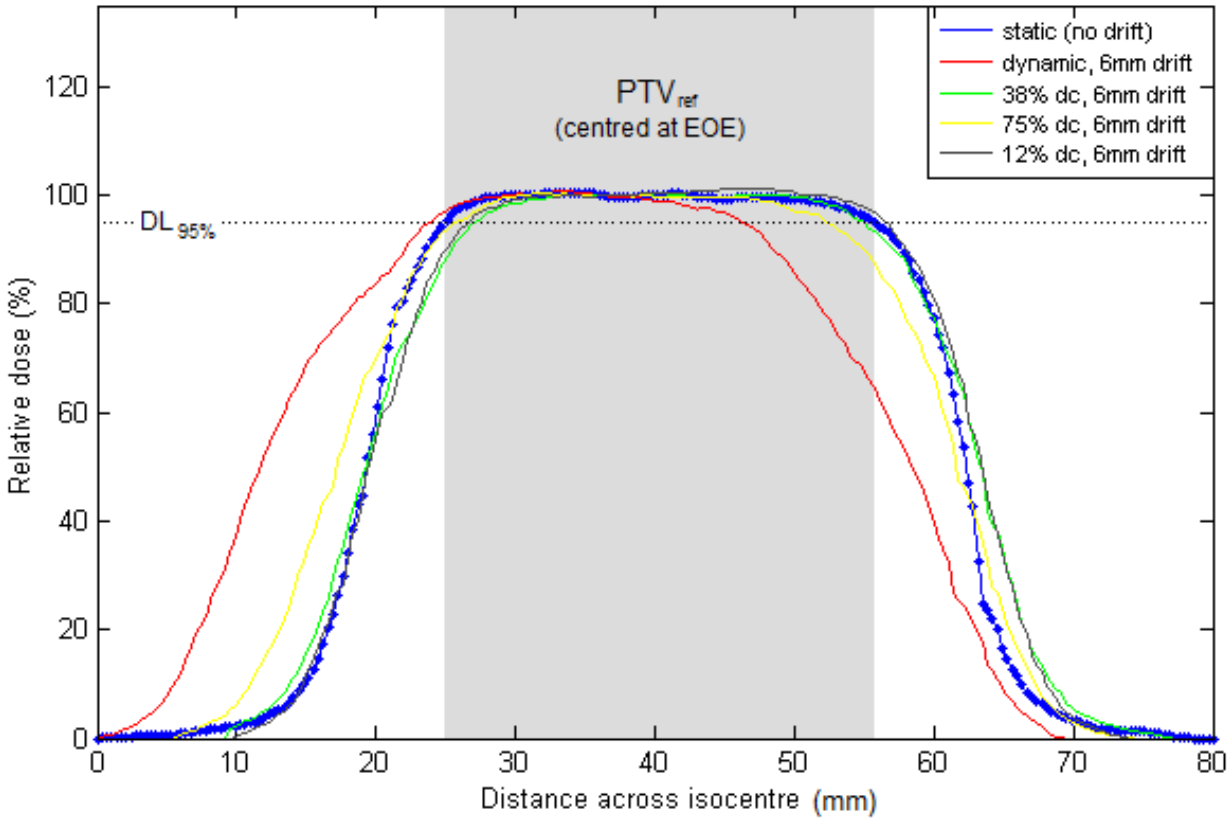

Figure 3.16: *Dose profiles measured in the plane of film. The unblurred/static profile (blue profile) served as reference. The remaining profiles correspond to dose delivery under the effect of a 6 mm baseline drift without (red profile) and with gating applying duty cycle of 75 (yellow profile), 38 (green profile) and 12% (grey profile).*

It is expected that relatively larger magnitudes (i.e. $> 6mm$) of baseline drifts could result in a more significant amount of dose being delivered outside $\text{PTV}_{(ref)}$ to the extent that compensating for such discrepancies by reducing the gating window, would not be sufficient. This observation can be better understood by looking at the dose profiles shown in Figure 3.17. These profiles were obtained from delivery sessions under the influences of 6mm, 9mm and 12mm baseline drift with control for respiration (gated with a 38% duty cycle) and without any control for respiration (un-gated). With respect to the reference distribution, the smearing of the dose distributions towards the EOE (left-hand) direction were compensated with gating for all the simulated drifts at the expenses of decreased dose to PTV. However, when considering the region towards the EOI (right-hand side), which represents healthy tissue, it appears that the benefits of gating were minimised. Gating resulted in even more dose smearing towards the EOI into the area representing healthy tissue, compared to ungated dose delivery.

In Figure 3.18, the dose area histogram for the region representing the surrounding healthy tissue around the PTV (area not enclosed by 95% isodose), is shown for the resulting dose distributions just discussed above for gated and ungated delivery sessions under the influences of baseline drifts of 6mm, 9mm, 12 mm. The static reference (blue) DAH has

also been added for comparison. All DAHs were evaluated relative to the static reference distribution, but in this case the area selected as region of interest (OAR) was the area not enclosed by the 95% isodose level in reference distribution. The larger peak seen for the static case for doses greater than 80% is because intrafractional motion and baseline drifts lead to a decrease in the cumulative dose to the PTV (underdose), which results in a decrease in the PTV area receiving doses less than the prescribed. This means that the area enclosed by high dose region inside the PTV is smaller, compared to the static case (see dose profiles).

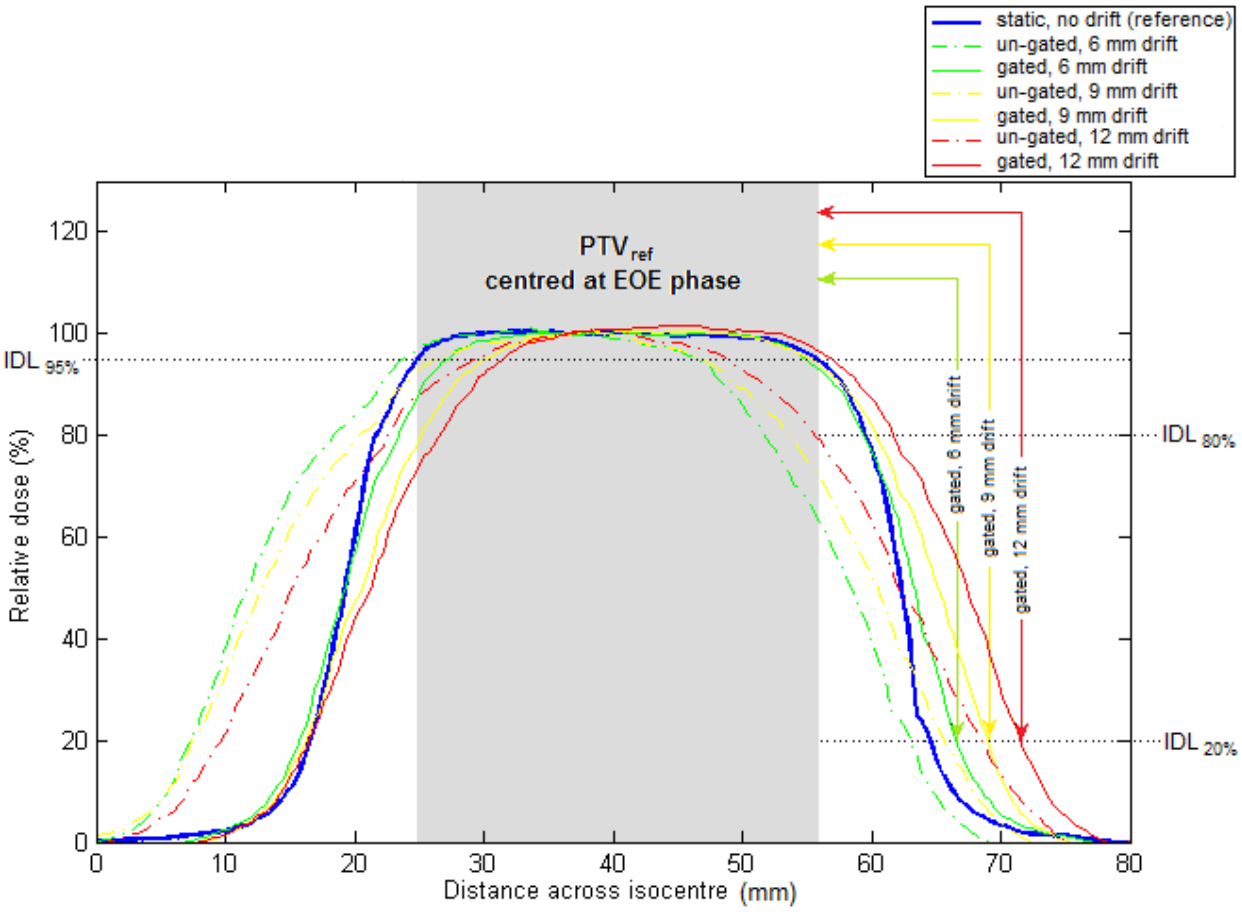

Figure 3.17: *Comparison of dose profiles corresponding to un-gated and gated dose distribution under the effects of 6, 9, 12mm baseline drifts*

Dose area histograms show that overall, with respect to the reference dose distribution and dose values between the 20% and 80% of prescribed dose, the overdosed area outside the $PTV_{(ref)}$, resulting from simulated drifts of 6, 9, and 12 mm, was decreased with gated beam delivery by approximately 20.1%, 32.6% and 31.3%, respectively. However, it can also be observed that gating led to a slightly increase in the area outside $PTV_{(ref)}$ receiving higher dose levels, i.e. $> 80\%$, compared to un-gated dose delivery, as illustrated in Figure 3.18.

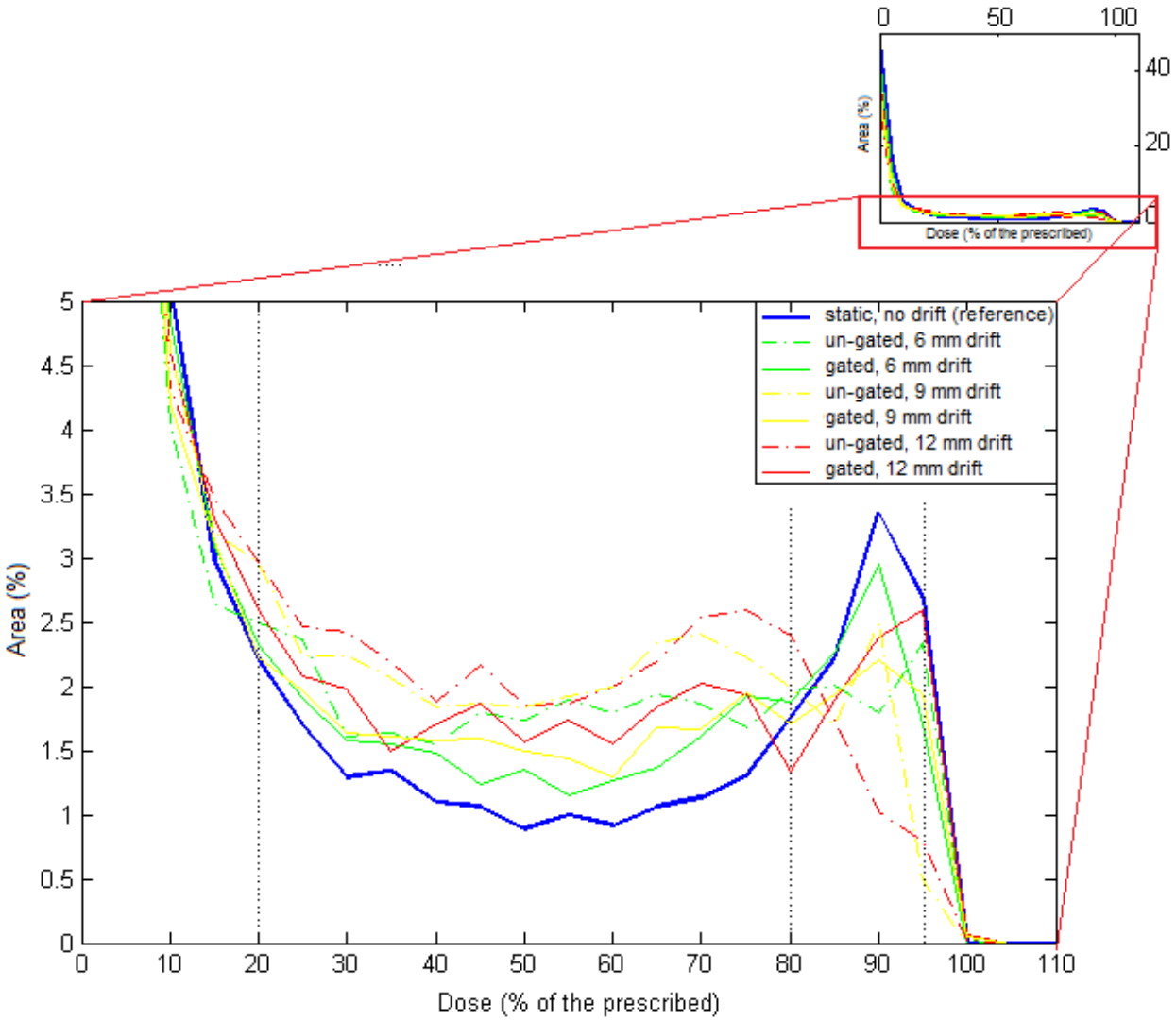

Figure 3.18: *Dose area histogram of the area outside PTV (region outside the 95% isodose level $IDL_{95\%}$), representing the surrounding healthy tissue.*

3.4 Summary

Phantom studies were conducted to investigate the dosimetric effects that intrafractional motion and baseline drift may have on the dose to the tumour substitute during gated beam delivery. Film dosimetry was based on dose distributions in the coronal plane through the centroid the tumour surrogate. Dose area histograms as well as dose profiles were generated allowing the quantification of the delivered dose to PTV and penumbra widening. Intrafractional motion led to an enlarged beam penumbra and hence to less conformal dose distributions, which resulted in an overall decrease in the cumulative dose to the PTV. Gated beam delivery improved dose conformity at the expenses of increased delivery times. For an amplitude-based approach and 38% reference duty cycle, gating allowed a 41% reduction in dose blurring caused by motion with a reduction of 31% in treatment efficiency. However, these dosimetric gains were compromised by the effects of baseline drifts, which caused a shift in dose distribution in addition to increased dose blurring. For instance, for the same

reference 38% duty cycle, baseline drifts between 3mm to 12 mm led to an increase in dose blurring by 10% - 70%. Compensation of baseline drift by reducing the gating window was possible only to a certain extent. Baseline drifts need to be considered during planning and require larger margins for compensation that intrafractional motion. Unfortunately, baseline drifts cannot be easily identified by means of 4D computed tomography (CT) for its integration into treatment planning. This calls for monitoring tumour position during delivery either by imaging or other means to identify variations in the tumour's residual motion within the gating window caused by baseline drifts. Real-time tumour tracking will potentially address these issues. Previous studies [16] have demonstrated the feasibility of EPID-based tumour visualisation and its markerless localisation but this has not been applied to RGRT. A feasibility study for EPID-based verification of tumour position during gated RT is to be investigated in the next chapter.

Chapter 4

Tumour Tracking Study

A method for real-time verification of tumour position is required to maximise the potential benefits of respiratory gated RT (RGRT), which may facilitate the safe reduction of treatment margins and ultimately dose escalation. RGRT is becoming widely available as a means for motion compensation of tumours affected by respiration, and is offered by several manufacturers of medical equipment. Although its benefits have been reported in numerous studies [23, 24, 25, 51], there are some issues associated with the use of such commercially available systems, in particular with those that rely on the monitoring of external surrogates to derive internal tumour position (i.e., optical reflector, pressure belt, spirometer), which rely on the fact that the correlation between surrogate and actual tumour motion remains stable over time. However, it has been identified that the degree of such correlation can vary intra-/interfractionally [45, 46, 54], suggesting that the use of external surrogates alone is not sufficient for guiding the delivery of gated treatment beams. This calls for the direct monitoring of tumour position during treatment.

Most of the existing approaches for treatment verification and direct determination of tumour position during gated RT have resorted to using fiducial implants, which are monitored and tracked by means of either kV fluoroscopy [44] or megavoltage imaging systems [59, 56]. This is accomplished at the cost of increased risk of infection involved with the implant procedure, and additional exposure of patient to considerable levels of imaging dose. By the time this work was initiated, reports on methods for imaging and tracking lung tumours in real-time during gated RT with focus on minimum treatment invasiveness (markerless) and exposure of the patient to imaging dose, were scarce. In this work a dedicated software package, denoted PortalTrack developed at the University of Wuerzburg, was utilised. PortalTrack is capable of determining tumour position directly in portal images without implanted fiducial markers using the Megavoltage (MV) treatment beam (exit dose) and the electronic portal imaging device (EPID). Using PortalTrack and the EPID system only as image-guidance tool will address issues with regards to the invasiveness of the implant procedure, while at the same time discarding the need for additional imaging hardware, which will prevent the additional exposure of patient to imaging dose.

In this work, the suitability and potential of PortalTrack for markerless position verification of lung tumours during RGRT is investigated. The issue of discrepancies between external surrogates and internal tumour motion in RGRT is also addressed. To accomplish this, it was evaluated whether or not *(1)* it is feasible to track lung tumours during RGRT

without markers using PortalTrack, *(2)* the tracking information is enough to detect subtle changes in tumour motion within gating window, and *(3)* whether tumour tracking can potentially improve the accuracy and effectiveness of gated treatment as performed by a third party gating system.

4.1 Method and Materials

A dedicated software package, denoted *PortalTrack*, was utilised for real-time imaging and tumour tracking. PortalTrack was written in Visual Basic (Microsoft Corporation, Redmond, WA) and it acquires, stores, and displays portal images in real-time. A more detailed description of the performance of this software has been previously reported by Baier *et al.* [50]. Briefly, the software interacts directly with the frame grabber card making use of the existing dynamic link libraries provided by the manufacture of the EPID system, and hence manipulate the image acquisition process of the flat panel [50]. PortalTrack is capable of detecting the tumour position in portal images without using implanted fiducial markers (markerless tracking). Briefly, the projected trajectory is obtained by defining a beam specific mask over a representative portal image in which the target has been identified. This mask serves as reference window, which is instructed to move pixel-wise within a certain region (search range) over consecutive portal images. An intensity-based root-mean square difference algorithm is responsible for searching the best matching mask position in every consecutive portal image of the acquired EPID movie. The details of this process and feasibility of tracking moving tumours with megavoltage portal imaging have been described previously in the work by Meyer *et al.* [16]. Previous studies with PortalTrack have reported a mean tracking accuracy of 0.36 mm $\pm$ 0.12 mm for phantom studies and 1.0 mm $\pm$ 1.1 mm for realistic lung tumours during SBRT [39]. The suitability of PortalTrack for tumour tracking and motion compensation by means of robotic HexaPOD treatment couch has also been investigated and shown promising capabilities [42].

To investigate the suitability and potential of PortalTrack for the tumour position verification during RGRT, EPID movies and the external respiratory signals were synchronously acquired for the motion phantom during delivery sessions of 200 MUs each. The centroid of the tumour substitute was placed in the linac isocentre and a 6 MV radiation beam at 0^o gantry angle. For simplicity, a square field size (4 cm x 4 cm) was chosen to ensure the target substitute was always within the beam. EPID movies were acquired at $\approx$ 2 fps (frames per second). All deliveries were performed on an Elekta Synergy S (Elekta, Crawley, UK) equipped with an MV amorphous silicon (*a*-Si) EPID. Retrospectively, all EPID movies were loaded into PortalTrack and analysed by simulating gated delivery and tumour tracking for hypothetical gating windows with varying threshold levels.

4.1.1 Simulation of Gated Delivery

Gated treatments was simulated by manipulating the acquired EPID movies to create intermittent periods of beam-on (gates) and beam-off as the movies were played. To accomplish this, an amplitude threshold level was set on the external respiratory curve to define a hypothetical/or imaginary gating window in the surrogate space, separating the portion of

breathing cycle chosen to be encompassed by the gating window, i.e. end-of-exhalation, from the rest of breathing trace. Any time the external signal falls below the predefined threshold, it is considered to be within the gating window (beam-on). Furthermore, since both the external signal and EPID movies were acquired in a synchronous fashion, the portal images corresponding to the time signal remained within the gating window were selected to represent periods of beam-on (gate), whereas those that did not to represent periods of beam-off. Additionally, for the purpose of this study, a new feature was implemented into PortalTrack, which allowed the handling of intensity fading of portal images. With this tool, portal images could be either set to retain their default intensity value, i.e. a visible image, or obscured (completely faded), i.e. a dark image. Subsequently, all frames which were not inside the gating window, corresponding to beam-off time, were obscured leaving those corresponding to beam-on only visible. This is illustrated in Figure 4.1

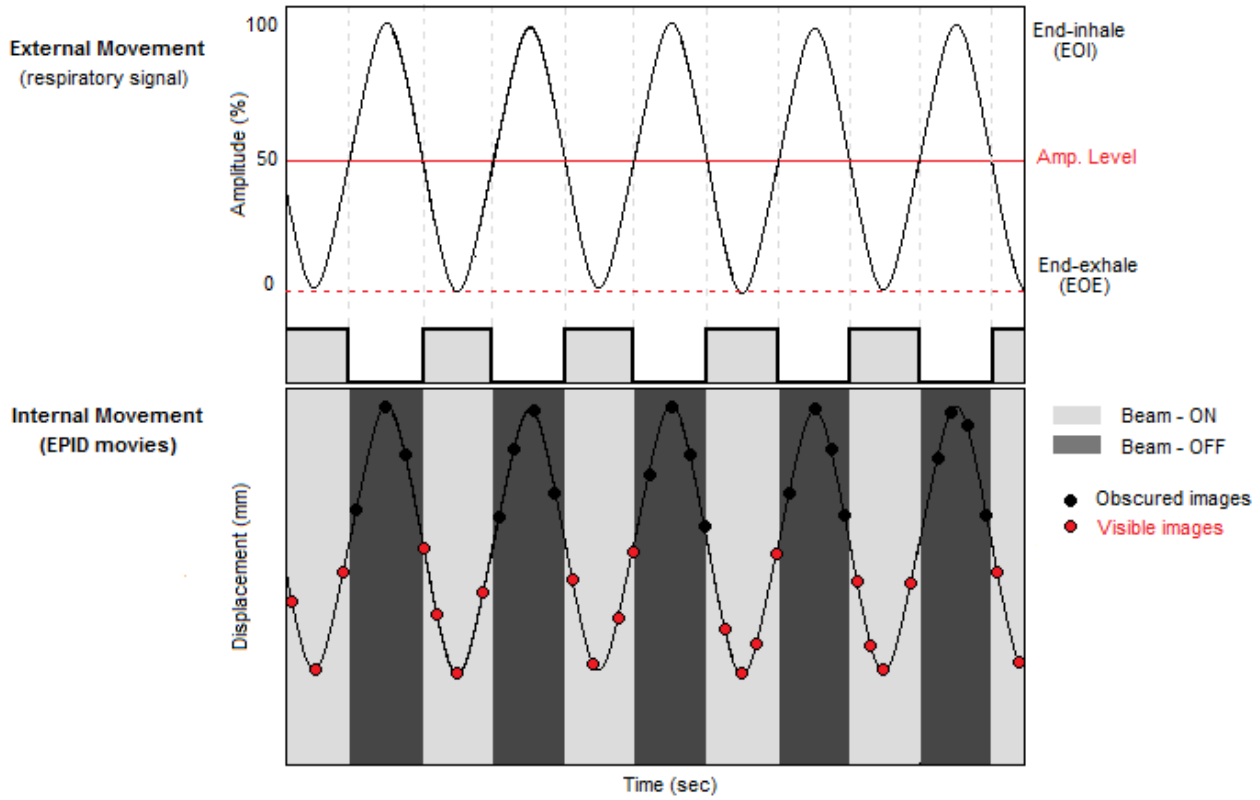

Figure 4.1: *Simulation of gated delivery by obscuring the frames which are not inside hypothetical gating window*

With the above-mentioned approach, gated treatments with different duty cycles of clinical relevance (15% - 60%) were simulated. The gating window was chosen to encompass the respiratory signal's EOE. An amplitude-based gating approach was simulated in the sense that a fixed gating window was set on external breathing signal, mimicking the use of commercially available gating systems. The obscuring of frames is analogous to acquiring images with the electronic portal imaging device during a realistic gated treatment procedure. Moreover, when in cine mode the EPID continuously acquire images even when the MV beam is turned off (blank images). These blank images are equivalent to those that are

obscured for the purpose of this study.

4.1.2 EPID Tracking

Tumour tracking was performed during each simulated gated treatment. Thus, only the frames acquired during beam-on time were available (or visible) to PortalTrack to detect the positions of the moving target inside the gating window. A representative portal image, with the target showing less imaging artifacts (high contrast), was selected (see Figure 4.2(b)) for the definition of a reference mask. Based on the shape of the target a reference mask was defined by drawing an annular contour around the high contrast edges of the target, as shown in figure 4.2(b). For automatic tracking the mask was moved pixel-wise (with a pixel equivalent to a resolution of 0.25 mm) within a user-defined search region of 30 pixels in each direction for any consecutive portal image acquired inside a hypothetical gating window. The position of the moving tumour substitute is directly determined in each portal images by the tracking algorithm, which minimised the mean sum of squared differences (MSSD) of pixels in the current mask position and in the reference mask to find the best matching position of tracked target, as described by equation 4.1.

$$MSSD(I_{ref}, I_j) = \frac{1}{N-1} \sum_{i=1}^{N} (B_i - A_i)^2 \tag{4.1}$$

where A is the region defined by the reference mask in representative portal image I_{ref}, B is the corresponding region over the consecutive portal images, and N corresponds to the total number of pixels [16]. Absolute values, representing the trajectory determined in pixels values, were converted into millimeter. All positions detected in portal images were stored and used to quantify target motion inside the gating window. This study was only concerned with motion along the SI direction, since it is the predominant direction of motion observed for tumours in the lung [27, 39].

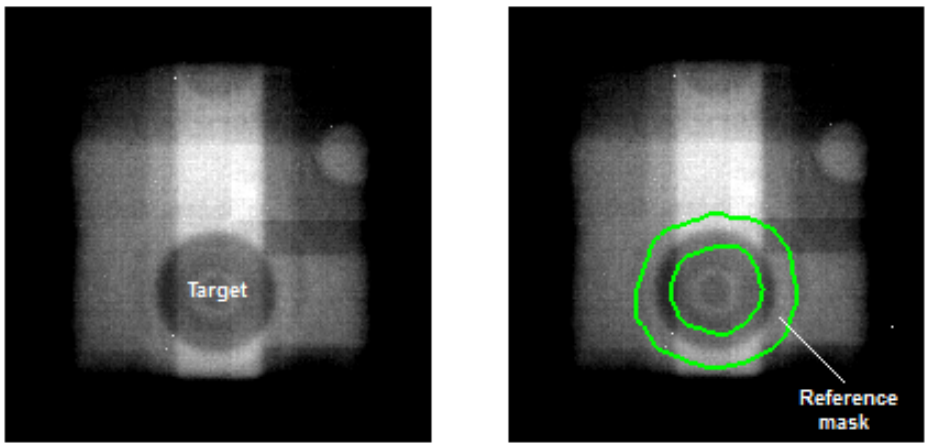

Figure 4.2: *(a) Selection of representative portal image showing the target to be tracked, and (b) definition of reference mask (right) over the characteristic non-homogeneous edges of the target.*

4.1.3 Data Analysis

Measurements of the Residual Motion

The residual motion as well as the probability density function (PDF) were used as measures to quantify target motion inside the gating window and its variability. The residual motion is the target motion during the time the gate is open (beam-on time) [46, 47, 59], and its value gives an estimate of the intrafractional variability of tumour motion inside the gating window. Tracking information was used to determine the residual distribution ($PDF_{residual}$), comprising all the target positions detected inside the gating window. The range of $PDF_{residual}$, measured at $95^{th} percentile$, gives an estimate of the magnitude of residual motion within a given gating window. The selection of the $95^{th} percentile$ as measure of residual motion was based on the literature concerning measurements of residual motion by other group studies [17, 45, 46, 59].

Discrepancies in the Internal/External correlation

Irregularities in the trajectories of tumour substitute were also simulated in order to investigate their impact on RGRT. As mentioned previously, variations in the internal/external correlation represents a major limitation to external-based gating techniques. Discrepancies between the internal and external signal were simulated, in analogy with previous study in Chapter 3, by keeping the external signal constant while simulating various baseline drifts in the trajectories of the tumour substitute during simulated gated treatments. Henceforth, all baseline drifts were simulated digitally in PortalTrack by once again manipulating the EPID movies. A feature in PortalTrack allowed the user to shift the portal images pixel-wise either along the longitudinal (y axis) or the lateral (axis) directions depending on the intended direction of drifts. Shifting the frames digitally did not affect the functionality of the tracking algorithm. Therefore, measurements of residual motion were conducted for both regular and irregular paths of the tumour substitute. All resulting PDFs$_{(residual)}$ were described in terms of their standard deviation (SD), mean (m) and range to measure residual motion and its intrafractional variability.

Determination of Ideal PDFs

Due to the characteristics of the flat panel, the maximum frame rate of image acquisition approximately 2 frames/sec. Therefore, PortalTrack was limited to acquire information regarding the target motion inside the gating window every 0.5 sec. To investigate whether the tracking information was sufficient to quantify residual motion, piecewise cubic Hermite interpolation was applied to motion data acquired from EPID movies. This allowed to assess the advantages of having a higher acquisition rate of frames, and thus an increased number of data points (positions inside the gating window) compared to a lower acquisition rate of $\approx$ 2 frames/sec.

Data interpolation was applied to all simulated trajectories of the tumour substitute. The same procedure, as above, was used to determine the residual motion inside equivalent (same duty cycles) hypothetical gating windows. Interpolated motion data inside a given gating

window, was interpreted as the true target motion, which represented the ideal probability density function (PDF_{ideal}). The range at 100^{th} percentile of such ideal PDF constituted the 'true' residual motion. This value of true residual motion was compared against the value determined with PortalTrack on the 2 frames/sec movies to evaluate how close PortalTrack can retrieve reliable information regarding the target motion inside the gating window. All data analysis was performed using MATLAB R2009b (The MathWorks, Inc., Natick, MA).

4.2 Results and Discussions

4.2.1 Measurements of Residual Motion

The residual motion of the tumour substitute driven by the motion phantom was measured during simulated gated treatments for 5 hypothetical gating windows with duty cycles between 15% and 60%. For this section, only motion path 1 of the tumour substitute, represented by a sinusoidal curve with an amplitude of $\approx$ 9 mm and cycle length of 4 sec, was analysed. Figures 4.3(a-b) illustrate the positions of tumour substitute determined with PortalTrack during two simulated gated treatments with duty cyles of 50% and 25%. An amplitude threshold level set on the external signal defined the gating window. The shaded regions represent the beam-on time (gates), whereas the red dots represent the positions of the target detected by PortalTrack inside the gating window. The two horizontal dashed lines drawn on the internal signal plots indicate the range of residual motion resulting from applying 50% and 25% gating duty cycles to external signal, respectively. In addition, the histograms representing the distribution of target positions obtained during simulated gated (red histogram) and un-gated deliveries (grey histogram), are also given for each case. The un-gated distributions corresponds to the whole motion range (peak-to-peak) of the target (grey trajectories), which may be equivalent to applying a 100% gating duty cycle to external signal, representing the maximum magnitude of residual motion. The potential of gated beam delivery to reduce intrafraction motion is more clearly illustrated by comparing the un-gated distributions against those determined with PortalTrack ($PDF_{residual}$).

Measurements of residual motion based on tracking information showed a reduction of the substitute tumour motion with gating beam delivery. For duty cycles of 15%, 25%, 35%, 50% and 60% the measured residual motion at the 95th percentile were 1.75 mm, 4.1 mm, 5.11 mm, 8.56 mm and 9.25 mm, whereas the standard deviations of residual PDFs determined with PortalTrack were 0.77 mm, 1.38 mm, 1.82 mm, 2.65 mm and 3.26 mm, respectively. Results showed a relationship between residual motion and gating duty cycle, with a decreasing trend in residual motion as smaller gating duty cycles were applied, as observed in Figure 4.4(e).

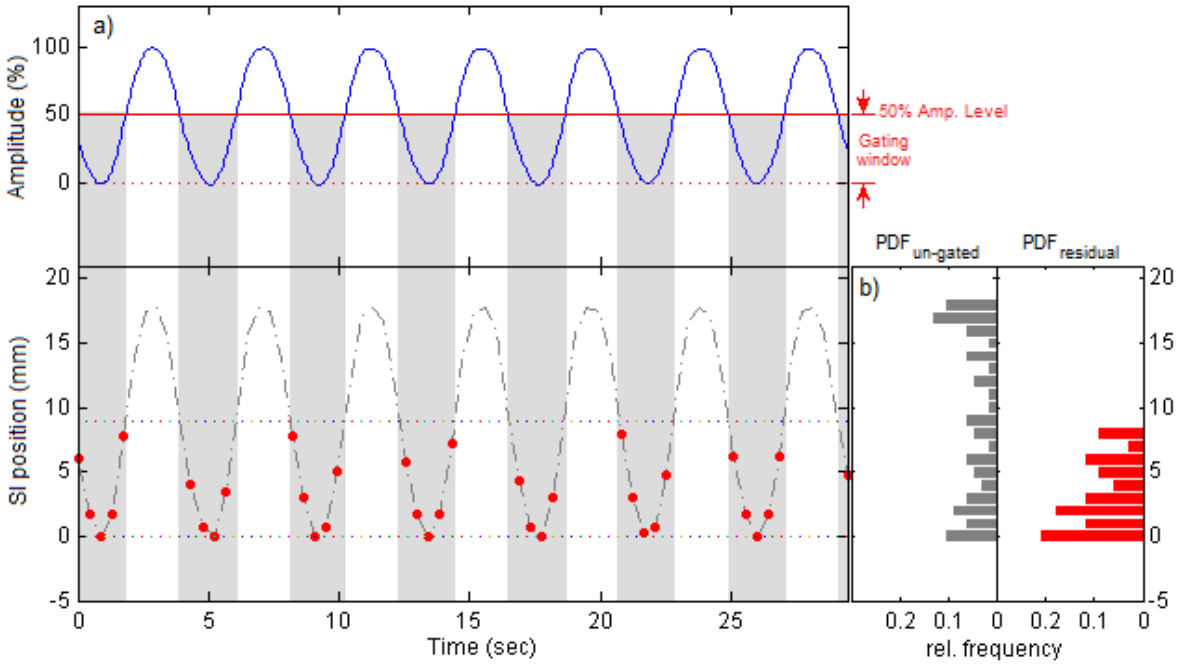

(a) Target positions detected in the superior-inferior direction (red dots) during simulated gated treatment with 50% dc

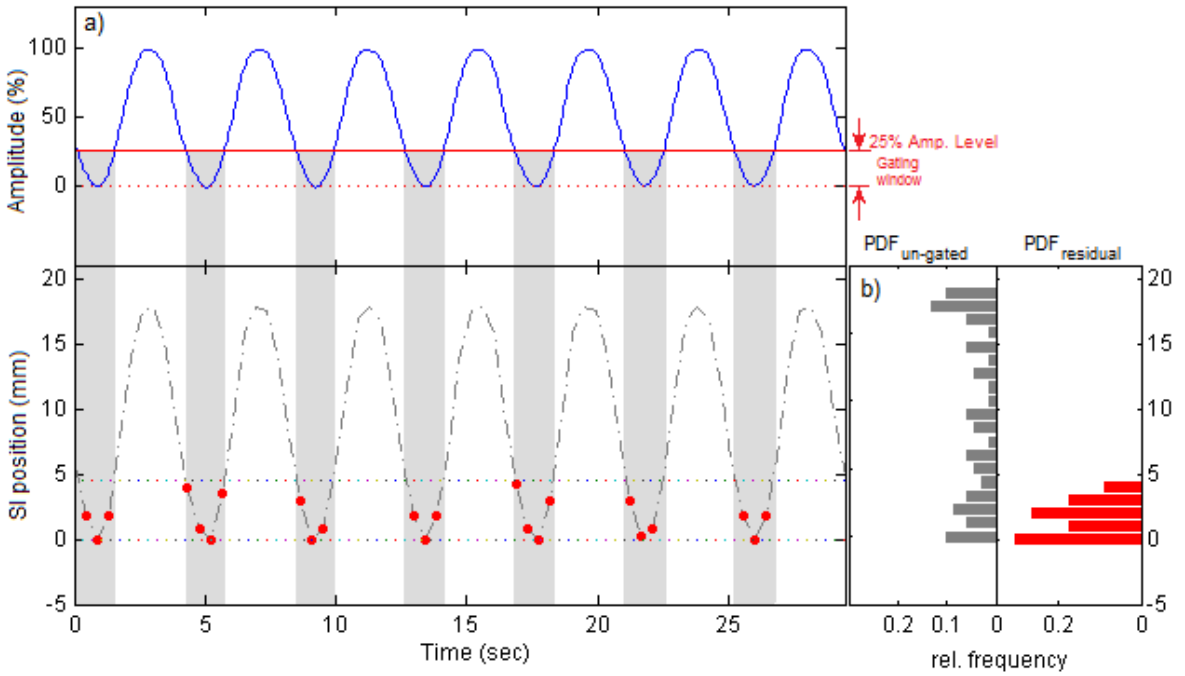

(b) Target positions detected in the superior-inferior direction (red dots) during simulated gated treatment with 25% dc

Figure 4.3: *Positions of tumour substitute determined with PortalTrack (red dots) during the time the external signal falls inside the gate (shaded regions) for simulated gated treatments with duty cycles of 50% (a) and 25% (b), and resulting distribution histograms, $PDF_{residual}$, (red histograms)*

Moreover, a reduction in the standard deviations of the determined PDFs$_{residual}$, representing the spread of detected positions inside the gating window, was also observed. With gating, the standard deviations of residual PDFs were reduced by 27% - 50%, relative to the un-gated distribution with 6.57 mm standard deviation. Although these results seem intuitively obvious with regard to the functionality of gated delivery, PortalTrack gave an extra degree of confidence to gated treatment by allowing the direct monitoring of target motion in the linac beams-eye-view during treatment. This represents a significant improvement compared to gated treatment procedures conducted in the absence of an image-guided tool for verification of treatment.

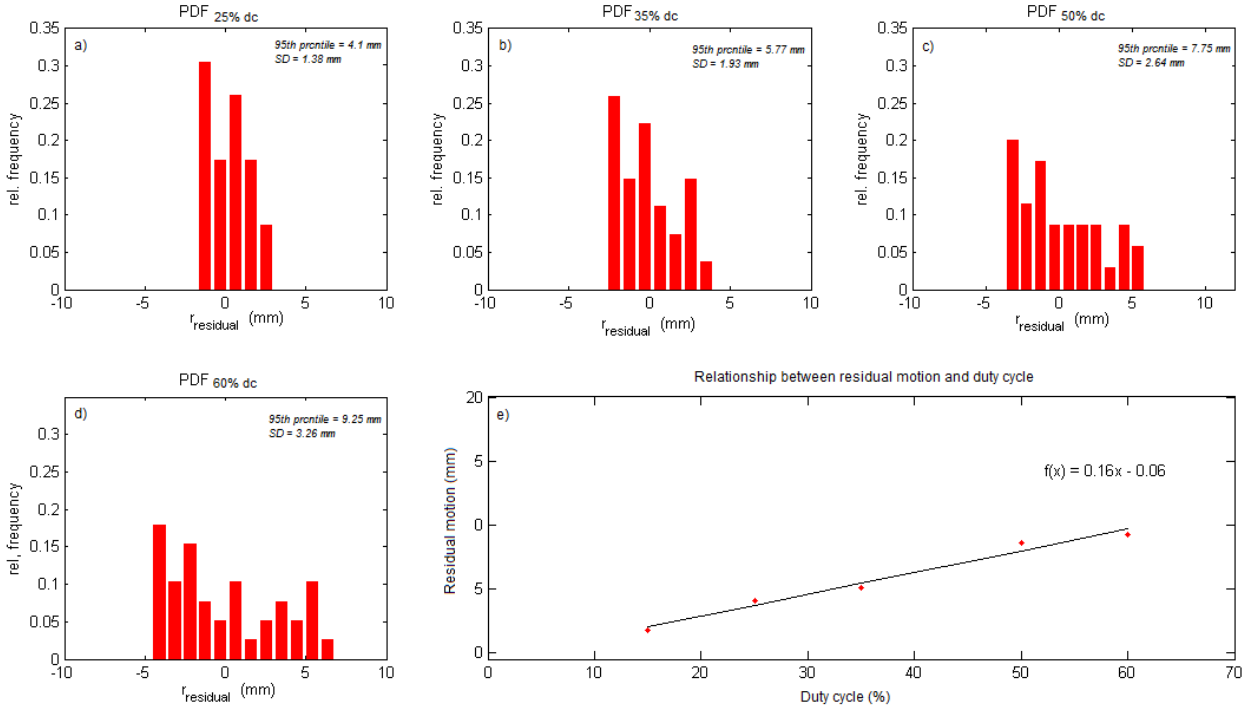

Figure 4.4: *Residual motion distribution histograms for applied gating duty cycles of 25%(a), 35%(b), 50%(c) and 60%(d). The residual motion as function of gating duty cycle show a linear relationship (e).*

4.2.2 Variations in Residual Motion

The objective of this section was to investigate the effects irregularities in the target trajectories, as well as discrepancies in the external/internal correlation on residual motion. Intra-/interfractional variations in both the internal tumour mobility and breathing patterns have been reported in the literature [26, 27, 28, 39, 45, 46]. For instance, the external signal may drift downwards as the patient relaxes. As a result, clinicians are required to monitor the external signal during treatment and once a drift is identified the treatment may be interrupted [17, 26]. However, if there is no information regarding the tumour position during treatment there is no way to identify variations in the internal trajectory of the tumour. Large fluctuations in residual tumour motion have been reported [46, 56]. Even

at the same external duty cycle the tumour may exhibit more or less residual motion intra-/interfractionally. The lack of monitoring means uncertainty [17], which may result in gating errors leading to false negatives and false positives [29, 47].

Baseline drifts of 3 mm and 6mm, which are within the ranges of those found in the literature regarding the tracking of lung tumours in stereotactic body radiotherapy (± 4 mm) [39], were simulated. Only the internal trajectories of tumour substitute were perturbed whereas the external signals were kept un-changed through simulated gated treatments. All drifts were simulated towards the EOE direction of respiration. The effects a regular (path 1) and an irregular exhibiting a baseline drift of ≈ 3 mm (path 2), with a reference 35% dc gating window, is illustrated in Figure 4.5. Such irregularity led to a systematic shift of exhale positions, deviating from their intended position, which was defined by the gating window (the region within the two horizontal dotted lines drawn in the internal signal plot). This irregularity is reflected in the spread of $\mathrm{PDF}_{(residual)}$ in the direction of drift (red histogram), causing an increase in standard deviation of the residual PDF from 1.93 mm to 2.52 mm (30% increase) and in residual motion from 5.77 mm to 8.42 mm (46% increase), compared to gated delivery with same gating duty cycle in the absence of baseline drift. Moreover, such deviations of the target from reference position could represent incidences of target underdosage.

It is expected that a larger drift could result in a more significant increase in residual motion, which in turn could lead to incidences of false positives (beam-on at the wrong target position [29]), such as in the case shown in Figure 4.6. For this example, a 6 mm drift resulted in an increase in residual motion up to 11.37 mm with same reference duty cycle, which constitutes a percentage increase between 36% to 97%, compared to path 1 and path 2, respectively. This could have adverse effects on accuracy and efficacy of external based gating. Furthermore, such irregularity would have passed unnoticed in the absence a verification tool such as PortalTrack in order to detect possible deviations of the target from reference position, which may not be manifested in the external signal pattern. These observations are comparable to those pointed out in the work by Nelson *et al* [56]. Investigators found unexpected tumour motions during gated treatment, which was not reflected in the analysis of the external signal, leading to significant magnitudes (> 2 cm) of residual tumour motion.

Overall, baseline drifts were detected and tracked with PortalTrack during simulated gated deliveries. In Figure 4.7, the residual PDFs determined with PortalTrack, as well as, their calculated parameters of standard deviation and ranges of residual motion, resulting from simulated gated treatments with duty cycle of 15%, 25%, 35%, 50% and 60%, are shown for paths (1-3). The first column corresponds to a regular (path 1) trajectory of tumour substitute, whereas the second and third columns corresponds to irregular trajectories exhibiting drifts of 3 mm (path 2) and 6mm (path 3). In contrast to a regular path of tumour substitute, a 3 mm drift led to increases in standard deviation of residual PDFs from 1.48 mm to 4.11 mm and in residual motion from 5 mm to 13.32 mm, whereas for the case of 6 mm drift from 2.15 mm to 4.37 mm and from 7.59 mm to 15 mm, respectively. A correlation between baseline drift and residual motion was observed. Baseline drifts led to an increase in residual motion by a value approximately equivalent to the magnitude of the simulated drift.

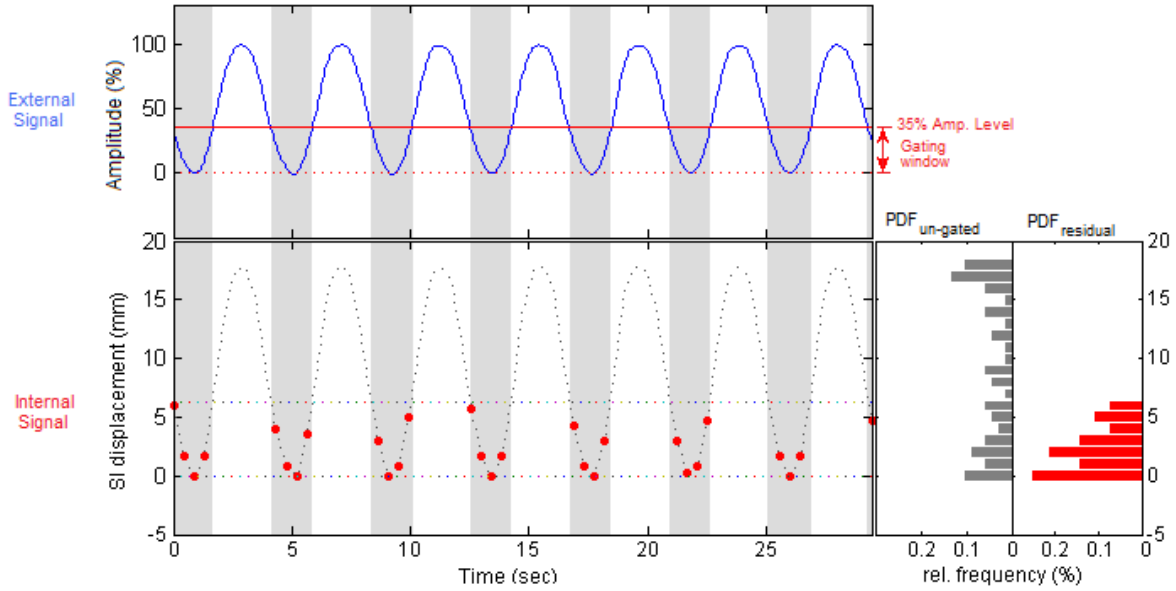

(a) Regular trajectory (path 1) of target detected within a 35% gating window

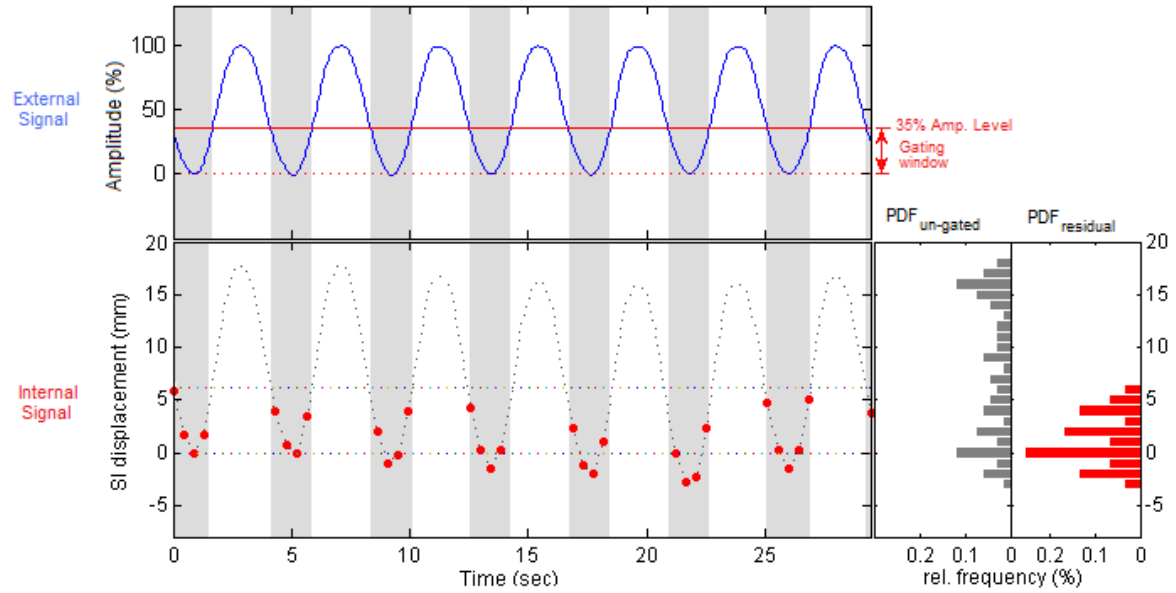

(b) Irregular target trajectory exhibiting baseline drifts ≈a 3 mm (path 2) detected within a 35% gating window

Figure 4.5: *Two examples of target tracking during simulated gated delivery with a 35% dc reference gating window for a regular (a) and another irregular (b) trajectory of tumour substitute. A 3mm baseline drift led to deviations in the target's path from the intended position.*

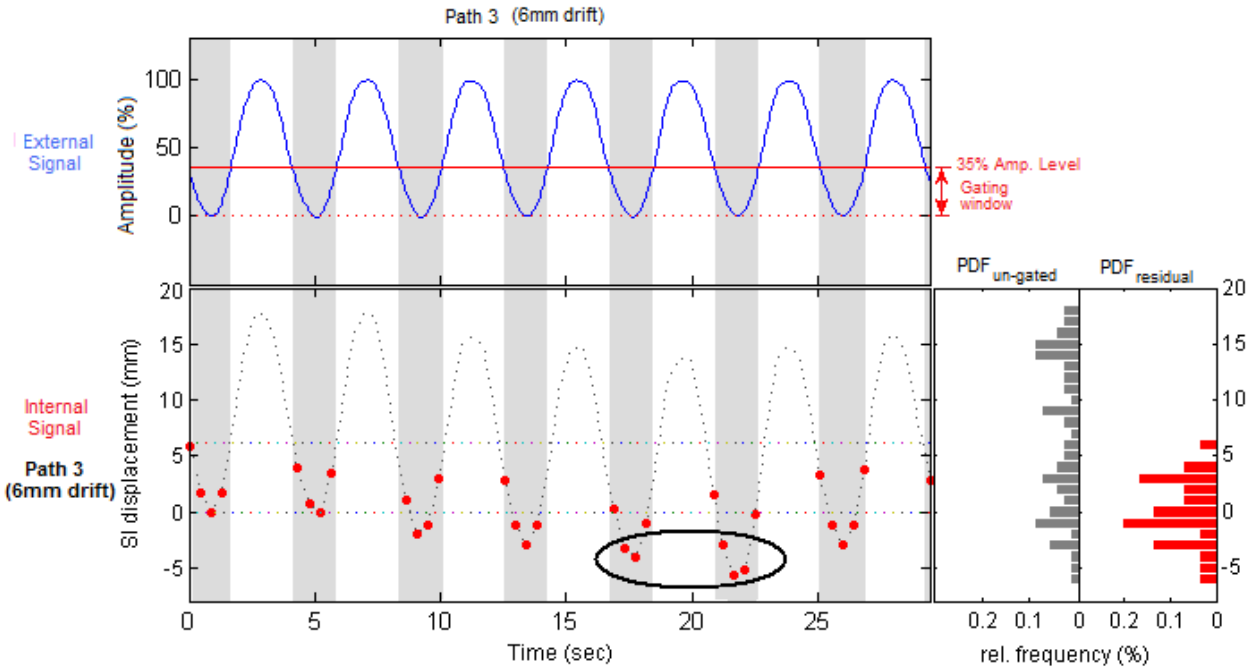

Figure 4.6: Motion path of tumour substitute exhibiting a 6 mm baseline drift. Such irregularity leads to significant deviations from target's intended position, increasing the chances of marginal miss

Simulations showed that increases in residual motion may be compensated, to a certain extent, by narrowing the gating window. For instance, for a simulated trajectory exhibiting a drift of 3 mm the residual motion was reduced by 62.5% with a 15% dc compared to a larger gating window of 60% dc. Whereas, a reduction in residual motion of about 49% was only observed for target under the influences of larger 6 mm drift. However, at the expenses of prolonged delivery times, as demonstrated in previous chapter (Chapter 3, section 3.2.1).

4.2.3 Comparison with Ideal PDFs

This section investigates the trade-offs between faster (ideal) image acquisition and the current frame rate of the system. The system presented herein offered a frame rate of ≈ 2 frames/sec due to the hardware characteristics of the amorphous silicon flat panel detector, whereas the time needed by tracking algorithm to find each position (best match) of tracked object in portal images was on average 0.3 sec $\pm$ 0.1 sec, which could be reduced by a factor of 4 by skipping every second row and column within the search range during the search for best match, as reported in the work by Wilbert *et al.* [42]. As a result of this, it was evaluated whether the tracking information was sufficient to quantify residual motion as well as other irregularities in the internal target paths that could have been underestimated.

Simulated trajectories obtained from tracking the tumour substitute in EPID movies were interpolated to 0.05 sec intervals, corresponding to a frame rate of 20 frames/sec. This rate was roughly similar to the sampling frequency at which the external signal was acquired.

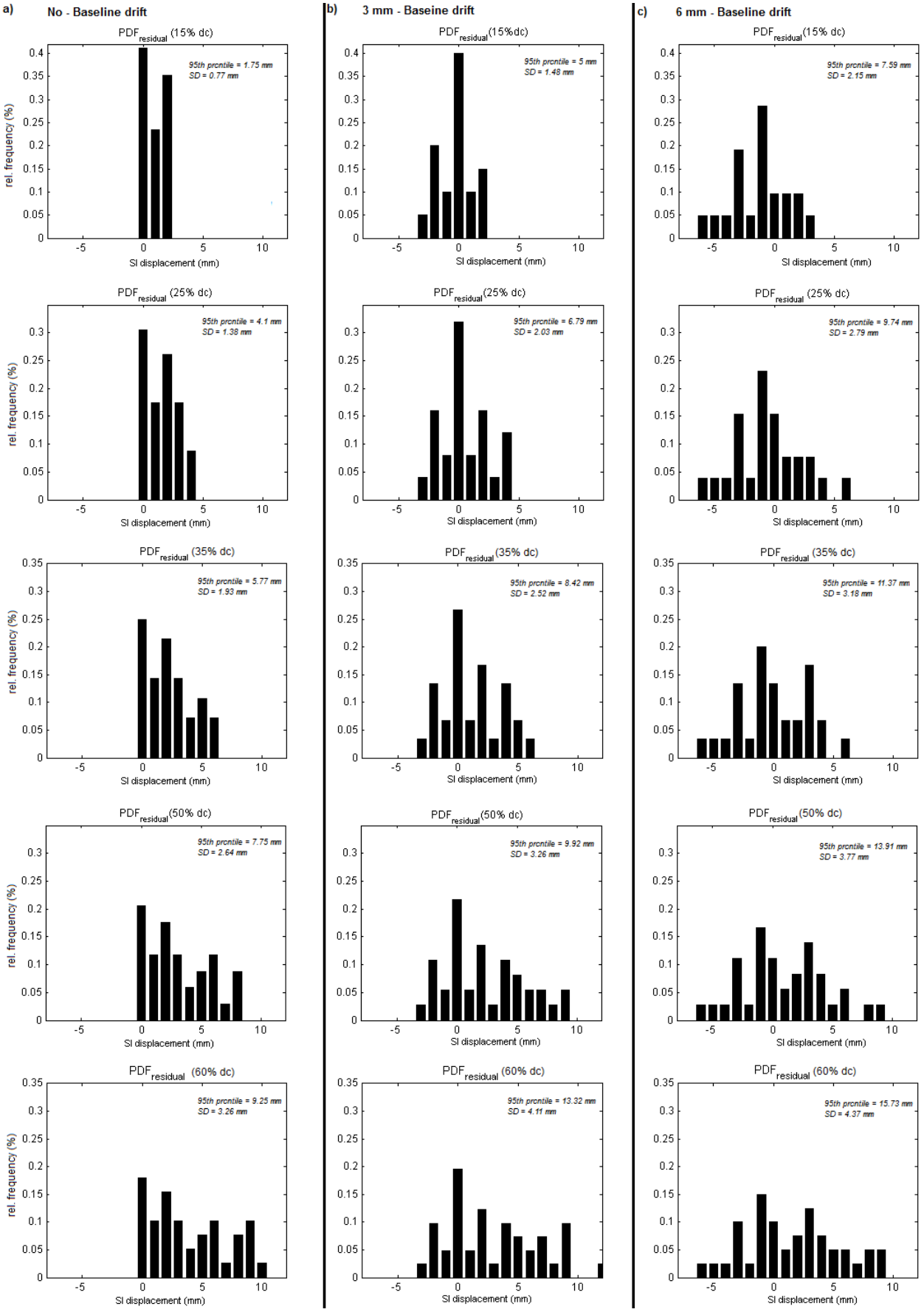

Figure 4.7: Resulting residual PDFs ($PDF_{residual}$) corresponding to motion paths 1 (left column), path 2 (middle) and path 3 (right column)

The comparison of ideal PDFs, obtained from interpolated data, against those determined with PortalTrack ($PDF_{residual}$) is illustrated for the three cases (paths 1-3) shown in Figure 4.8. The 95th percentile of PDF$_{(residual)}$ in a 35% duty cycle window served as reference value of gating efficiency. From this figure, it can be observed that most of the positions in or near the end-exhale were detected by PortalTrack. Furthermore, exhale positions were tracked even when the target exhibited baseline drifts, provided that the target moves within gating window. This is better illustrated by the residual PDF corresponding to path 1 (regular/no-drift) showing a peak around the end-exhale phase, Overall, the shapes of residual PDFs resemble those of ideal PDFs for the three cases, with their standard deviations and calculated values residual motion of residual PDFs differing by 0.01 mm and 0.52 mm, 0.07 mm and 0.8 mm, 0.08 mm and 0.07 mm for path 1, path 2 and path 3, respectively.

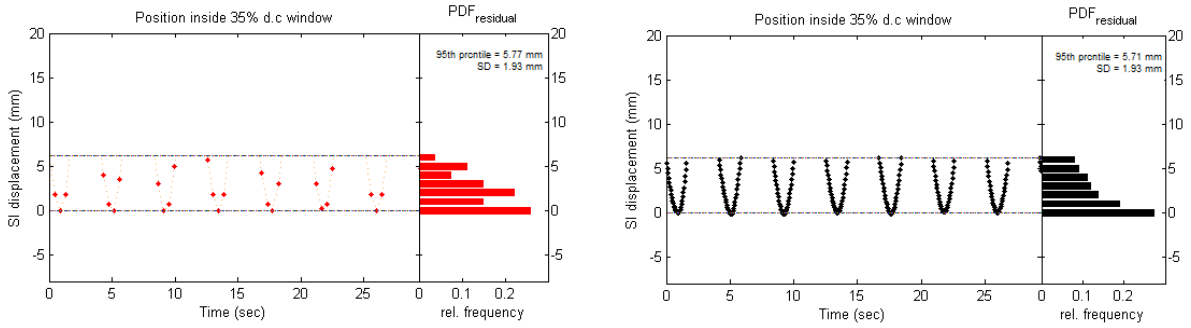

(a) Path 1

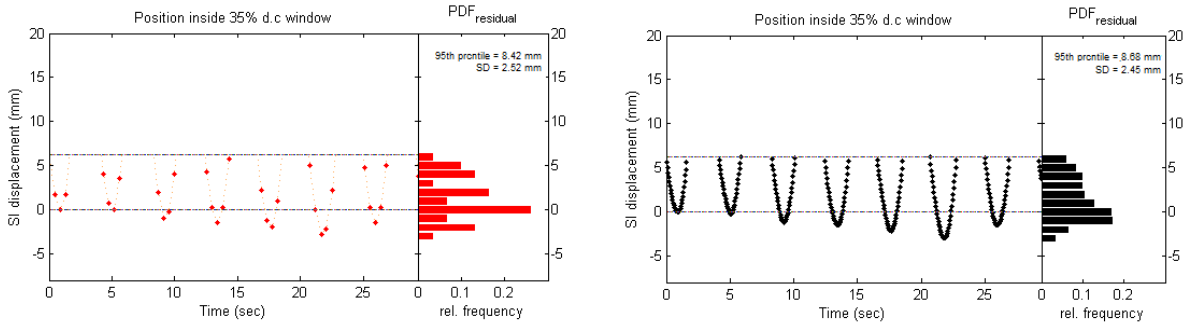

(b) Path 2

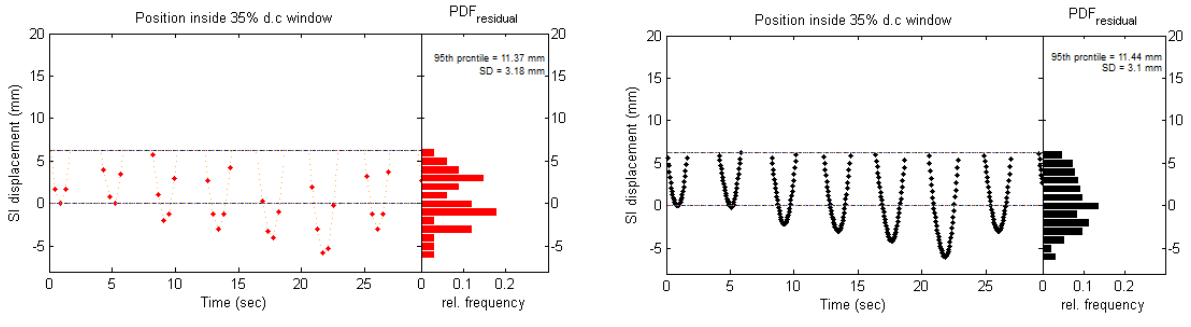

(c) Path 3

Figure 4.8: Comparison between the position information obtained by PortalTrack (in red) and interpolated data at 0.02 sec intervals (in black) representing the true target motion inside the gating window. A reference gating window with 35% dc was used for all simulated delivery sessions.

A summary of measured parameters of standard deviation, mean and residual motion for both residual ($PDF_{residual}$) and ideal (PDF_{ideal}) position distribution histograms corresponding to regular and irregulars trajectories, is given in Table 4.1. For the simulated gated treatments with hypothetical gating windows of 15%, 25%, 35%, 50% and 60% duty cycles, the differences between the *'true'* values of residual motion and those determined with PortalTrack $\Delta\,|PDF_{ideal} - PDF_{residual}|$ ranged from 0.05 mm to 1.08 mm with a mean difference of 0.4 mm ± 0.3 mm. Figure 4.9 compares the residual motions measured with PortalTrack and those representing their true values obtained from interpolated data for target paths (1-3) and simulated gated deliveries with duty cycle between (15% - 60%). The shifts in the measurements of residual motion corresponding to path 2 and path 3 relative the path 1 are explained by the effects of baseline drifts, which led to a systematic shift in exhale positions and hence in an increase in the residual motion within the gating window. The magnitude of the shift is proportional to that of the simulated drift. These increases in residual motion are correlated with increases in the margins that would be required to compensate for the effects of baseline drifts, in addition to the margins already allocated for the compensation of residual motion taken into account during treatment planning process based on 4DCT or a fluoroscopy session. From Figure 4.9 it can be observed that PortalTrack gives a very close estimate of the true residual motion.

Table 4.1: *Comparison of measurements of residual motion and standard deviation of position distributions determined with PortalTrack ($PDF_{residual}$) and those obtained using interpolated data (PDF_{ideal}), representing an ideal system capable of faster processing compared to PortalTrack. For all the PDFs the mean (m) and standard deviation (m) are given.*

Path #	DC %	$PDF_{m\pm SD}$ (mm)		$\mathrm{PDF}_{95^{th}prctile}$ (mm)		
		PortalTrack	*Ideal*	*PortalTrack*	*Ideal*	$\Delta\ 95^{th}prctile$
1	15	0.80 ± 0.77	0.89 ± 0.84	1.75	2.44	0.69
	25	1.50 ± 1.38	1.51 ± 1.38	4.09	4.14	0.05
	35	2.02 ± 1.93	2.19 ± 1.93	5.77	5.71	0.06
	50	3.06 ± 2.64	3.17 ± 2.72	7.75	8.12	0.35
	60	3.87 ± 3.26	3.82 ± 3.25	9.25	9.68	0.43
2	15	0.01 ± 1.48	-0.04 ± 1.43	5	5.22	0.22
	25	0.73 ± 2.03	0.67 ± 1.95	6.79	7.12	0.33
	35	1.29 ± 2.52	1.35 ± 2.45	8.42	8.68	0.25
	50	2.09 ± 2.99	2.32 ± 3.19	9.92	11.01	1.07
	60	3.52 ± 4.11	2.96 ± 3.70	13.32	12.53	-0.79
3	15	-1.27 ± 2.15	-1.08 ± 2.2	7.59	8.19	0.6
	25	-0.06 ± 2.79	-0.30 ± 2.65	9.74	9.83	0.09
	35	0.41 ± 3.18	0.37 ± 3.1	11.37	11.44	0.07
	50	1.39 ± 3.77	1.42 ± 3.78	13.64	13.91	0.27
	60	2.29 ± 4.37	2.16 ± 4.32	15	15.73	0.73
						0.41 ± 0.31

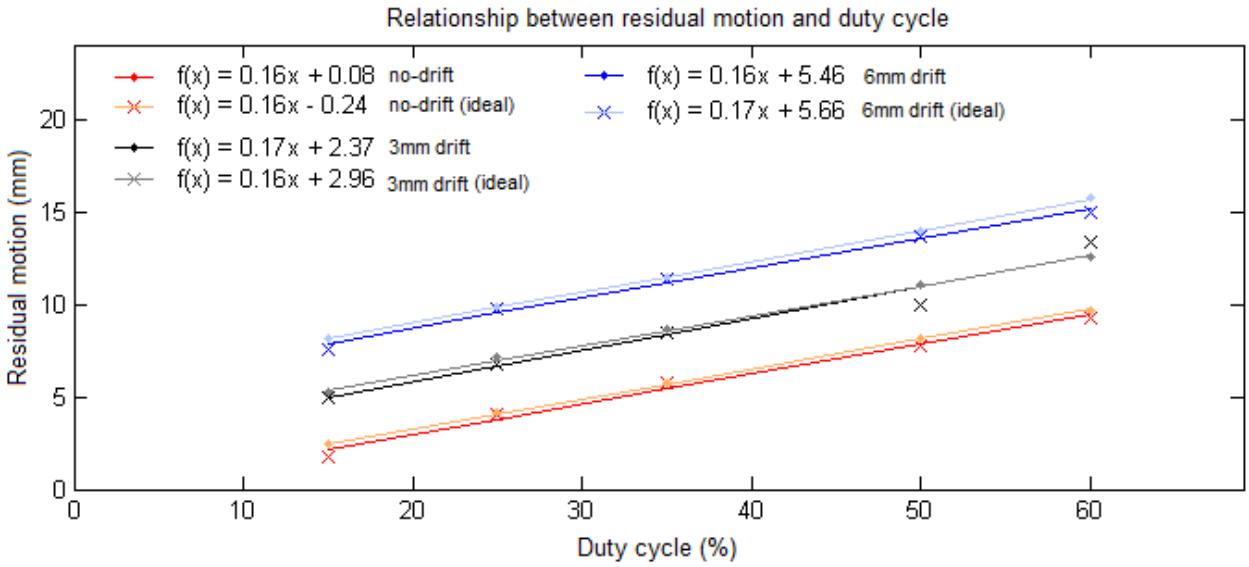

Figure 4.9: Comparison of determined residual motions with PortalTrack and their ideal values for motion path $1_{nodrift}$ (data points in red/light red), path $2_{3mmdrift}$ (data points in black/gray) and path $3_{6mmdrift}$ (data points in blue/light blue).

4.3 Summary

This study evaluated the suitability of a clinical tool for real-time tumour position verification during gated beam delivery. The approach is based on the direct imaging and tracking of moving targets in portal images, acquired during beam-on time, without the aid of implanted markers and using the therapeutic MV treatment beam. Under the simulation of gated beam delivery, different gating duty cycles were applied and the target residual motion during beam-on time measured. Simulations showed that PortalTrack is capable of measuring target motion within the gating window. Measurements of residual motion showed a relationship between gating duty cycle and residual motion, with smaller duty cycles leading to less residual motion inside the gating window. Although such results supported the functionality of gated beam delivery, whose main goal is to reduce target motion within the treatment portal, PortalTrack gave added confidence in the simulated treatment procedure since it allowed for the direct monitoring of the target motion during dose delivery.

Investigations of the effects of baseline drifts on residual motion indicated a clear correlation between both parameters. Baseline drifts led to an increase in residual motion by a factor approximately equivalent to the magnitude of exhibited drift. Compensating for baseline drifts would require larger margins than those initially assigned during treatment planning based motion characteristics, i.e. peak-to-peak motion amplitude, of the tumour acquire through fluoroscopy or 4DCT.

Tracking information was sufficient to quantify residual motion. The relative slow frame rate of the tracking system did not constitute a limitation when estimating values of residual motion. Residual motion determined with PortalTrack was very close to the true residual motion, with a mean difference of 0.41 mm $\pm$ 0.31 mm for all simulated trajectories and

gated treatments. Furthermore, tracking information showed that variation in residual motion, such as those resulting from baseline drifts, may be compensated by adjusting the gating window, however only to a certain extent, as there may be cases in which the residual motion is so large that it cannot be dealt with by only narrowing the gating window. Such tracking information could potentially be used to update/validate the degree of external/internal correlation, using the tracking information as the true tumour signal, to correct possible variations in the external signal which may arise during treatment [47]. Alternatively, tracking information can be used to adjust or adapt the gating window to compensate for variations in residual motion, as suggested by Aristophanous *et al.* [17].

Chapter 5

Clinical Study

In this section, the feasibility of the approach presented in the previous chapter was evaluated by means of a clinical case study. The objective of this study was not to quantitatively prove or disprove the degree of internal/external correlation, but to investigate the possibility of treatment verification with PortalTrack which may improve the safety and effectiveness of external based gated RT.

5.1 Method and Materials

Data Acquisition

The approach for tumour position verification was retrospectively evaluated based on patient data collected at the Department of Radiation Oncology, University of Wuerzburg. The subject was a lung cancer patient treated with stereotactic body radiotherapy (SBRT) with a prescribed dose of 57.6 Gy delivered over 3 fractions using 6 fields per fraction. During treatment delivery, EPID movies were acquired by megavoltage imaging of the treatment beam, producing a projection of the tumour onto the plane of the electronic portal imaging device (EPID) (see Figure 5.1). The tumour position is determined in portal images of acquired EPID movies, which represented the internal signal. At the same time, the three dimensional (3D) breathing motion of the abdomen of the patient was recorded by tracking an optical marker placed on the abdomen of the patient with an infrared camera (Polaris, NDI, Waterloo, Ontario, Canada), referred to as external signal (see Figure 2.5). Overall, this resulted in the synchronised acquisition of both internal and external datasets during treatment. For this study only the one dimensional (1D) anterior-posterior (AP) component of the external signal was used for the simulation of gated treatment, hence mimicking the use of commercially available gating systems. Moreover, only tumour motion in the superior-inferior (SI) direction was studied since this is the predominant direction of motion observed for tumours in the lung [27, 39].

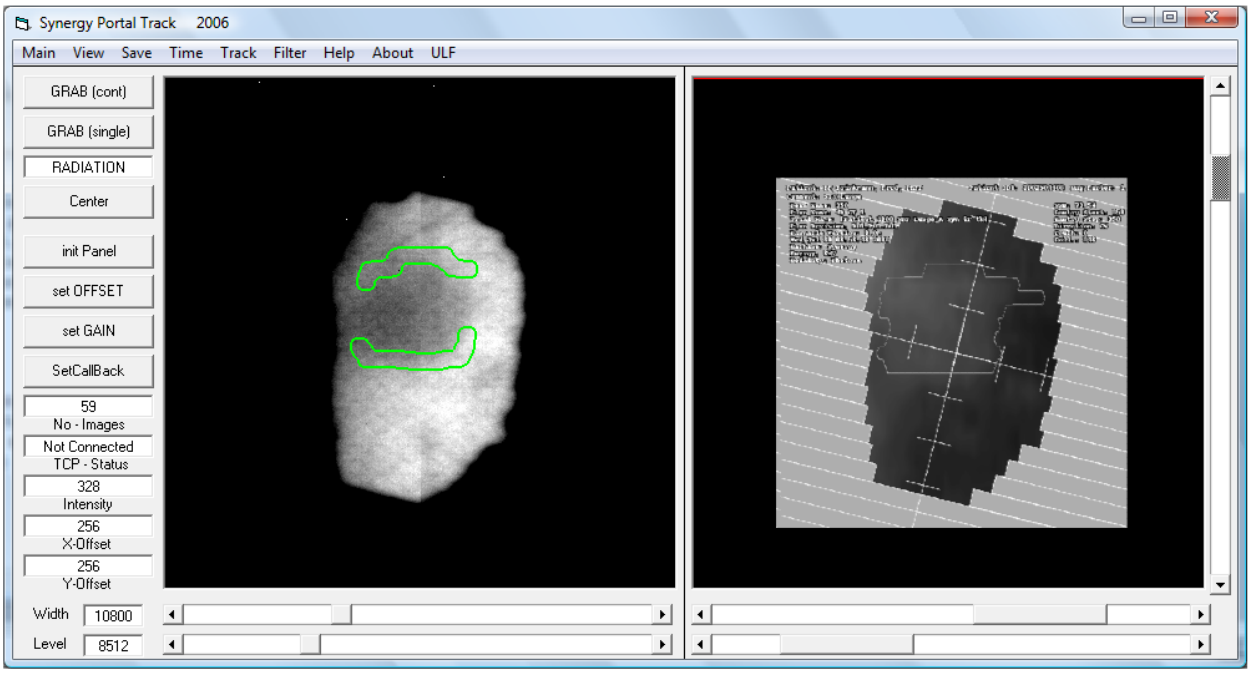

Figure 5.1: *Display window from PortalTrack showing a lung tumour being tracked in the beam's-eye-view (left panel), and corresponding DRR (right panel) used for the definition of the search mask (green annular contour).*

Gating Window Definition

For the simulation of gated treatment both external and internal signals were first analysed over a treatment observation time, corresponding to the first 30 seconds of treatment, to define gating parameters, i.e. gating duty cycle, whether to gate at EOE or EOI. In a real gating procedure, such parameters are defined based on the information provided by fluoroscopy or 4DCT imaging of the patient. During observation time an external amplitude (EA) and an end-exhale baseline (Ext. baseline) were determined by taking the average of all the peak-to-peak amplitudes and end-exhale positions of the external signal. A fixed gating window was defined by the distance between the end-exhale baseline and a reference 35% amplitude threshold level, referred to as external upper limit (Ext. UL), set on the external respiratory signal (red horizontal line), as illustrated in figure 5.2(a). The choice of the reference 35% duty cycle, resulted in $\approx$ 6 mm residual tumour motion, which was assumed to be clinically allowed for the simulation of gated treatment as indicated in the literatute [18, 29]. The gating window remained unchanged (fixed) throughtout fraction delivery (6 fields), mimicking an amplitude-based gating approach with fixed gating window. Obscuring of portal images, which were not in inside the gating window, was performed as discussed in the previous chapter.

Permitted Range of Residual Tumour Motion

Additionally, a reference frame by which possible deviations of tumour from its intended position could be judged, i.e. permitted range of residual motion, was defined during treatment

observation time. As result of the 35% dc gating window set on the external signal, it was assumed that no more than 6 mm residual motion was allowed. During pre-treatment time the internal signal, which was available over the entire time, was retrospectively analysed in the same fashion as the external signal. An internal tumour motion amplitude (IA) of 16.7 mm ± 2.9 mm was determined by taking the average peak-to-peak motion amplitude all breathing cycles found over the observation time. An internal baseline (Int. baseline) was also defined by taking the average of all end-exhale tumour positions found over treatment observation time. A transformation factor (TF), the ratio of external amplitude (EA) to internal amplitude (IA), allowed to translate the external to internal amplitude and vice versa. The permitted range of residual motion was defined by the distance between the internal baseline (Int. baseline) and the internal upper limit (Int. UL), which was calculated by dividing the reference gating window (35% of EA) by TF. Defining this permitted range of residual motion will allow the appreciation of variations in the internal mobility of the tumour, as well as in the reproducibility of tumour exhale positions, relative to the planned position, which may arise during treatment. In an idealised gated treatment the exhale positions should be fairly stable and fall within this range to ensure adequate tumour coverage.

Figure 5.2 shows all the parameters defined for both internal and external signals over pre-treatment time. On the external signal plot the gating window is defined by Ext. UL (35% amplitude level in red) and Ext. baseline (Figure 5.2 (a)), whereas on the internal signal plot the permitted range of residual motion by the Int. UL and Int. baseline (black horizontal dashed line) (Figure 5.2 (b)). The red dots represent the tumour positions obtained from tracking the tumour in portal images during beam-on time.

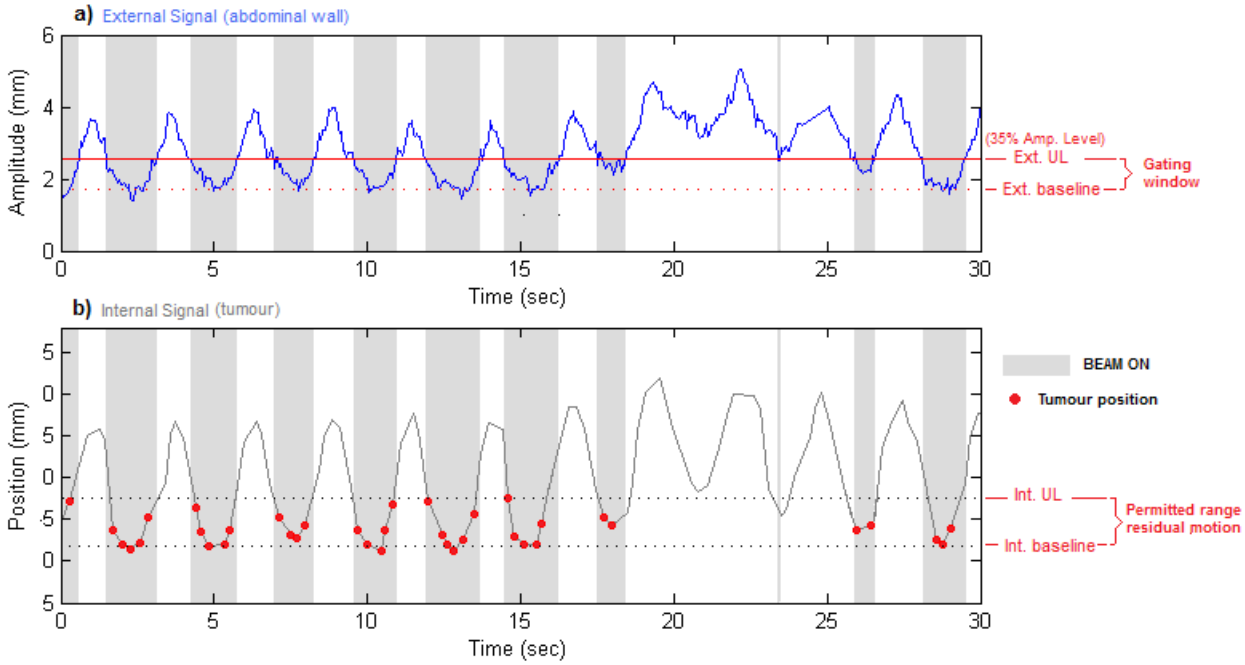

Figure 5.2: *Definition of gating window on external respiratory signal (a), and permitted range of residual motion (b) during pre-treatment observation time (first 30 sec of treatment).*

Tumour Tracking

The definition of the reference mask for tumor tracking was based on the digitally reconstructed radiographs (DRR) generated for each beam during treatment planning. This was conducted in order to help identify the tumour in the reference image to ensure that the tracking algorithm follows the actual tumour and not projections of other anatomical regions [42]. The contour of the macroscopic tumour was overlaid and stored with the DRR. Both the EPID movies and DRRs were loaded into PortalTrack for simulation of gated treatment and tumour tracking. From each EPID movie a representative portal image, in a corresponding phase of the breathing relative to the DRR, was selected for mask definition. The reference mask was drawn by retracing the tumour contour in DRR and at the same time drawing the reference mask over the representative portal image. In some cases, a characteristic nonhomogeneous part of the tumour visible in representative portal was sufficient for mask definition avoiding the need to encompass the whole tumour, as shown in Figure 5.3. All pixel values within the defined reference mask were stored. As in the previous chapter, the mask was instructed to move pixel-wise, relative to the previous frame over a search range of 30 pixels in each direction. The tumour was tracked in portal images during simulated gated treatment and determined positions were stored to determine residual PDFs.

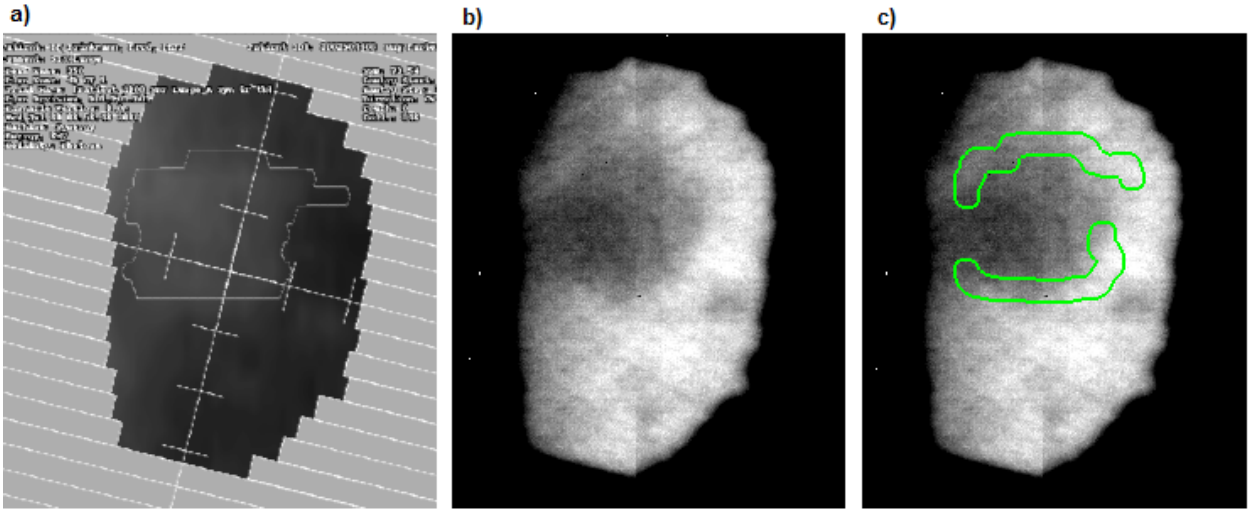

Figure 5.3: *a) Digitally reconstructed radiograph (DRR) showing the tumour and CTV. (b) Representative portal in corresponding phase of breathing relative to DRR, and (c) definition of reference mask based on macroscopic tumour contour defined on DRR.*

Tumour Position Verification

For this study, the residual motion metric was based on the work by Berbeco *et al.* [59], by calculating $r_{(residual)}$, which is the difference between each gated data point (tumour position determined in each portal image along superior-inferior direction), $y_{(i)}$, and the daily average gated position, $y_{(daily,ave)}$, which is the average tumour position obtained by tracking the tumour in all portal images acquired during beam-on time for the fields in one fraction, as shown by equation (5.1). Doing this, allowed one to factor out the interfractional (day-to-

day) error components when calculating the residual tumour motion during fraction delivery, thus highlighting possible intrafractional (beam-to-beam) variations in residual motion for a given day.

$$r_{(residual)} = (y_{(i)} - y_{(ave)}) \tag{5.1}$$

This difference ($r_{(residual)}$) formed a residual motion distribution histogram ($PDF_{residual}$) comprising all target positions detected inside the gating window. For each beam, their corresponding residual distribution histograms ($\text{PDF}_{residual}$) were described in terms of their standard deviations and 95^{th} percentiles. Furthermore, deviations in the end-of-exhale tumour positions, which crossed downwards pass the predefined internal baseline (Int. baseline), were measured to give an estimate of the magnitude of exhale fluctuation, as suggested in the work of Nishioka *et al.* [26].

5.2 Results and Discussion

A total of 386 portal images were acquired during fraction delivery corresponding to treatment fields (1-6) at gantry angles 240^o, 195^o, 285^o, 350^o, 130^o and 150^o, respectively. Simulations showed that tumour motion can be monitored and tracked during RGRT with PortalTrack. In figure 5.4 and 5.5, both the external, guiding the onset of the gates, and the internal, tumour positions detected during beam-one, movement plots are illustrated. For each beam, the gating window is drawn on the respiratory signal, which remained constant throughout all six fields. The shaded regions represent the time during which the gate was open. At the instance when the respiratory signal falls in the gate, tumour position is obtained from tracking tumour in portal images (red dots). In addition, the resulting residual motion distribution histograms (red histograms) are given, representing the distribution of all tumour positions determined with PortalTrack during beam-on time ($PDF_{residual}$). Furthermore, the tumour trajectories obtained without any control for respiration (un-gated delivery), shown in the background (gray dotted path) of each internal signal plot, as well as corresponding histograms (gray histograms) are also included for two reasons: *(i)* to highlight the possible occurrence of false negatives (beam off while tumour is inside gating window) and false positive (beam on while the tumour is outside gating window), which may have arisen from changes in the internal/external correlation during treatment; and *(ii)* to use tracking information to evaluate the efficacy of gated delivery to reduce interfractional tumour motion in both the absence or presence of possible intrafractional variations during treatment.

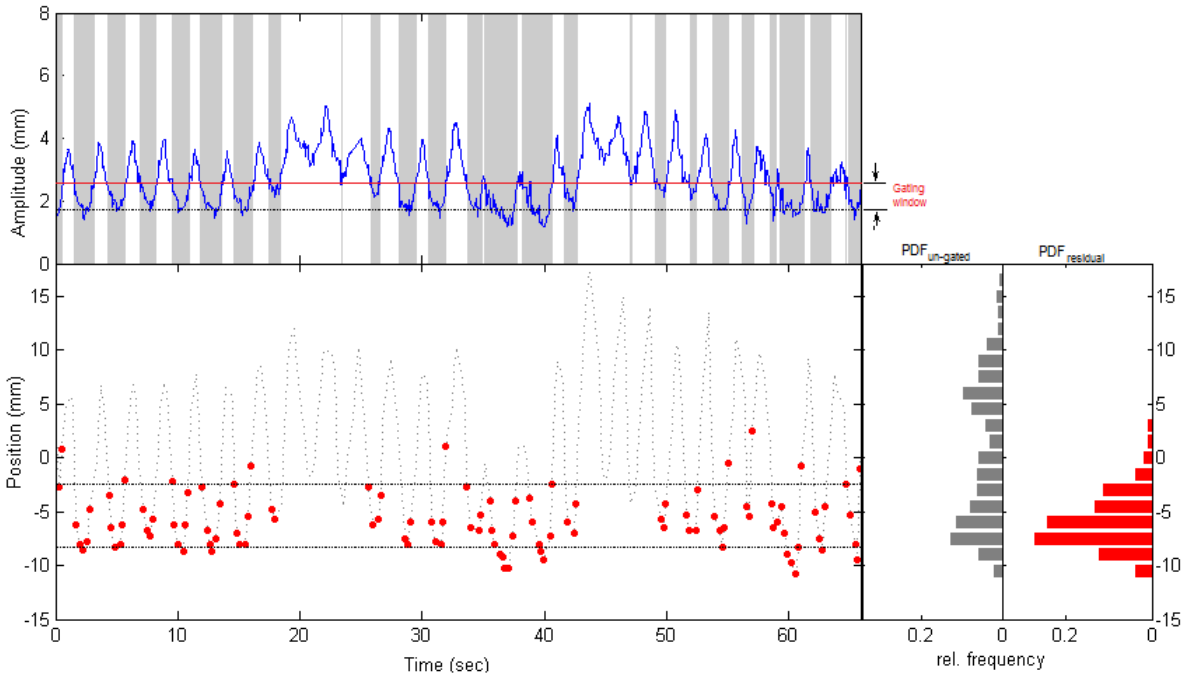

(a) Beam 1 (Gantry 240^o)

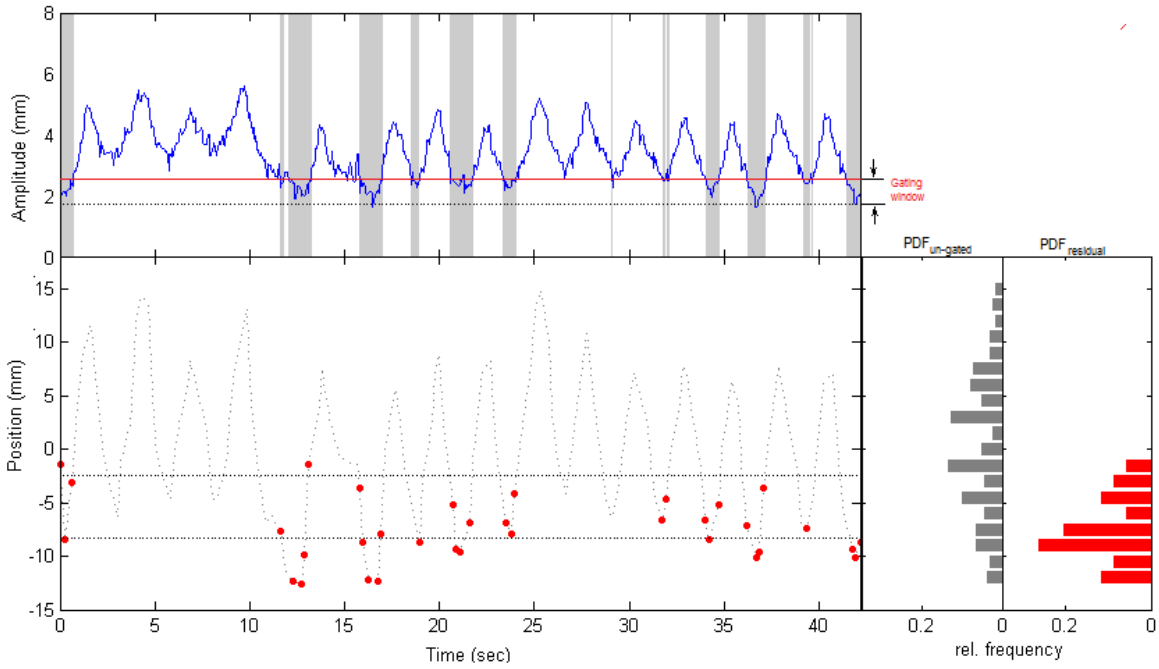

(b) Beam 2 (Gantry 195^o)

Figure 5.4: Fraction one beam 1-2

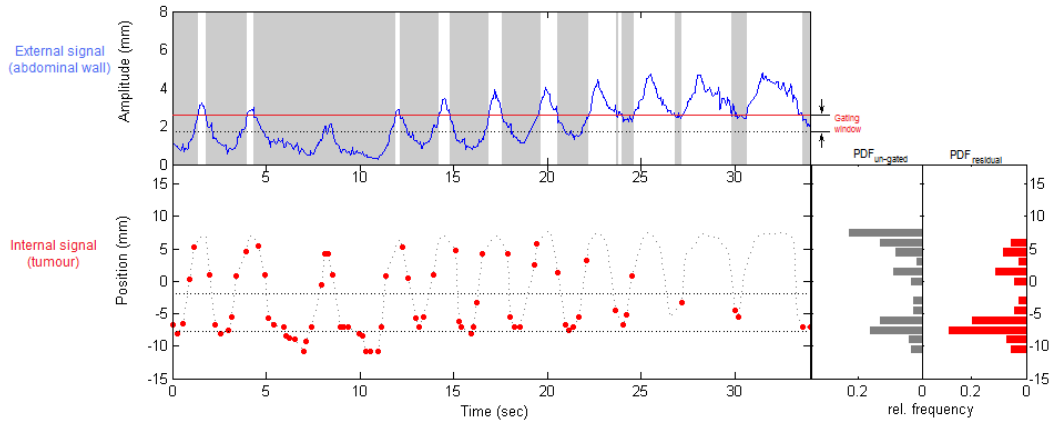

(a) Beam 3 (Gantry 285^o)

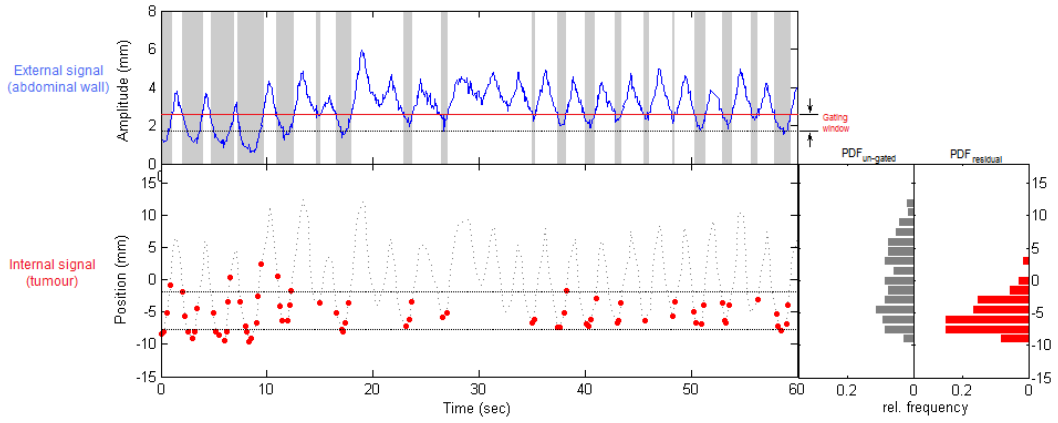

(b) Beam 4 (Gantry 350^o)

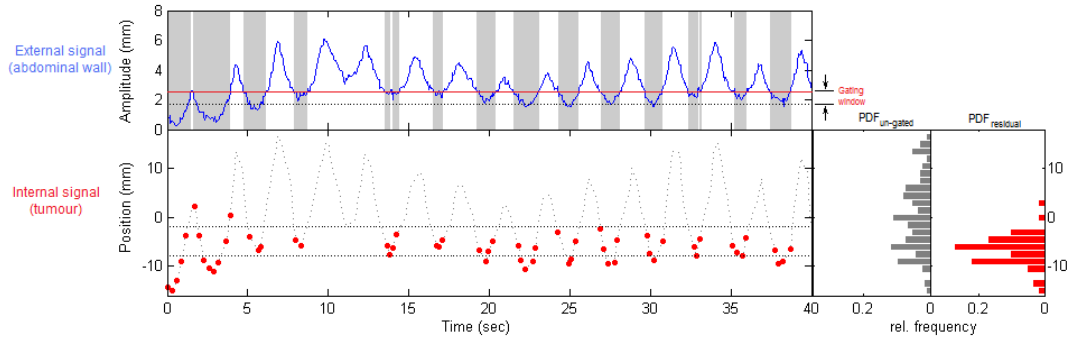

(c) Beam 5 (Gantry 130^o)

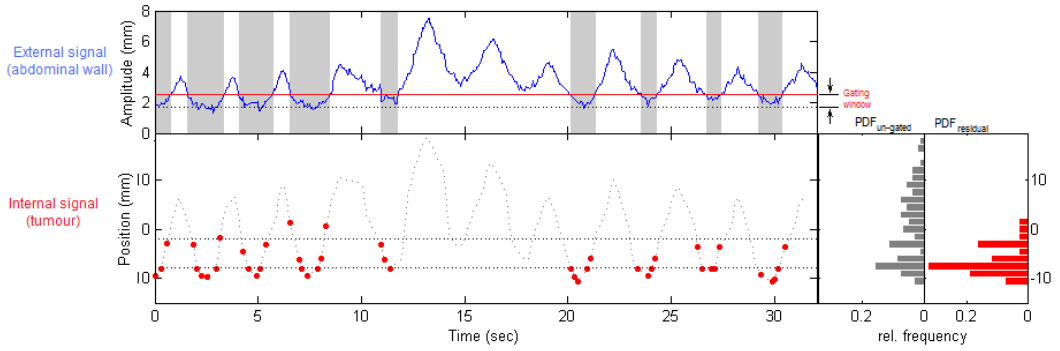

(d) Beam 6 (Gantry 150^o)

Figure 5.5: Fraction one beam 3-6

Baseline drifts as well as sudden cycle-to-cycle irregularities in the end-of-exhale tumour positions were detected and quantified. It was observed that such irregularities led to considerable variations in residual motion, which may in turn result in marginal miss. By inspecting both synchronised external/internal movement plots for beams (1-6), it can be seen that in some time intervals the respiratory patterns behaved in an irregular manner, exhibiting amplitude variations, baseline drifts, as well as sudden (cycle-to-cycle) variations in exhale positions. Such variations made it difficult to consistently and accurately capture the exhale positions to guide the gating of treatment beams. Tumour tracking information showed that in most cases the patterns exhibited by the external signal were translated into internal tumour movements detected during beam-on time. Maximum detected fluctuations of the exhale tumour positions ranged from 1.35 mm to 6.67 mm for fields (1-6), as shown in Table 5.1.

Table 5.1: *Measured residual motion at 95^{th}percentile and standard deviations (SD) of $PDFs_{residual}$ determined with PortalTrack throughout fraction delivery. $\Delta_{residual}$ represents the percentage difference between measured and clinically assumed value of residual motion*

Beam #	$PDF_{residual}$		$\Delta_{residual}$	Max. exhale
	SD (mm)	95% range (mm)	$\lvert measured - allowed \rvert$ (%)	fluctuation (mm)
1	2.5	8.7	49	2.5
2	2.9	10.5	80	4.3
3	4.9	15.9	171	2.4
4	2.4	8.1	38	1.3
5	3.0	9.4	62	6.6
6	2.9	9.4	61	2.4

5.2.1 Intrafraction Variations in Residual Motion

Table 5.1 gives a summary of calculated parameters for beams (1-6). The standard deviations of residual motion distribution histograms ($PDF_{residual}$) ranged from 2.4 to 4.9 mm, with beam 4 exhibiting the smallest and beam 3 the largest deviation. The measured residual motion measured at 95^{th}*percentile* ranged from 8.1 to 15.9 mm, which constituted a percentage difference (increase) in residual motion between 38% to 171%, relative to the clinically allowed value of $\approx$ 6 mm. Large fluctuations in residual motion are observed from beam-to-beam. There was a decrease of 49% between beam 3 and beam 4 and then a gradual leveling through the remaining fields. It is interesting to note that beam 3 and beam 4 also represented the maximum and minimum measured values of residual motion. Taking a closer look at the external/internal signals for beam 3 (gantry angle 285^o), it can be observed that external signal exhibited baseline drifts, which resulted in longer gates/beam-on time (wider shaded regions) as the signal shifted downwards. Subsequently, a longer gate means that a higher percentage of the tumour motion amplitude is allowed to move within the treatment

portal. This is reflected in the spread of tumour positions (red dots) beyond the defined range of permitted residual motion (towards the inhale phase of respiration), which in turn is manifested by the increase in the range of $\text{PDF}_{residual}$ (red histogram), and hence residual motion. The clinical implications from this would be that if small margins are designed during the process of treatment planning to encompass the PTV region, comprised by CTV and assummed permitted range of residual motion ($\approx$ 6 mm), with a given isodose level (i.e. 95% isodose), the tumour will move away from high dose region, leading to a poor tumour coverage, and possibly marginal miss.

It is worth noting that for the case of beam 3, such high measured magnitude of residual tumour motion is mostly due to variation in the external respiratory pattern and represents a worst case scenario of gated treatment, which is included in this study for comparison purposes. In a realistic treatment procedure with an external-based gating system the treatment would have been interrupted once the drift was identified by monitoring the patient's respiratory trace during treatment. Breath couching would have avoided this also by means of either audio instructions or visual feedbacks with the attempt to maintain a reproducible breathing pattern during dose delivery [29]. Tracking information showed that the internal tumour paths during beam-on time seemed to hardly resemble the motion characteristics exhibited by the external signal. For this case, it is observed that most of end-of-exhale tumour positions (10 out 12) were detected within the assumed permitted range of residual motion, whereas external signal exhibited baseline drifts, shifting downwards (posteriorly) for the first 11 seconds and then anteriorly for the rest of the delivery. This represents a typical example of degraded internal/external correlation, which constitutes a major limiting factor to the success of external-based gating techniques that lack an image-guided tool for treatment verification, as noted in the literature [18, 26, 28, 29, 45, 47, 54]. However, the importance of PortalTrack is that tumour tracking information can be used to validate the internal/external correlation to update or readjust the gating window.

Furthermore, by comparing both un-gated and gated distributions, it can be observed that with gated delivery the standard deviations of tumour positions were reduced by 21.3% - 61.3%, compared to the case in which no control for respiration was performed. The distribution of tumour motion in the SI direction for the combination of the resulting $\text{PDF}_{residual}$ correponding to all the six fields is shown in Figure 5.6. The distributions has its mean at zero, which representes the daily average tumour position. The asymmetry of the distribution is explained by the presence of the above-mentioned irregularies taking place during simulated treatment. The skew of the distribution towards the inhale direction (to the right side of the distribution) is mostly attributed to the effects of baseline drifts observed during dose delivery for beams (3-5). The 95^{th} percentile of this distribution, which indicates the limit within which 95% of the data points (detected tumour positions inside the gating window throughout fraction delivery) are located, is 15.9 mm as opposed to 6 mm. Furthermore, assuming a peak-to-peak tumour motion amplitude of $\approx$ 16.7 mm, as determined during treatment observation time (method section), it shows that gating reduced intrafraction motion by roughly 5% of its magnitude that would otherwise result without any control for respiration (un-gated). This is in agreement with the work by Korreman *et al* [45], in which it was found that even with gating the reduction in the mean tumour motion was low (6%), mostly due to baseline drifts and variations in the internal/external correlation.

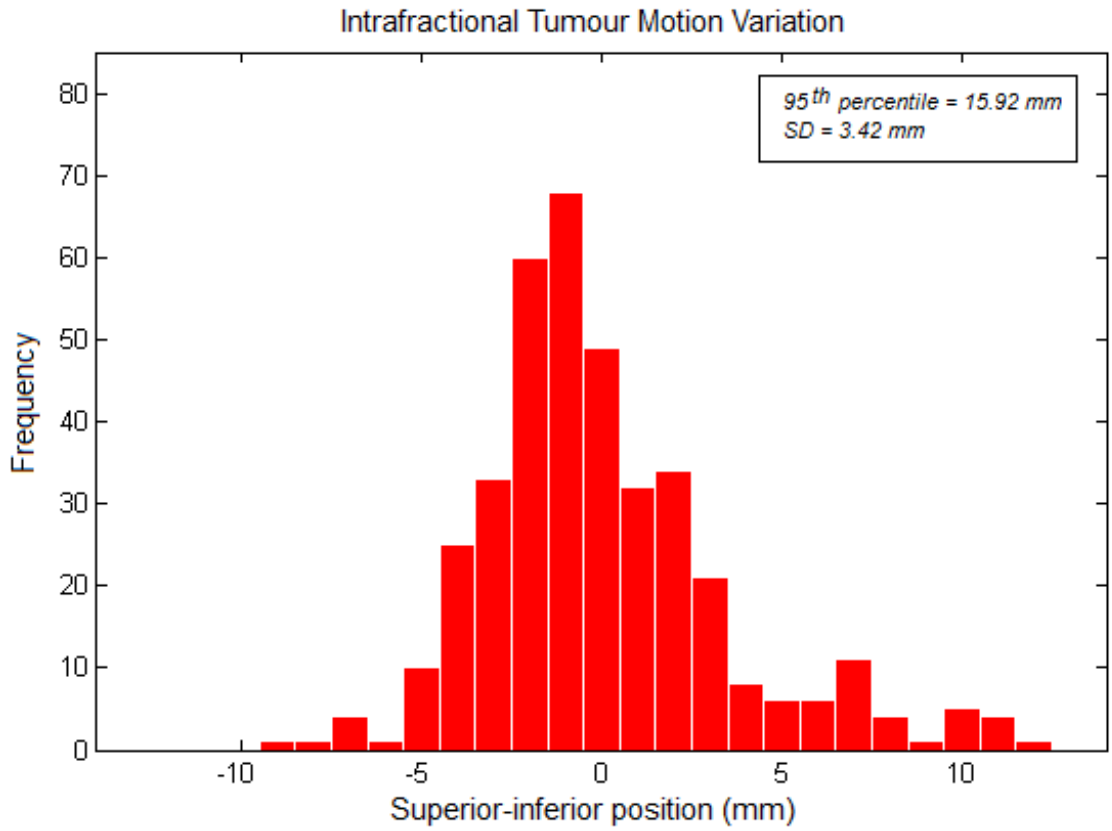

Figure 5.6: *The intrafractional superior inferior (SI) tumour displacement detected in each of the 336 images acquired during simulated gated treatment*

Detection of False Positive/Negatives

The detection of incidences of false positives, which are of more clinical concern since more dose would be given to healthy tissue [29, 47, 54], can be represented by those tumour positions detected distantly away from defined permitted range of residual motion. In other words, finding the tumour outside the permitted range meant that the tumour was located outside the high dose region, or even outside of the field in the case of those positions with significant deviations from permitted range. This will be the case provided that only 6 mm residual motion was taking into account for the purpose of treatment planning based on a 35% duty cycle for gated treatment. For example, in the case of beam 5 (breathing cycle 1), detected tumour positions 1-3 (end-exhalation) would represent cases in which the treatment portal was irradiated without having the tumour within the beam's-eye-view. This may be also observed in beam 2 (breathing cycles 5-6), beam 3 (cycles 1-8) and henceforth. These observations would have been better illustrated provided that a real gated treatment procedure was performed using small treatment margins designed during treatment planning to explicitly compensate for the clinically allowed residual motion ($\approx$ 6 mm). This represents a limitation in the study since gated treatment was simulated, patient was treated with SBRT using an ITV concept encompassing the whole tumour motion range.

On the other hand, the appreciations of false negatives (beam off at the right target position) from these simulations are difficult due to the fact the external signal directed

the onset of the gates, which means that no portal images were available to verify if the tumour was within the treatment portal. To highlight the presence of such effects the whole motion range of tumour trajectories, representing un-gated treatment, were added in the background (gray dashed paths) of each internal signal plot. Beam 2 showed the most cases of false negatives, which in some cases the exhale positions of external signal did not fall within gating window, whereas the tumour did. In a real clinical procedure this would have prolonged the treatment.

5.2.2 Margin Determination

In an idealised gated treatment, the treatment scenario should mimic the scenario considered during treatment planning [30]. Therefore, if the tumour coverage is to be kept constant throughout the course of treatment, the residual tumour motion should be kept constant and within the range of residual motion taken into account during treatment planning process. Subsequently, tracking information was utilised to retrospectively quantify a margin surrogate required to compensate for variations in residual motion for each beam and maintain tumour coverage. To accomplish this, the measured (95^{th} range) and clinically allowed (permitted movements range) values of residual motion were compared. The distances between the internal baseline and the $5^{th}percentile$, and between the internal upper limit and the 95^{th} percentile of a distribution were used as measures to quantify adequate margins magnitudes in both exhalation and inhalation directions.

Table 5.2 gives a summary of calculated parameters for beams (1-6). The distances between the 5^{th} percentile and internal baseline ranged from 0.2 to 7.6 mm, whereas between the 95^{th} percentile and internal upper limit from 0.8 to 4.1 mm. Assuming that the range of permitted tumour movements is enclosed by the 95% isodose, and a homogeneous dose to tumour is wanted, the margins must be increased by 1.2 mm, 4.1 mm, 2.4 mm, 0.8 mm, 3.9 mm and 2.1 mm in the exhalation direction, and by 1.6 mm, 0.6 mm, 7.6 mm, 1.5 mm, 0.2 mm and 1.5 mm in inhalation direction for beams (1-6), respectively.

Table 5.2: *The standard deviation of residual distributions and determined margin surrogates for fields 1-6. For each $PDF_{residual}$ the mean (m) and standard deviation (SD)determined tumour positions are given.*

Beam #	$PDF_{residual}$ $m \pm SD$ (mm)	distance Int. baseline to $5^{th}percentile$ (mm)	distance Int. UL to $95^{th}percentile$ (mm)
1	-5.8 ± 2.6	1.2	1.6
2	-7.5 ± 2.9	4.1	0.6
3	-3.9 ± 4.9	2.4	7.6
4	-5.5 ± 2.5	0.8	1.5
5	-6.7 ± 3.0	3.9	0.2
6	-6.8 ± 2.9	2.1	1.5

5.3 Summary

The feasibility of markerless tracking lung tumours for the verification of respiratory gated treatment was investigated with a case study. Gated treatment was simulated based on motion data obtained from a lung patient that underwent stereotactic body radiotherapy, from which both EPID movies and the external respiratory signal were synchronously acquired. EPID movies were retrospectively analysed in PortalTrack by simulating gated delivery and tumour tracking. The external signal directed the onset of the gates and the tumour was directly tracked in portal images acquired during beam-on time.

Simulations showed that tumour motion can be monitored and tracked during respiratory gated RT. PortalTrack was able to quantify the residual tumour motion as well as it's variations. Measurements of residual motion showed that large fluctuations in residual motion can occur intrafractionally. Irregularities in the internal tumour trajectories, such as baseline drifts and sudden cycle-to-cycle variations in the exhale tumour positions were detected and quantified within the predefined gating window. Such irregularities may lead to considerable variations in residual motion, which may in turn result in poor tumour coverage and in some cases even in marginal miss if the tumour residual motion is too large.

An evaluation of the internal tumour positions detected during beam-on time with PortalTrack showed that the external-based gating alone is not sufficient for precise gated lung treatment. There were incidences in which the pattern observed on the external signal were not reflected on true tumour positions detected within the gating window. A verification system is required in which the respiratory tumour motion can be imaged and quantified to the extent that a baseline (mean tumour position or exhale position) can be identified or established [45]. As suggested by Engelsman [34], it is more relevant to compensate for baseline drifts as they require larger margins than those required to compensate for breathing induced motion. Portaltrack has shown potential to detect baseline drifts. Information from PortalTrack may be used for treatment verification or the adaptation of the gating window such as reported in a recent work by Aristophanus *et al* [17]. Another direction would be to use tracking information for the adaptation of the treatment couch to correct for baseline drifts [42].

Chapter 6

Concluding Remarks

6.1 Summary

This thesis investigated the potential of RGRT to compensate for the effects of respiration induced motion and the suitability of real-time tracking for tumour position verification during treatment. Results have indicated that gated beam delivery for treating mobile tumours in the lung is advantageous, although its benefits can be further improved with the aid of a treatment verification tool. Dynamic phantom studies showed that RGRT has the potential to mitigate the effects of intrafractional tumour motion on dose distributions, reducing dose blurring effects by enabling steeper dose gradients, which led to improved dose conformity. Dose delivery in the presence of intrafractional motion without any compensation for respiration degraded dose conformity, enlarging the beam penumbra by 121% compared to dose delivery in absence of intrafractional motion. Conversely, gating allowed the reduction in dose blurring by 28% - 46% with gating duty cycle between 12% dc - 75% dc. The clinical significance of these findings are that decreasing dose blurring effects with gating leads to sharper dose distributions, thus resulting in more dose being delived to the PTV while sparing more healthy surrounding tissue or other OAR which may be in the close proximity to high dose gradient, i.e. heart. It was observed that reducing the duty cycle led to dose distribution that resembled those of the static distribution, however, suboptimal in terms of treatment efficiency.

In real practice, the use of external sensors as surrogates for internal tumour motion may be a source of uncertainties. It should not be considered a priori that the correlation between external signal and internal tumour mobility will remain stable throughout treatment. In fact, in the case of respiration such assumption is difficult make since different driving mechanisms, i.e., diaphragm, intercostal muscles [18] are involved during respiratory activity. Therefore, it was of interest to test the performance of the gating system under the influences of discrepancies in external/internal correlation as well as irregular tumour paths. Results showed that the dosimetric benefits of gated delivery were overshadowed by the influences of baseline drifts during dose delivery. Baseline drifts resulted in the systematic deviation of tumour position from planned position, leading to a shift in dose distributions in addition to increased dose blurring. For a reference gating window with 38% dc, baseline drifts of 3 mm to 12 mm led to an increase in dose blurring by 10% - 70%. Moreover, compensating for such irregularities by only adjusting the gating window proved to be limited. The clin-

ical implications of baseline drifts are that eventhough the tumour motion amplitude may be small, the systematic shift in its mean motion path would required larger margins for compensation. Baseline drifts can not easily be identified by means of 4DCT for its integration into treatment planning process, which may have even more detrimental consequences in terms of healthy tissue toxicity when smaller field sizes are used such as in the case of RGRT. More importantly, such drift would be unnoticed unless tumour motion is directly monitor during dose delivery. Real-time verification of the tumour position is essential to maximise the potential benefits of RGRT.

The suitability of PortalTrack for the verification of RGRT was investigated in simulations of gated treatment using the motion phantom, and demonstrated its feasibility with a clinical case study. The results showed that it is possible to determine and track tumor motion and variability during RGRT. During treatment the tumour was visualised in the beam's eye views and its residual motion as well as deviations from intended position (gating window) measured. Larger irregularities in tumour trajectories as well as in the external respiratory patterns of the patient were observed, which further justified the need for real-time verification during treatment. Measurements of residual motion ranged between 8.1 mm to 15.9 mm, which constituted a relative difference of 38% - 171% compared to the allowed residual motion of 6 mm, with the major part of these discrepancies arising from baseline drifts and sudden fluctuations of the exhale tumour positions inside the gating window. These results are comparable to those reported in the work of Berbeco *et al.* [46]. Investigators assessed the validity of external/internal correlation assumption of external-based gating, reporting intrafractional (beam-to-beam) variations in residual motion $> 300\%$. Exhale fluctuations up to 6.7 mm were observed. Recently, Nishioka *et al.* [26] reported exhale fluctuations up to 12.7 mm for cohort group of 12 lung cancer patients using the real-time tumour tracking (RTRT) system. The clinical significance of the results coming from this thesis is that if a patient is to be treated with gating under free breathing, with the gating window set to encompass the exhalation portion of the breathing cycle, which is commonly done in clinical procedures, it is important to be aware that exhale positions may fluctuate. However, future work is required, involving more clinical data, to further support these arguments.

Simulations of gated treatment resulted in the loss of motion data that could have otherwise been used to determine residual PDFs and hence altered their distributions. For the phantom studies, all the EPID movies were acquired during the delivery of 200 MUs, which resulted in a certain number of breathing cycles during whole dose delivery. If gated beam delivery had been performed, delivery times would have been prolonged depending on the duty cycle applied, resulting in more breathing cycles recorded during EPID movies acquisition. Conversely, during simulations of gated treatment delivery times were not prolonged and the frames which were not inside the gating window were only obscured and discarded, leaving only few breathing cycles and hence less data available for tumour tracking and determination of PDFs.

Evaluations of EPID moves were limited to detecting baseline drifts and other irregularities during beam-on time only, whose magnitudes could have been under estimated in case the irregularity lasted longer than the gate, moving outside the gating window during beam-off. Moreover, in the context of RGRT it seems to be more appropriate to refer to baseline drifts as systematic changes of exhale positions [26, 30], which can be quantified by

measuring their fluctuations relative to gating window. Figure 5.5 (b) shows the SI tumour position detected inside the gating window where a drift in exhale tumour position of about 9.26 mm was observed during beam-on time. However, this drift extended over 13 mm when non-gated delivery was considered. Moreover, EPID movies only provided 2D projections of the tumour in the plane perpendicular to central beam axis, limiting to detect intrabeam irregularities only, in fact, it is expected interbeam irregularities to be of larger magnitudes compared to intrabeam when considering the 3D motion of lung tumours and associated irregularities.

6.2 Future Work

An important aspect for bringing the present approach into the clinical routine is the feasibility of the tracking process with real tumours. The approach presented herein showed to be useful with a clinical case in which the tumour could be identified and tracked in portal images. This clinical case was intentionally selected because of the high visibility of tumour in portal images. However, the continuous tumour monitoring in portal images may not be feasible in some cases due to poor image contrast. There is still work to be done in terms of improving image quality. Alternatively, the makerless tracking process in EPID movies could be improved with the aid external respiratory signal combined with mathematical models of the correlation between the abdominal motion and tumour motion as suggested in a recent study by Wilson and Meyer [60].

Besides real-time tumour localisation, prompt linac response to the gating signal is required for the success of RGRT [29]. In this work, an immediate response of the linac was assumed during gated treatment simulations. This could have contributed to a non-negligible uncertainty when selecting portal images to either be obscured or remain visible. In a future work, it would be worth integrating the latency of the response to the gating signal during simulations, based on the mechanical characteristics of the linear accelerator, and evaluate the effect on residual PDFs. Furthermore, this study mainly focused on detecting baseline drifts and exhale fluctuations leaving phase shifts (also referred to as time shift [54]) between the external and internal signals unattended. Detecting such shifts are crucial to validate/update the external/internal correlation. An analysis of the correlation between the external respiratory signal and the tumour trajectories detected inside the gating window with PortalTrack could be addressed in a future work.

6.3 Conclusions

The need for a verification system is of utmost importance in the safe implementation of external-based gating to ensure that tumour motion inside the gating window is reproducible and enable corrections in case discrepancies arise throughout the course of treatment. Simulations showed that by making use of standard components of linear accelerator and a cost-effective solution such as PortalTrack the effectiveness of commercially available gating system could be improved. One major goal was to investigate whether tracking information was suitable/sufficient to quantify the residual motion as well as other systematic and

un-expected fluctuations in the internal tumour trajectories inside the gating window, with the process limited by the acquisition rate of portal images at approximately 2 frames/sec. Comparisons of measurements of residual motion determined with PortalTrack and that of a more ideal system, with an acquisition rate of 20 Hz, showed differences ranging from 0.1 mm to 1.1 mm and a mean of 0.4 mm $\pm$ 0.3 mm for all the simulated trajectories. This indicates that the main characteristics of the tumour trajectories inside the gating window were preserved at sampling rate of 2Hz and that PortalTrack gave a close estimate of the true residual motion. Although it is obvious that a sampling rate of $\approx$ 2 Hz could affect the accuracy of detecting sudden tumour positions that may take place between to sampling points, gated treatments are normally planned to encompass the more stable end-of-exhalation phase of respiration, where the tumour is expected to spend longer time. Results indicated that PortalTrack detected and tracked exhale tumour positions and fluctuations satisfactorily. PortalTrack has shown great potential for the verification of tumour position during RGRT and the tracking information could possibly be used for adaptive treatment delivery procedures for the compensation of respiration and variability.

Acknowledgment

First of all I would like to thank Dr. Juergen Meyer for his supervision, guidance, valuable discussions, and specially for inspiring me with the subject regarding the management of respiratory motion in radiation therapy. I also greatly appreciate being given the opportunity to meet and work together with people undertaking cutting edge research on the subject. I would like to thank Dr. Florian Cremers, the Chief Medical Physicist of University Medical Centre Hamburg-Eppendorf (UKE) in Germany, for giving the opportunity to join the medical physics group and work on my research project alongside a multidisciplinary team. Also for making sure that I had all the required resources available for the realisation of this research work.

I would like to thank Medical Physics Expert, Mr. Kurt Baier from the University of Wuerzburg, Germany, for letting me work with his fascinating tracking software, support with upgrades and implementation of new features, as well as welcoming hospitality in Wuerzburg. I would like to thank Dr. Juergen Wilbert and Dr. Anne Richter, also from the University of Wuerzburg, for providing me with clinical data. I would like to thank Volker Platz from UKE for his support, discussions and for always making sure that I had an accelerator available for measurements, as well as letting me spend all those hours needed to learn the operation and use of the gating system. I would also like to thank Dr. Bern Bobmann from UKE for the feedbacks on this manuscript. I would like to thank Rene Werner, from the University of Luebeck in Germany, for his support with Matlab routines. I would also like to thank Lukas Henze for the friendly company at the office. Finally, I would like to thank my wife for her support in any possible way throughout all this work.

Bibliography

[1] E Brambilla, W D Travis, T V Colby, B Corrin, Y Shimosato: *The new World Health Organisation classification of lung tumours.* European Respiratory Journal, 18: 1059-1068, 2001

[2] A Jemal, F Bray, J Ferlay, E Ward, D Forman: *Global Cancer Statistics.* CA: A Cancer Journal for Clinicians, 61(2):69-90, 2011

[3] S D Cox, J Y Chang, R Komaki: *Image-Guided Radiotherapy of Lung Cancer*, Informa Healthcare USA, Inc., 52 Vancerbilt Avenue, New York, NY 10017, 2008.

[4] T Bortfeld, R Schmidt-Ullrich, W De Neve, D E Wazer: *Image-Guided IMRT*, Springer-Verlang Berlin Heildergerg, 2006.

[5] W Curran, C Scott, C Langer, R Komaki, J S Hauser, B Movsas, et al.: *Long term benefits is observed in a phase III comparison of sequential vs concurrent chemo-radiation for patients with unresectable NSCLC: RTOG 9410.* In: Proceeding of the American Society of Clinical Oncology, 621a, 2003

[6] S Webb: *Intensity Modulated Radiation Therapy.* Institute of Physics, Dirac House, Temple Back, Bristol BS1l 6BE, UKE, 2001.

[7] S Webb: *Intensity modulated radiation therapy (imrt): a clinical reality for cancer treatment.* The British Journal of Radiology, 78: S64-S72, 2005.

[8] S Webb: *The physical basis of imrt and inverse planning.* The British Journal of Radiology, 76: 678-689, 2003.

[9] W Schlegel, T Bortfeld, A L Grosu: *New Technologies in Radiation Oncology*, Springer-Verlag Berlin Heidelberg, 2006.

[10] M van Herk: *Errors and margins in radiotherapy*, Seminars in Radiation Oncology, 14(1):52-64, 2004

[11] M. Guckenberger, T. Krieger, A. Richter, K. Baier, J. Wilbert, R. Sweeney, M. Flentje: *Potential of image-guidance, gating and real-time tracking to improve accuracy in pulmonary stereotactic body radiotherapy.* Radiotherapy and Oncology, 91:288-295, 2009.

[12] International Commission on Radiation Units and Measurements: Prescribing, recording, and reporting photon beam therapy. ICRU Report 62, Bethesda, 1993.

[13] L Ekberg, O Holmberg: *What margins should be added to the clinical target volume in radiotherapy treatment planning for lung cancer*. Radiotherapy and Oncology, 48:71-77, 1998.

[14] M van Herk, P Remeijer, C Rash, J V Lebesque: *The probability of correct target dosage: dose-population histograms for deriving treatment margins in radiotherapy*, International Journal of Radiation Oncology Biology and Physics, 47(45):1121-1135, 2000.

[15] R I Berbeco, H Mastafavi, G C Sharp, S B Jiang: *Towards fluoroscopic respiratory gating for lung tumours without radiopaque markers*. Physics in Medicine and Biology, 50:4481-4490, 2005.

[16] J Meyer, A Richter, K Baier, J Wilbert, M Guckenberger, M Flentje: *Tracking moving objects with megavoltage portal imaging: A feasibility study*. Medical Physics, 33:1275-1280, 2006.

[17] M Aristophanous, J Rottmann, S Park, S Nishioka, H Shirato, R Berbeco: *Image-guided adaptive gating of lung cancer radiotherapy: a computer simulation study*. Physics in Medicine and Biology, 55:4321-4333, 2010.

[18] J P Keall, M Murphy, M van Herk, : *The management of respiratory motion in radiation oncology report of AAPM Task Group 76*. Medical Physics, 33(10): 3874-3900, 2006.

[19] J Willner, K Baier, E Caragiani, A Tschammler, M Flentje: *Dose, volume, and tumour control prediction in primary radiotherapy of non-small-cell lung cancer*. International Journal of Radiation Oncology Biology and Physics, 52 (2):382-389, 2002.

[20] D Dosoretz, D Galmarini, J Rubenstein, M Katin, P Blitzer, S Salenius, R Dosani, M Rashid, G Mestas, S Hannan: *Local control in medically inoperable lung cancer: and analysis of its importance in outcome and factors determining the probability of tumour eradication*. International Journal of Radiation Oncology Biology and Physics, 27(3):507-516, 1993.

[21] J Belberdos, JJ Sonke: *State-of-the-art lung cancer radiation therapy*, Expert Reviews Anticancer Therapy, 9(10):1353-1363, 2009.

[22] L Fang, R Komaki, P Allen: *Comparison of outcome for patients with medical inoperable Stage I non-small-cell lung cancer treated with two dimensional vs. three dimensional radiotherapy.* International Journal of Radiation Oncology Biology and Physics, 66(1):108-116, 2006.

[23] J P Keall, V R Kini, S S Vedam, R Moham*Potential radiotherapy improvements with respiratory gating*. Australasian Physical and Engineering Sciences in Medicine, 25:1-6, 2002.

[24] H.D. Kubo, B.C. Hill: *Respiration gated radiotherapy treatment: a technical study*. Physics in Medicine and Biology, 41:83-91, 1996.

[25] R W M Underberg, F J Largerwaard, B J Slotman, J P Cuijpers, S Senan: *Benefits of respiration-gated stereotactic radiotherapy for stage I lung cancer: An analysis of 4DCT datasets*. International Journal of Radiation Oncology Biology and Physics, 62:554-560, 2005.

[26] S Nishioka, T Nishioka, M Kawahara, S Tanaka, T Hiromura, K Tomita, H Shirato: *Exhale fluctuation in respiratory-gated radiotherapy of the lung: A pitfall of respiration gating shown in a synchronized internal/external maker recording study*. Radiotherapy and Oncology, 86:69-76, 2008.

[27] Y Seppenwoolde, H Shirato, K Kitamura, S Shimizu, M van Herk, J V Lebesque, K Miyasaka: *Precise and real-time measurement of 3D tumour motion in lung due to breathing and heartbeat, measured during radiotherapy*. International Journal of Radiation Oncology, Biology and Physics, 53(4):822-834, 2002.

[28] T J Nøttrup, S S Korreman, A N Pedersen, L R Aurup, H Nyström, M Olsen, L Specht: *Intra- and interfraction breathing variations during curative radiotherapy for lung cancer*. Radiotherapy and Oncology, 84:40-48, 2007.

[29] S.B. Jiang: *Technical aspects of image-guided respiratory-gated radiation therapy*. Medical Dosimetry, 31:141-151, 2006.

[30] S S Korreman, T J Nøttrup, G F Persson, A N Pedersen, M Enmark, H Nystrom: *The role of image guidence in repiratory gated radiotherapy*. Acta Oncologica, 47:1390-1396, 2008.

[31] M Guckenberger, A Kavanagh, S Webb, M Brada: *A novel respiratory motion compensation strategy combining gated beam delivery and mean target position concept - A compromise between small safety margins and long duty cycles*. Radiotherapy and Oncology, 98:317-322, 2011.

[32] H Shirato, K Suzuki, G C Sharp, K Fujita, R Onimaru, M Fujino: *Speed and amplitude of lung tumor motion precisely detected in four-dimensional setup and in real-time tumor tracking radiotherapy*. International Juornal of Radiation Oncology, Biology and Physics, 64(4):1229-1236, 2006.

[33] T Bortfeld, S B Jiang, A Rietzel: *Effects of motion on total dose distributions*, Seminars in Radiation Oncology, 14(1):41-51, 2004.

[34] M Engelsman, G C Sharp, T Bortfeld, R Onimaru, H Shirato: *How much margin reduction is possible through gating or breath hold?*. Physics in Medicine and Biology, 50:477-490, 2005.

[35] M Engelsman, E M F Damen, K De Jaeger, K M van Ingen, B J Mijnheer: *The effects of breathing and set-up errors on cumulative dose to a lung tumour*, Radiotherapy and Oncology, 60:95-105, 2001.

[36] J Meyer,K Baier, J Wilbert, M Guckenberger, A Richter, M Flentje: *Three-dimensional spatial modelling of the correlation between abdominal motion and lung tumour motion with breathing.* Acta Oncologica, 45:923-934, 2006.

[37] L Ma, C Herrmann, K Schilling: *Modeling and prediction of lung tumor motion for robotic assited radiotherapy.* 2007 IEEE/RSJ International Conference on Intelligent Robots and Systems (IROS 2007), San Diego, CA, 189-194, 2007 (unpublished).

[38] J J Sonke, R T Lebesque, M van Herk: *Variability of four-dimentional computed tomography patient models*, International Journal of of Radiation Oncology Biology and Physics, 70:590-598, 2008.

[39] A Richter, J Wilbert, K Baier, M Flentje, M Guckenberger: *Feasibility study for markerless tracking of lung tumour in stereotactic body radiotherapy.* International Journal of Radiation Oncology Biology and Physics, 78:618-627, 2010.

[40] J W H Wolthaus, J J Sonke, M van Herk, J S A Belberdos, M M G Rossi, J V Lebesque, E M F Damen: *Comparison of different strategies to use for four-dimensional computed tomography in treatment planning for lung cancer patients*, Physics in Medicine and Biology, 70(4):1229-1238, 2008

[41] R D Timmerman, L Xing: *Image-Guided and Adaptive Radiation Therapy*, Lippincott Williams and Wilkins, 2009.

[42] J Wilbert, J Meyer, K Baier, M Guckenberger, K Herrmann, R Hess, C Janka, L Ma, T Mersebach, A Richter, M Roth, K Schilling, M Flentje: *Tumor tracking and motion compensation with an adaptive tumor tracking system (ATTS): System description and prototype testing.* Medical Physics, 35:3911-3921, 2008.

[43] M van Herk, M Witte, J van der Geer: *Biological and physical fractionation effects of random geometrical errors*, International Journal of Radiation Oncology Biology and Physics, 57:1460-1471, 2003.

[44] H Shirato, S Shimizu, T Kunieda, K Kitamura, M Van Herk, K Kagel, T Nishioka, S Hashimoto: *Physical aspects of real-time tumour tracking system for gated radiotherapy.* International Juornal of Radiation Oncology, Biology and Physics, 48(4):1187-1195, 2005.

[45] S S Korreman, T J Nøttrup, A Boyer: *Respiratory gated beam delivery cannot facilitate margin reduction, unless combined with respiratory correlated image guidance.* Radiotherapy and Oncology, 86:61-68, 2008.

[46] R I Berbeco, S Nishioka, H Shirato, G T B Chen, S B Jiang: *Residual motion of lung tumours in gated radiotherapy with external respiratory surrogates.* Physics in Medicine and Biology, 50:3655-3667, 2005.

[47] H Wu, Q Zhao, R I Berbeco, S Nishioka, H Shirato, S B Jiang: *Gating based on internal/external signals with dynamic correlation updates.* Physics in Medicine and Biology, 53:7137-7150, 2008.

[48] X A Li, P J Keall, C G Orton: *Respiratory gating for radiation therapy is not ready for prime time.* Medical Physics, 34:867-870, 2007.

[49] M J Murphy: *Tracking moving organs in real time.* Seminars in Radiation Oncology, 14(1): 91-100, 2004.

[50] K Baier, J Meyer: *Fast image acquisition and processing on a TV camera-based portal imaging system.* Medical Physics, 15:122-125, 2005.

[51] X A Li, C Stepaniak, E Gore: *Technical and dosimetric aspects of respiratory gating using a pressure-sensor motion monitoring system.* Medical Physics, 31(1): 145-154, 2006.

[52] T Lin, L I Cervino, X. Tang, N Vasconcelos, S B Jiang: *Fluoroscopic tumor tracking for image-guided lung cancer radiotherapy.* Physics in Medicine and Biology, 54:981-992, 2009.

[53] R Berbeco, S Nishioka, H Shirato, G Chen, S Jiang: *Clinical feasibility of using an EPID in cine mode for image-guided verification of stereotactic body radiotherapy.* International Journal of Radiation Oncology Biology and Physics, 69:258-266, 2007.

[54] D Ionascu, S Jiang, S Nishioka, H Shirato, R Berbeco: *Internal-external correlation investigations of respiratory induced motion of lung tumors.* Medical Physics, 34(10):3893-3903, 2007.

[55] C Grohman, R Werner, D Alberts, F Cremers: *Analysis of dose shifts induced by organ movements during treatment with TomoTherapy using a motion phantom and GafChromic EBT films.* University Medical Centre Hamburg-Eppendorf, World-Congress_UKE, Germany, 2009.

[56] C Nelson, G Starkschal, P Balter, R Morice, C Stevens, J Chang: *Assessment of lung tumour motion and setup uncertainties using implanted fiducials.* International Journal of Radiation Oncology Biology and Physics, 67:915-923, 2007.

[57] J W H Wolthaus, C Schneider, J J Sonke, M van Herk, J S Belderbos, M M Rossi, R T Lebesque, E M Damen: *Mid-Ventilation CT scan construction from four-dimensional respiratory-correlated CT scans for radiotherapy planning of lung cancer patients*, Physics in Medicine and Biology, 65(5):1560-1571, 2006.

[58] Y Tsunashima, T Sakae, Y Shioyama, K Kagei, T Terunuma, A Nohtomi, Y Akine: *Correlation between the respiratory waveform measured using a respiratory sensor and 3D tumour motion in gated radiotherapy.* International Journal of Radiation Oncology Biology and Physics, 60(3):951-958, 2004.

[59] R Berbeco, T Neicu, E Rietzel, G Chen, S Jiang: *A Technique for respiratory-gated radiotherapy treatment verification with an EPID in cine mode.* Physics in Medicine and Biology, 50(16):3669-3679, 2005.

[60] P L Wilson, J Meyer: *A spring-dashpot system for modelling lung tumour motion in radiotherapy.* Computational and Mathematical Methods in Medicine, :1-14, 2009.